Creep and Mechanical Properties of Carbon Fibre Reinforced PEEK Composite Material

by

Jonathan H. Enns

A Thesis Presented to

The University of Manitoba

in Partial Fulfillment of the Requirements for the Degree of

Master of Science

in Mechanical Engineering

Winnipeg, Manitoba

CREEP AND MECHANICAL PROPERTIES OF CARBON FIBRE REINFORCED PEEK COMPOSITE MATERIAL

BY

JONATHAN H. ENNS

A Thesis submitted to the Faculty of Graduate Studies of the University of Manitoba in partial fulfillment of the requirements for the degree of

MASTER OF SCIENCE

Abstract

Constant load creep tests of unidirectional carbon fibre/PEEK (polyetheretherketone) composite material (APC-2) were performed in three point bending. Testing concentrated on the creep behaviour of APC-2 in the longitudinal fibre direction although some transverse tests were run. Testing temperatures ranged from room temperature to 220 °C. It was found that unidirectional APC-2 in the longitudinal direction is susceptible to sudden creep failure (even after creeping for 64 hours) at stresses below the ultimate stress. Creep failure occurs even though the creep strains observed are very small (less than 0.0004 in/in). Creep increases with temperature while the strength, stiffness, and strain to failure decrease with temperature in the longitudinal direction. Plots of log compliance versus log time are linear for the longitudinal tests with a marked increase in slope at the glass transition temperature. The transverse plots of log compliance versus log time displayed a close correspondence to the WLF equation above the glass transition temperature. The use of the WLF equation and the generation of a master curve for the unidirectional tests is not appropriate due to the dominant properties of the carbon fibres. The creep tests performed indicate that the phenomenon of creep rupture in flexure is of significance and must be understood and characterized especially if the material is subjected to large loadings or large temperature gradients.

Acknowledgments

I wish to thank Don Mardis and Ron Crampton for their help in constructing the loading frame. Kim Majury for the temperature controller, and Dr. Cahoon for supporting me and giving me a free hand to perform this work.

Contents

List of Figures

List of Tables

1 Introduction

Fibre reinforced composite materials are continuing to see greater use in the aerospace and transportation industry. Carbon reinforced composite materials have seen and are continuing to see greater use as primary structural components in aircraft. Advanced fibre composite materials offer very high strength to weight ratios and high stiffness to weight ratios. Epoxy (thermosetting) composite materials have been used in the past in primary and secondary applications, replacing metallic parts using aluminium alloys to improve design and for weight reduction.

Thermoset composites and aerospace alloys are now being challenged by fibre composite systems using thermoplastic resins as the matrix [1,2,3]. The matrix used in epoxy composite materials are thermosetting polymers. These materials achieve their strength and stiffness by the extensive cross-linking (bonding) of the polymer chains. This cross-linking (commonly referred to as 'curing') can occur at room temperature or at elevated temperatures. The bonds between the polymer chains cannot be broken without severe degradation of the material occurring. This means that reforming of an epoxy composite material is not possible. A thermoplastic composite material uses a thermoplastic polymer as the matrix. These materials do not undergo the extensive crosslinking which occurs in thermosetting materials therefore they can be reheated and reformed without any degradation. Poly-ether-ether-ketone (PEEK) represents the first thermoplastic engineering polymer to be considered as a resin for advanced structural composite materials. Of the new advanced thermoplastic composite materials available, PEEK carbon fibre reinforced material is the most

well known and researched.

Thermoplastic materials such as PEEK offer higher toughness, greater chemical and environmental resistance and better thermal stability than epoxy composite materials. These are critical properties for high peformance and tactical aircraft. The processing advantages of thermoplastic materials offer great potential over epoxy composites, allowing postforming operations such as stamping, extrusion, molding, reuse and remolding of scrap material. In many cases the processing operations available with thermoplastic composite materials may allow design simplifications [1,2]. Table 1 shows the projected cost and weight reductions possible by replacing an aluminium alloy with thermoplastic composite materials. As well, thermoplastics allow for welding operations and provide for easier repairability. It is clear that the general class of thermoplastic matrix fibre composites has distinct advantages over metals or thermosetting composites. However they are a new class of materials and their mechanical properties have not been completely explored nor fully understood. Therefore an investigation was undertaken to determine the high temperature creep properties of PEEK matrix carbon fibre unidirectional composite material. The purpose was to characterize creep behaviour and to provide some results suitable for use in design using the composite. The material chosen for study was APC-2 because it was readily available commercially.

Table 1: Westland 30-300 Stabilizer Costs and Weights [1].

Material:	Al-Alloy	Thermoset CFR Epoxy	Thermoplastic APC-2 and CFRPEI	Optimized Thermoplastic APC-2 and CFRPEI
Weight	100%	70%	70%	68%
Manufacturing Cost	100%	76%	52%	44%

2 Literature Review

2.1 PEEK

PEEK (Poly-Ether-Ether-Ketone) is a relatively new material developed by ICI (Imperial Chemical Industries) and has only been available commercially as a carbon fibre reinforced material since 1982. The use of thermoplastic polymers for resin systems has been slow due to their high viscosity and the difficulty of impregnating brittle carbon fibres. It is only recently that polymer science has developed the technology to impregnate carbon fibres with thermoplastic engineering resins.

The interest in PEEK and other thermoplastics such as Phillips polyphenylene sulphide (PPS) is due to their handling and processing potential and their high temperature property retention. Standard epoxy or thermosetting composite materials are usually provided in the form of a preimpregnated sheet (i.e. the fibre reinforcement is preimpregnated with the resin but not fully cured) and must be laid up and processed in an autoclave to allow the resin to cure. The preimpregnated epoxy composite ('prepreg') has been partially polymerized and must be stored in cold storage as the epoxy resin will cure at room temperature in a matter of a few hours or days. Even in cold storage epoxy resins possess a shelf life of only six months. Once cured, an epoxy resin cannot be molded or formed to any degree whatsoever. Thermoplastic prepregs have unlmited shelf life and can be stamped, molded, and processed a number of times.

PEEK is a semi-crystalline polymer with crystallinities on the order of 30% [4]. This semi-crystalline structure provides PEEK with excellent chemical resistance,

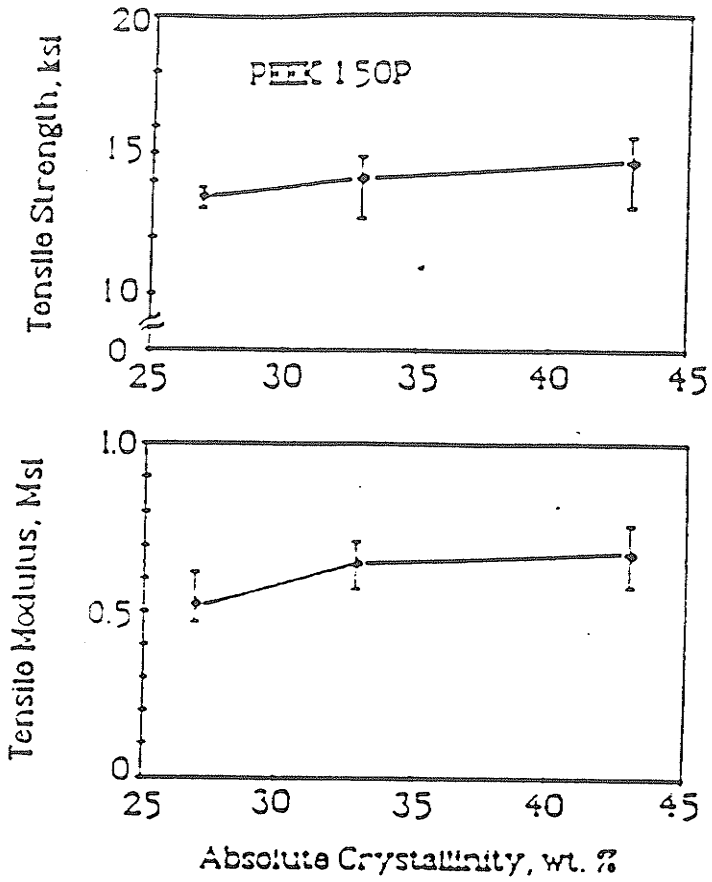

Figure 1: Tensile strength and modulus of PEEK 150P resin as a function of degree of crystallinity [4].

strength, and stiffness. Figure 1 shows the effect of the degree of crystallinity on the strength and stiffness of the PEEK resin. With increasing crystallinity however there is a correlating decrease in toughness (Figure 2). Table 2 shows some of the properties of the neat PEEK resin.

PEEK has a glass transition temperature (T_g) of 143 °C and a melt temperature (T_m) of 340 °C. PEEK has a continuous use temperature of 200 °C [6] but can go as high as 300 °C for short durations [7] although properties are severely reduced at this temperature.

Various types of reinforcement are available with PEEK; from continuously rein-

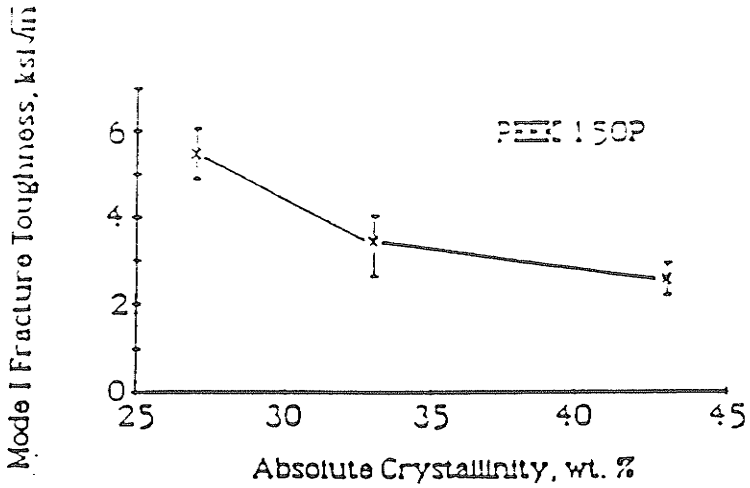

Figure 2: Mode I toughness of PEEK 150P resin as a function of crystallinity [4].

Table 2: PEEK: Neat Resin Properties [5].

$T_g - ^\circ C$	143
$T_m - ^\circ C$	343
Yield Strength - ksi(kPa)	14.5(100)
Modulus - ksi(MPa)	450(3.1)
Strain - %	> 40
Fracture Energy $-\frac{in-lb}{in^2}(kJ/m^2)$	$> 23(4.04)$

forced PEEK with glass and carbon fibre reinforcement in a cross-woven, cross-ply, or unidirectional format and available as a prepreg, to chopped and random fibre orientation for use in injection molding. PEEK reinforced with 61% by volume of continuous Hercules AS-4 type carbon fibre is referred to by the trade name APC-2, or aromatic polymer composite. APC-2 is the material studied in this investigation.

2.2 Properties of PEEK Composite Material

The mechanical and thermal properties of APC-2 and other PEEK composite materials are superior to most other thermoplastics and its properties are fully comparable or greater than those of state of the art epoxy composite materials. PEEK composites

Table 3: Mode I Toughness Test: G_{IC} (Delamination Resistance) $-\frac{in-lb}{in^2}(kJ/m^2)$ [3].

Epoxy/Graphite Cloth	1.34(0.24)
PEEK/Graphite Cloth	11.4(3.14)
Epoxy/Unidirectional Graphite	0.8(0.14)
PEEK/Unidirectional Graphite	8.0(1.4)

Table 4: Effect of Temperature on Flexural Strength of APC-2 [9].

Temp(^oC)	Axial Flexural Strength MPa/ksi	Transverse Flexural Strength MPa/ksi
23	2076/301	148/21.5
80	–	129/18.7
120	1776/258	116/16.8
180	1038/151	66/9.6

have better high temperature performance and property retention than most epoxies. The upper end use temperature of most epoxy resins is around 177 °C where the elevated temperatures begin to cause material breakdown and degradation. PEEK can operate in excess of these temperatures as required by advanced aircraft. Tables 3-5 show some of the properties for carbon fibre/PEEK composites, namely APC-2. There is a considerable range in the value of properties obtained depending on the testing methodology. The testing of composite materials is not fully standardized so some variation can be expected. Much of the testing that has been performed is comparative and qualitative in nature.

2.2.1 Environmental Resistance

PEEK composites are highly unreactive and possess excellent chemical and solvent resistance. PEEK composites retain virtually all of their strength in the fluids and solvents to which they might be exposed [3,9,10]. PEEK has good moisture resis-

Table 5: Mechanical Properties of Unidirectional APC-2 [4].

Flexural Stress - ksi(MPa)	273(1.88)
Flexural Modulus - msi(MPa)	19.4(134)
Short Beam Shear Strength - ksi(kPa)	15.2(105)
Compressive Stress - ksi(MPa)	150 – 160(1.03 – 1.10)
Fracture Energy, G_{IC} - $\frac{in-lb}{in^2}(kJ/m^2)$	10.7(1.88)
Longitudinal Tensile Strength - ksi(MPa)	309 – 356(2.13 – 2.45)
Longitudinal Tensile Modulus - msi(MPa)	19.4 – 20.5(134 – 141)
Transverse Tensile Strength - ksi(kPa)	11.9(82)
Transverse Tensile Modulus - msi(MPa)	1.3 – 1.5(8.96 – 10.3)
In-Plane Shear Strength - ksi(kPa)	44 – 47(303 – 324)
In-Plane Shear Modulus - msi(MPa)	0.74 – 0.91(5.1 – 6.9)

tance and good property retention in wet environments whereas epoxies tend to swell considerably under continued exposure in many solvents and in moist conditions and can weaken substantially.

Studies have also shown that PEEK composites have good resistance to thermal cycling, radiation, and good resistance to both combined [11,12]. It was found that the mechanical properties at high temperatures were improved by irradiation. This is caused by an increase in the glass transition temperature of the PEEK matrix and the formation of cross-linking due to irradiation. These studies indicate the potential of PEEK composites such as APC-2 and the next generation of thermoplastic composite materials currently being developed.

2.2.2 Toughness of PEEK Composites

The lack of toughness of epoxy composites have eliminated them from many applications. The toughness of PEEK allows the replacement of metallic parts where toughness is a requirement and light weight is desirable. PEEK is an inherently tough

material and its toughness has been well characterized.

Various tests are used to characterize the toughness of composite materials; damage tolerance tests, Izod impact toughness tests, and mode I and II interlaminar fracture toughness tests. Damage tolerance tests include such tests as compression after impact tests (CAI) and these have shown that APC-2 has almost twice the damage tolerance as an untoughened epoxy and tolerance equivalent to a toughened epoxy composite [13]. An earlier investigation showed that APC-1 (predecessor to APC-2) possessed about 5 times the damage tolerance of a standard epoxy composite, AS4/3501-6 [14].

The double cantilever beam test is used to characterize the mode I interlaminar fracture toughness, G_{IC}. This test was used to measure the G_{IC} of APC-2 and Hercules AS4/3501-6 epoxy composite material. The failure modes of the two materials were quite different[14]. The crack growth of the epoxy was very stable and was mainly controlled by the crosshead displacement. The failure mode of APC-1 and APC-2 consist of slow crack growth followed by fast crack growth, crack arrest, and slow crack growth again. Slow crack growth or ductile growth was accompanied by plastic deformation of the PEEK matrix. Examination of the fracture surface revealed the areas where the crack had propagated slowly and darker areas with beachmarks where fast propagation had occurred. Much more resin had adhered to the fibres in the PEEK composite than in the epoxy composite indicating better fibre-matrix adhesion. This fast growth/slow growth behaviour is typical of most thermoplastic composites.

A G_{IC} value can be calculated for the slow crack growth mode and the fast crack

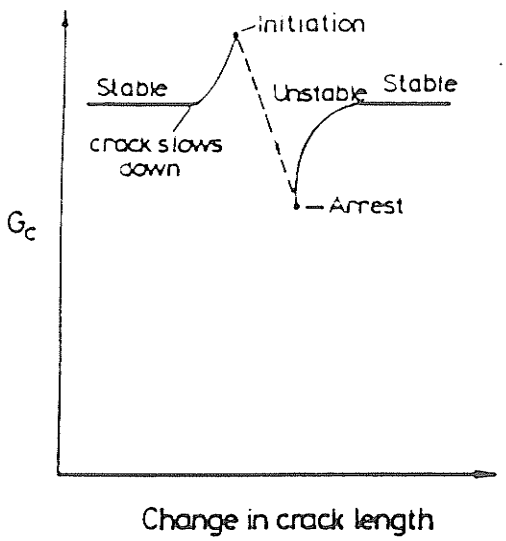

Figure 3: A schematic diagram showing the rise in G_C prior to unstable fracture [21].

growth mode. This is possible due to the visibility of the points of initiation for each mode. Figures 3 and 4 illustrate this fast growth/slow growth fracture behaviour. Figure 5 shows the toughness values obtained for APC-2 and other composite systems as a function of strain rate. The good toughness obtained for PEEK is due to the toughness and ductility of the PEEK matrix and the excellent carbon fibre-matrix adhesion which occurs.

2.2.3 Low Temperature Properties

The low temperature properties of APC-2 have been investigated and show that APC-2 may be of interest in cryogenic applications [17]. The strength and modulus of APC-2 is greater at 4.2 K than at room temperature due to the differential thermal expansion of the PEEK resin and the carbon fibres. The coefficient of expansion for PEEK is 47×10^{-6} while for carbon fibres it is around -0.5×10^{-6}. This results in significant residual stresses in the carbon fibres and an increase in strength and mod-

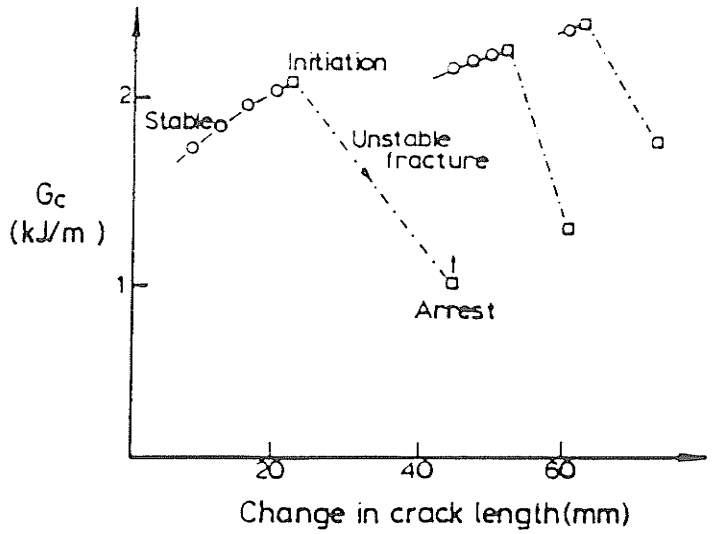

Figure 4: Typical results from DCB2 tests showing the buildup of G_C with crack length [21].

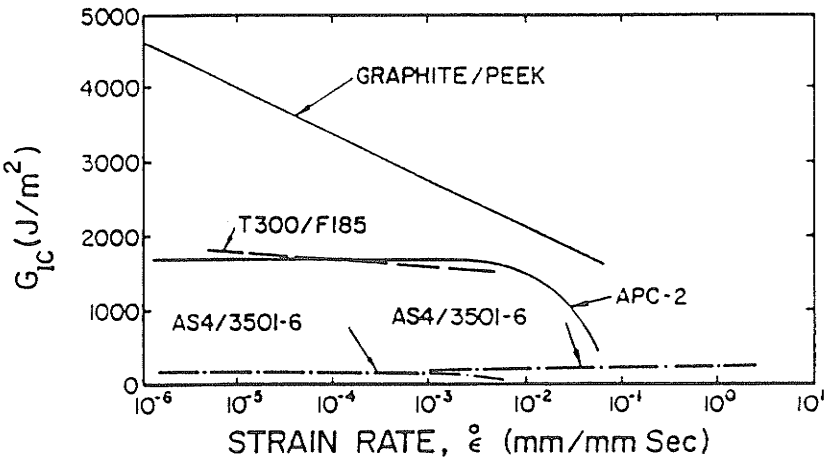

Figure 5: Relationships between interlaminar fracture energy and strain rate of four composite materials [15].

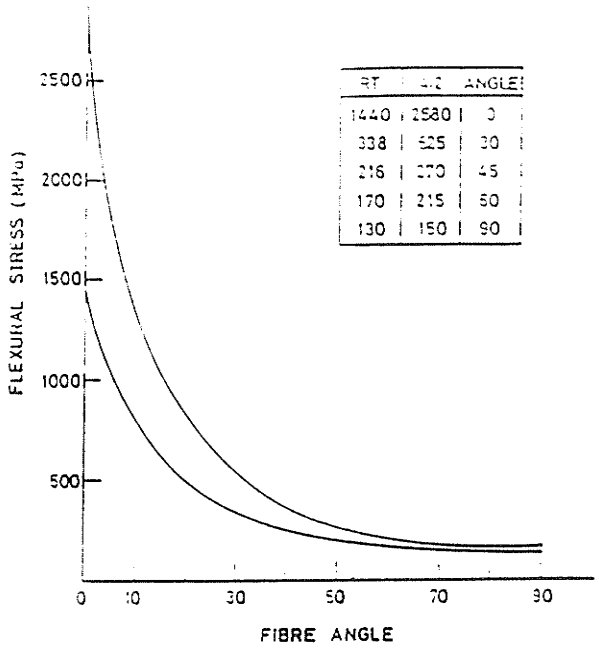

Figure 6: Flexural strength as a function of fibre angle [17].

ulus at very low temperatures (see Figure 6 and 7). Even at these low temperatures, microductility of the PEEK matrix was observed for cross-ply laminates.

2.2.4 Fatigue

Fatigue resistance is another critical property for any material for use in primary structural applications, particularly on aircraft. Graphite/PEEK composites were found to be more fatigue resistant than a state of the art epoxy, HMF-133-76 [18]. The better fatigue resistance of PEEK composites may be due to their toughness and the high level of fibre-matrix adhesion.

2.2.5 Creep

One study has shown that the transverse creep properties of carbon fibre/PEEK composites have superior creep resistance over carbon fibre/epoxy composites[19].

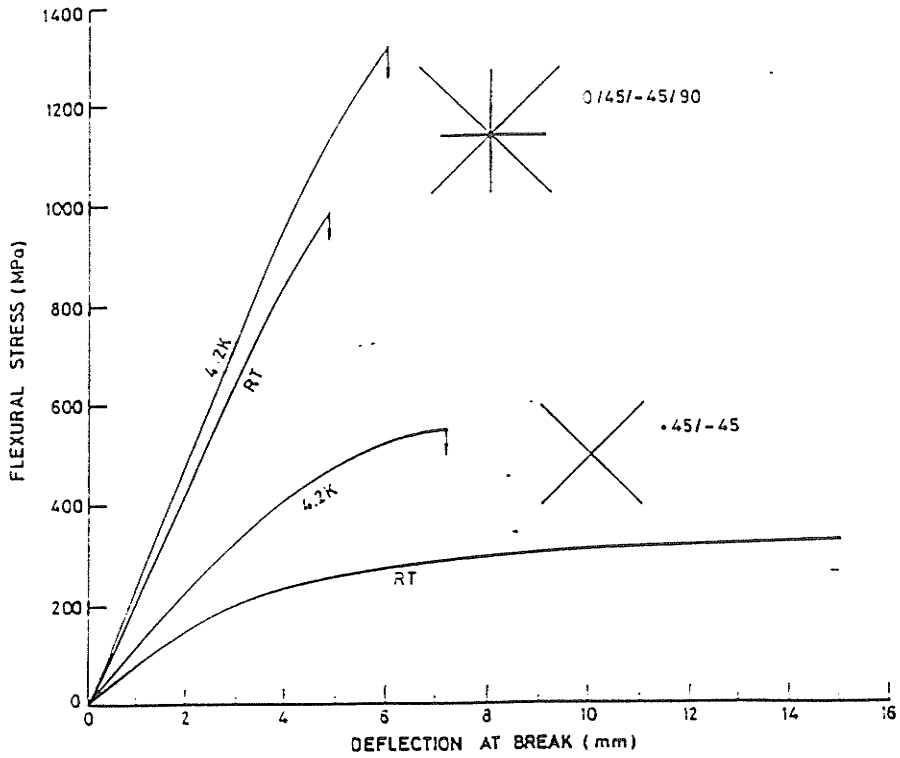

Figure 7: Flexural stress vs. deflection as a function of panel lay-up [17].

Another study has shown that for a cross-ply and transverse laminate PEEK showed greater creep strain although the difference in the transverse creep strain was on the order of 100 microstrains. These results were achieved at temperatures of 100 °C and less [30]. Similar results were observed in another study at room temperature. However the difference in performance at room temperature between PEEK and epoxy for creep resistance is marginal. At higher temperatures PEEK composites would be expected to outperform epoxy composites due to its better high temperature properties.

Relatively little creep data is available, although some work has been pursued using dynamic mechanic analysis (DMA) on composite materials, including carbon fibre PEEK composites. As well, constant load creep tests have been performed on

laminates of various layups and fibre orientations in tension. The experimental work for this thesis involves constant load creep tests in three point bending. This work will be discussed in further detail later along with a review of viscoelastic theory and other works.

2.3 Crystallinity of PEEK

The structure and morphology of the PEEK matrix affect the behaviour of the composite material. PEEK is a semi-crystalline polymer and there are two main levels to the crystalline morphology. The largest entities are the spherulites which are of the order of 10μm and consist of the three dimensional growth patterns of the much smaller underlying crystals. These crystals consist of lamellae about 5nm thick which grow outward until they impinge upon each other or on carbon fibres [20]. Crystallinity levels of 30% are typical and provide optimum properties although crystallinities of up to 40% can be obtained for very slow cooling rates. The carbon fibres in APC-2 have a diameter of 7μm and influence the growth patterns of the crystals.

Electron micrographs have shown that nucleation sites can be divided into three types [20]:

1) Nucleation from contact points between fibres or regions where the fibres are almost in contact:

This event could be the result of local shearing at the contact points enhancing the chances of nucleation by orienting the polymer chains or exposing specific nucleation sites at the surface of the fibres. Alternatively, this event could be the result of differential contraction stresses being exacerbated at the contact points of the fibre.

2) Nucleation at a free fibre polymer interface:

Surface nucleation occurs in APC-2 due to the presence of small graphitic crystals at the fibre surface. Differential contraction stresses may also play a part, although this process is not very significant.

3) Nucleation from within the matrix:

Crystallization due to lower processing temperatures favours matrix nucleation over nucleation at the contact points between adjacent fibres, although following the recommended processing procedures causes nucleation between adjacent fibres to predominate.

The crystallinity plays a major role in the behaviour of PEEK composite materials. Strength, modulus, toughness, and other related properties are all influenced by the level of crystallinity, which in turn is affected by the processing conditions. The adhesion of the matrix to the fibres also plays a role in determining the properties of the material and is related to the mechanics of nucleation.

3 Theory and Background

3.1 Mechanics and Behaviour

The mechanics and behaviour of composite materials can be quite complex. Continuous fibre reinforced composite materials are highly anisotropic. Two elastic contants are required to describe the elastic properties of an isotropic material while twenty-one are required for an anisotropic material with no planes of symmetry. A unidirectionally reinforced composite material is an orthotropic material and requires nine independent elastic constants to fully characterize the material. These materials have three mutually orthogonal planes of symmetry for mechanical properties and there are no interactions between the normal stresses and the shearing strains and conversely, there are no interactions between shearing stresses and normal strains.

In practical tests, the normal and shear moduli can be obtained in the three principal directions, as well as the three Poisson's ratios. In practice, few elasticity problems have been solved for orthotropic materials on account of the complexity of the stress-strain relations. The analysis becomes much more complicated and involved for off-axis composite materials and cross-ply laminates. The analysis is involved due to the interaction of two materials with very distinct properties. As a result, any detailed analysis involves finite difference and finite element analysis. Testing of unidirectional composite materials is relatively straightforward and necessary so as to characterize the principal material properties. These results can then be used to predict the materials behaviour for various other laminates; e.g. cross-ply, quasi-isotropic. For a unidirectional material, the 'Rule of Mixtures' applies quite well in

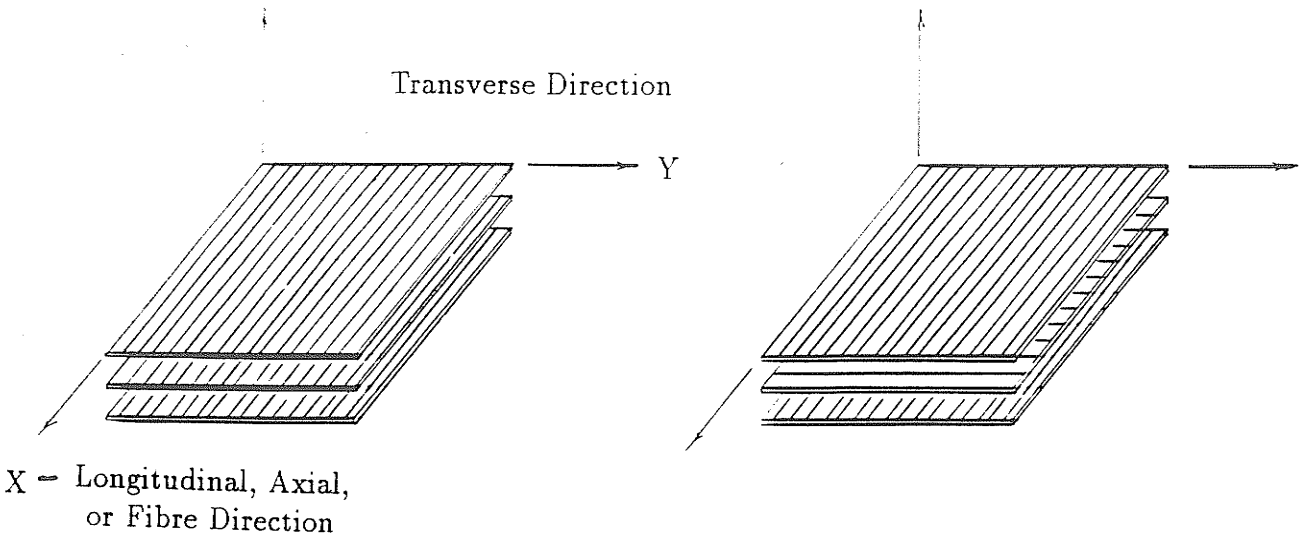

(a) Unidirectionally Reinforced Fibre Composite Material - 0° Layup.

(b) 0/90/0 Degree Cross-Ply Layup.

Figure 8: Schematic Representation of Continuously Reinforced Composite Materials.

the fibre direction for determining strength and modulus. Figure 8 helps define some of the parameters and variables involved in the field of composite materials.

The 'Rule of Mixtures' states that the strength or modulus of a composite material is equal to the summation of the volume fraction of each component multiplied by its respective strength or modulus. The strength of a composite material can be simply stated as

$$\sigma_{comp} = V_f \sigma_f + V_m \sigma_m$$

where V_f and V_m are the volume fractions of the fibre and matrix and σ_f and σ_m are the respective strengths of the fibres and matrix. For a high strength carbon fibre composite material the contribution of strength provided by the matrix becomes insignificant.

3.2 Adhesion

The adhesion of the matrix to the fibre provides the composite material with the basis for its strength. The fibres carry most of the load in a composite material so the matrix must be able to transfer and distribute the load evenly between the fibres. The matrix must fully adhere to the fibres and not allow slippage to occur otherwise the full load carrying capacity of the fibres will not be reached.

The fibre-matrix interface is specific to each fibre-matrix system. In APC-2, the carbon fibre reinforcement is Hercules AS-4 high strength carbon fibre with a volume percent of 61%, which is typical of most high strength carbon fibre composite materials. The interface in these materials plays a dominant role in determining the fracture toughness properties of composite materials and in their response to aqueous and corrosive environments. These environments can cause some thermosets to swell and delaminate.

Composite materials with weak interfaces have relatively low strength and stiffness but, in general, have high resistance to fracture. Materials with strong interfaces have high strength and and stiffness but tend to be brittle. APC-2 and some of the new toughened epoxies [15] have inherently tough matrices and display excellent toughness with excellent adhesion. However, resistance to fracture or fracture toughness is related to the ease of debonding and fibre pull-out during crack propagation. Fibre pull-out absorbs much energy and has the effect of crack blunting, thereby increasing fracture toughness.

3.2.1 Adsorption and Wetting

For good adhesion it is necessary that the resin cover every hill and valley of the fibre surface to displace air and obtain complete fibre wetting. Fibre wetting is extremely difficult for advanced themoplastics such as PEEK due to their high melt viscosity. The method of fibre impregnation for most thermoplastics is classified as proprietary knowledge although the methods involve film stacking, where thin films of the polymer are stacked with alternating layers of fibres and then molded under heat and pressure, or co-mingling (i.e. pairing or combining) of reinforcing fibres and fibres of the resin which are then aligned into mats and consolidated in a mold. Fibre wetting in epoxy composite materials is much easier as the resin is initially prepared in the form of a solution and the fibres are merely passed through this solution, where they are wetted. The wetted or resin coated fibres are then laid up in a specific orientation then cured in an autoclave. Volatiles are released as the resin cures and cross-linking occurs.

Good fibre wetting must occur if a strong bond is to be achieved. A strong bond will not be achieved if the fibre surface is contaminated, if air is entrapped at the fibre surface, or if large shrinkage stresses occur during the curing or consolidation process. These shrinkage stresses can lead to delamination between the fibre and resin which can not be healed. As well, the close packing of the fibres may prevent the resin from penetrating all of the fibres as the pressure from consolidation will force the fibres together and block the resin flow.

3.2.2 Bonding

Chemical bonding offers the main mechanism for the strength of the fibre-matrix interface. Coupling agents are often used on glass and carbon fibres. A chemical bond is formed between groupings on the fibre surface and a compatible chemical group in the matrix. The strength of the bond depends on the number and type of bonds. Interface failure will involve bond breakage.

In some cases it is possible to form a bond between two polymer surfaces by the diffusion of the polymer molecules on one surface into the molecular network of the other surface. The bond strength will depend on the amount of molecular entanglement and the number of molecules involved. The phenomena of interdiffusion has been called autoadhesion in relation to adhesives.

Mechanical adhesion may occur by the mechanical interlocking of the two surfaces. The tensile strength of the interface will be very low, however, the shear strength may be significant and depends on the surface roughness. Increased surface roughness also increases the surface area for chemical bonding.

3.2.3 Adhesion in APC-2

The importance of fibre-matrix adhesion in APC-2 has been studied [15,20]. The properties of APC-2 are governed by the tough ductile matrix and the strong interface bond.

The fibre-matrix adhesion level in APC-2 does not significantly influence the tensile modulus of the composite material as only good contact between the fibres and the matrix is necessary to yield maximum stiffness. Tensile strength is strongly de-

pendent on interface strength. The interface transfers stress between the matrix and the fibres. The stronger the interface the better the stress transfer capability. To reach the maximum strength of the composite, the fibres must fail due to overloading and not due to interface failure which will result in premature and localized failure. Tensile strength is quite sensitive to interface strength while compressive strength is less sensitive to the interfacial adhesion level as it is the compressive and shear moduli of the resin which determines the ability of the matrix to support the fibre in compression.

In transverse flexure of APC-2 [15] observation of the fracture surface revealed that although the crack may move close to the interface and prefers to follow the contours of the fibre surfaces failure is truly cohesive in the PEEK matrix. Transverse flexural strength in APC-2 is limited by the matrix strength. This cohesive failure mode allows considerable deformation of the matrix resulting in a ductile layer of PEEK adhering to the fibre surface. At temperatures as low as 4.2K this microductility and adherence of PEEK to the fibres was observed for cross-ply laminates [17]. It has also been shown that for APC-2, the optimum toughness can only be achieved when the fibre-matrix interface is stronger than the PEEK matrix. This is due to the high toughness of the PEEK matrix and its energy of plastic deformation. The strength of the fibre-matrix interface and the toughness of the PEEK matrix ensure that for an interlaminar crack the damage is restricted to either side of the main crack front so a very high value of toughness is obtained in comparison to other composite systems.

Other investigations have confirmed these results correlating the fibre-resin bond integrity with compression-after-impact (CAI) strength [13]. The CAI strength was

found to be twice that of an epoxy composite material.

4 Carbon Fibres

4.1 Introduction

APC-2 consists of 61% by volume AS-4 Hercules high strength carbon fibres (see Table 6). The properties of these carbon fibres and their method of production is illustrative and provides insight into the nature of carbon fibre reinforced materials and APC-2 in particular. Figure 8 shows some of the specific properties of engineering materials and illustrates the attractiveness of carbon-fibre reinforced materials.

4.2 Structure of Carbon

Elemental carbon exists in two forms; diamond and graphite. Buckminster fullerite ('buckeyballs' or C^{60}) is the third known form of elemental carbon recently discovered but is relatively rare. Diamond is metastable and converts rapidly to graphite when heated in a vacuum to about 1500°C. Graphite can be converted to diamond at high temperature and pressure. Graphite is extremely stable in an inert environment up to temperatures of 3000 °C.

Graphite has a layered structure, is highly anisotropic and is a good conductor of electricity parallel to the layers. The structure of the hexagonal form of graphite is shown in Figure 9 and has an *ab ab ab* stacking sequence along the c-axis with the

Table 6: Properties of Carbon Fibre Grades [23].

Fibre	Grade	Strength KSI (GPa)	Modulus MSI (GPa)
Magnamite AS-4	High Strength	450(3.1)	34.4(235)
Magnamite HMS	High Modulus	319(2.2)	38.4(265)
Magnamite AS-5	Commercial	305(2.1)	30.5(210)

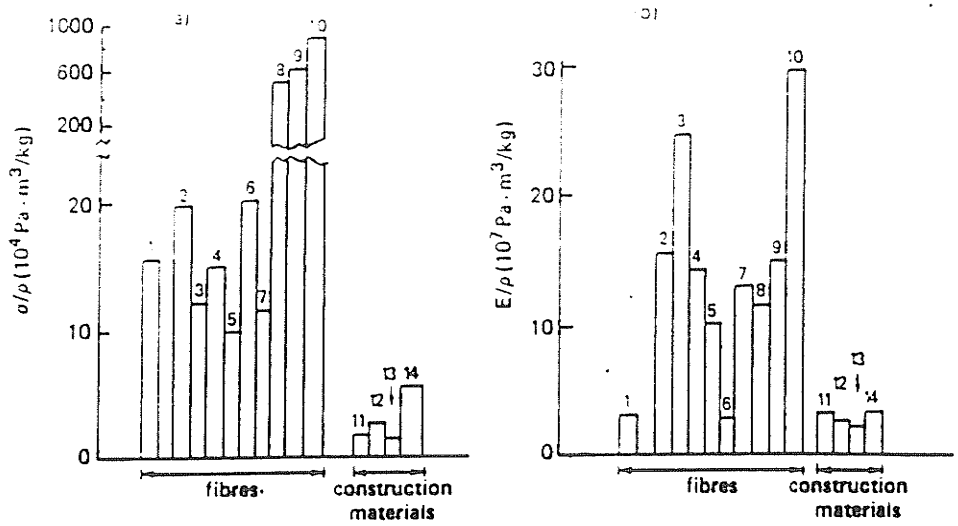

Figure 9: Specific values of strength and Young's modulus for carbon and other materials.

(a) Specific strength; (b) Specific modulus; (1) E-glass; (2) carbonized fibre; (3) graphitized fibre: (4) boron fibre; (5) boron carbide based fibre; (6) tungsten Fibre; (7) beryllium fibre; (8) saphire fibre (Al_2O_3); (9) silicon carbide based fibre; (10) graphite whiskers; (11) aluminium alloy; (12) titanium alloy; (13) magnesium alloy; (14) steel.

layer planes sitting in the *ab* planes. In the layers, each carbon atom is surrounded by three others in a planar trigonal arrangement so that the atoms and bonds form a hexagonal pattern. There are two forms of graphite; the hexagonal form discussed where succesive layers shift plus and then minus one bond length giving an *ab ab ab* stacking sequence. In the rhombohedral form succesive layers are displaced by one bond length giving an *abc abc* stacking sequence [24].

Within the planes of the graphite structure hybridization of the carbon atomic orbitals form three sp^2 orbitals inclined at 120° plus a π (2p) unhybridized orbital on each atom at right angles to the layer planes [24]. Tight bonding occurs in the layer planes due to the three sp^2 orbitals and as a result of this order, graphite is a good conductor of electricity parallel to the layer planes as there is virtually no energy gap between the atomic bonds in the layer planes. The conductivity parallel to the layer

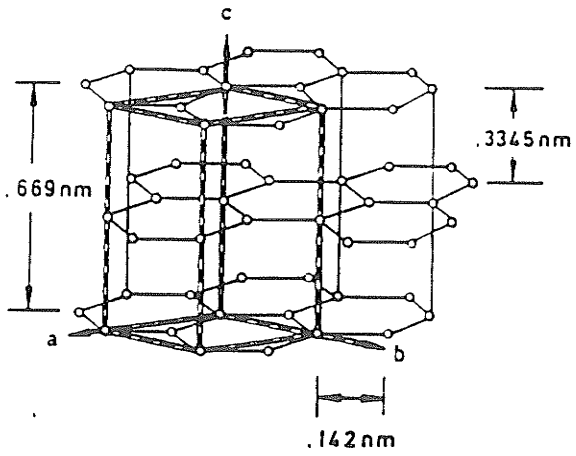

Figure 10: The structure of graphite and its unit cell; the hexagonal form [24].

planes is about 5000 times the conductivity perpindicular to the layer planes [24]. The bonding between the layer planes is by Van der Waals forces and the layer separation is 0.3345nm while the atomic separation in the layer planes is 0.142nm. The interaction between the layer planes is only about 1% of the tight bonding between atoms in the layer planes. The non-bonding 2p band is only partially filled and is narrow which reduces electron mobility.

The graphite layer planes may also be rotated individually about the c-axis to form a crystal in which the layer planes, while still parallel, are not ordered with respect to each other and any sense of stacking sequence is lost. This structure is known as turbostratic carbon and is the form which carbon fibres, including Hercules type AS-4, assume. Graphite refers strictly to the ordered three dimensional form. There is a close correspondence between most of the properties of graphite and turbostratic carbon. The layer spacing in turbostratic carbon is 0.344nm compared to 0.3345nm for graphite [24].

4.3 Structure of Graphite and Carbon Fibres

The carbon atoms in the layer planes of the graphite crystal have a very high elastic modulus (E) parallel to the layer planes of $155x10^6$ psi (155 msi or 1060 GPa) [24] due to the tight bonding in the layer planes. The elastic modulus is only 36.5 GPa perpendicular to the layer planes. Preferred orientation of the layer planes is necessary to attain a high modulus for polycrystalline graphite. Carbon whiskers have been obtained with a Young's modulus of 800 GPa parallel to the whisker axis. These whiskers consisted of sheets of carbon layer planes rolled up around the longitudinal axis.

Most commercial carbon fibres are made from a precursor which contains a high percentage of carbon. Carbon fibres can be made from cellulose, tar pitch, or from acrylic fibres like polyacrylonitrile (PAN). PAN fibres are the most commonly used precursor and are used for the manufacture of Hercules fibres. The structure of high strength and high modulus carbon fibres manufactured from PAN consist of crystalline units which are elongated, thread-like and fibrillar and there is sufficient evidence to attribute the response of the structure to a fibrillar model (Figure 11 [24]. This structure is formed from interlocking highly curved sheets of layer planes grouped into microfibrils which have a degree of preferred orientation with respect to the fibre axis. The sheets have no preferred orientation in the cross-section due to their high curvature except in some fibres heated to 2500°C which have a thin surface skin of highly ordered graphite. Residual strain induced by differential shrinkage is present in the structure and may influence the mechanical properties.

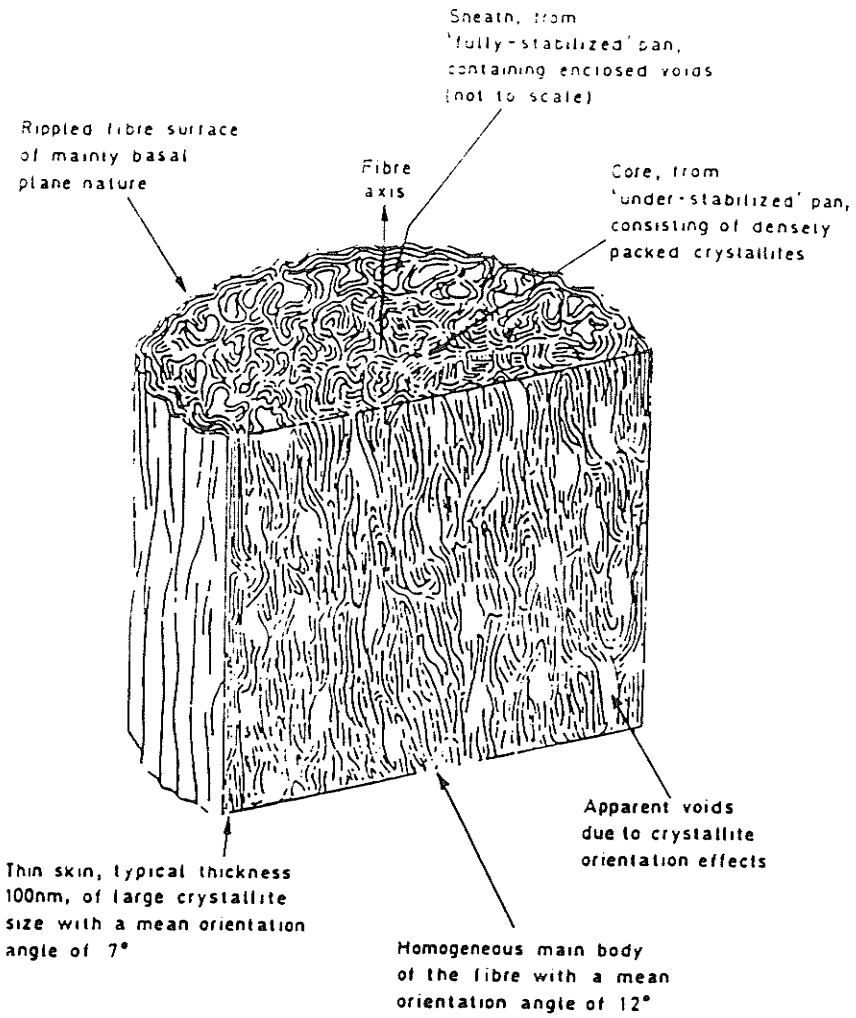

Figure 11: Schematic representation of the three-dimensional structure of a PAN based type I carbon fibre [24].

4.4 Properties of Fibres

The strength and modulus of continuous commercial carbon fibres are much less than single graphite crystals or oriented polycrystalline graphite whiskers although strengths of 450 ksi (3100 MPa) (Hercules AS-4) and moduli as high as 56.5 msi (390 GPa) (Torayca M40 fibres) with a corresponding strength of 2100 MPa are obtainable [23].

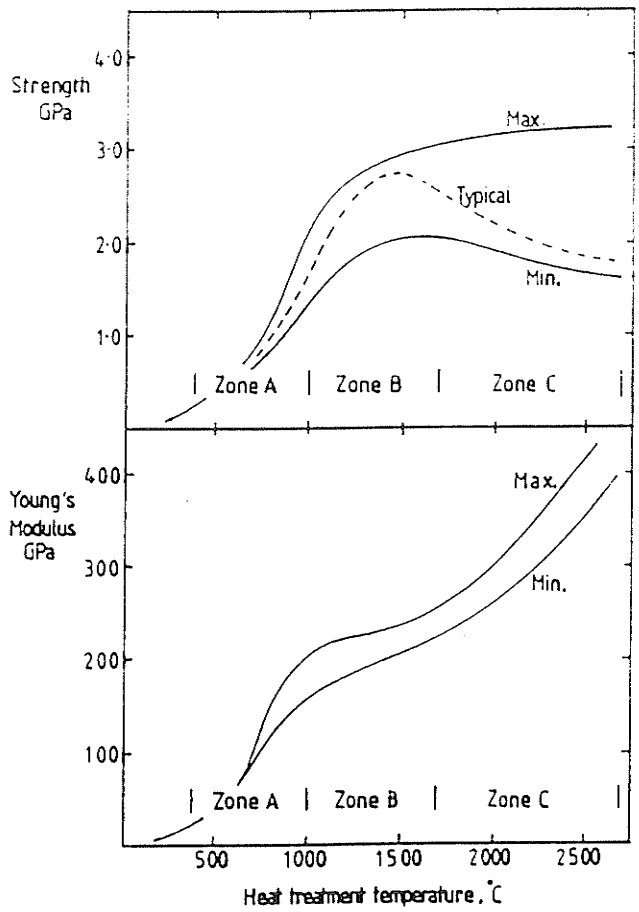

Figure 12: Strength and Young's Modulus versus heat treatment temperature [23].

The stiffness, thermal conductivity, thermal expansion, and electrical conductivity are all influenced by the size of the crystalline units or crystallites and by their misorientation. In carbon fibres made from PAN, this orientation depends upon the fibre heat treatment temperature (HTT) and improves with HTT (see Figure 12). Misorientations of 8 to 20 degrees are typical [24].

Thermal conduction in carbon and graphite is carried out by lattice vibrations and scattering of vibrational waves occurs at imperfections. The thermal conductivity of carbon fibres has been estimated by measuring the thermal conductivity of unidirectional composites and extrapolating the results for 100% fibre reinforcement.

Table 7: Thermal Properties of Various Materials [25].

Material	Linear Expansion Coefficient α $10^6 K^{-1}$	Specific Heat kJ/kg-K	Heat Conductivity W/m-K
Aluminium	22.4	0.897	211
Steel	9.44	0.453	$21 - 54$
Nickel	12.6	0.461	92
Graphite	-1.5	0.708	$70 - 120$
Glass(quartz)	0.5	0.9	1.4
Carbonized CF	$-0.5/-1.0$	0.671	$0.84 - 21$
Graphitized CF	$-1.0/-2.0$	0.671	$84 - 126$

Thermal conductivity ranges between 12 to over 100 Watts per meter per degree C for high modulus fibres (see Table 7).

The thermal expansion of the graphite lattice has been measured from 15 to 1800°C [24]. Turbostratic carbon will behave similarly. Up to about 400°C the dimension parallel to the layer plane was found to contract and above this temperature there is a small expansion. Significant thermal expansion does however occur perpindicular to the layer planes with the average coefficient of thermal expansion being found to be 28.3×10^{-6}. This behaviour is due to the the structural anisotropy of the carbon/graphite structure. Deformation of the crystal structure is much easier perpindicular to the layer planes due to the tight inter-atomic bonding within the layer planes. When the material is heated, the vibrations perpendicular to the layer planes are slower and of greater amplitude than those parallel to the layer planes. The lattice becomes stretched and a Poisson's contraction occurs parallel to the layer planes. Below 400°C this contraction exceeds the thermal expansion parallel to the layer planes, resulting in a negative thermal expansion along the fibre axis. At 400°C, the thermal expansion along the axis balances the Poisson contraction.

The thermal characteristics of carbon fibre and the resin matrix are particularly important when processing carbon fibre composite materials. High internal stresses are introduced due to the differences in the coefficients of expansion. Distortion and cracking may occur for a brittle matrix.

4.5 Processing of Carbon Fibres

Most commercial carbon fibres are made from PAN fibres and the processing must be carried out under very strict control as the integrity of the resulting carbon fibres is sensitive to initial conditions. PAN fibres have the ability to form a heterocyclic ladder polymer when heated to temperatures from 150 to 300 °C. When placed under tension during heating the PAN fibres develop a high degree of preferred orientation with respect to the carbon-carbon chains. Processing involves an initial oxidation stage, carbonization, and high temperature (graphitization) treatments throughout which the C-C orientation is maintained in the axial direction.

Oxidation is the essential PAN stabilization stage which allows the subsequent polymer degradative reactions to proceed without collapse of the fibres or the C-C orientation. During oxidation, some 5-10% of oxygen is taken into the fibre structure while a similar weight loss occurs from the evolution of hydrogen cyanide, water vapour, and other gasses. Fibre densification occures during this stage and there is a self-tensioning interaction relating to polymer orientation. In commercial manufacture the oxidation stage takes 1 to 4 hours.

Carbonization is performed in an inert atmosphere (usually high purity nitrogen) at above 1000°C. The weight of the fibre is reduced 50% with the loss of gasses such

as water , hydrogen cyanide, ammonia, carbon monoxide, carbon dioxide, nitrogen and hydrogen. The fibre contains at least 92% by weight of carbon after carbonization with residual nitrogen being removed progressively in the temperature range of 1000 to 1500 °C (Figure 11). During this process, the fibre changes from a textile fibre of low strength and low modulus with an extensability of 10% to a brittle ceramic fibre with high strength and high modulus with a strain-to-failure of only 1 to 2%. The fibre increases in density from 1400kg/m^3 to 1700kg/m^3. During this stage longitudinal shrinkage takes place as the open organic polymer chains form the tight hexagonal-ring layers of carbon atoms resulting in the typical turbostratic structure of carbon fibres. Processing times during oxidation are on the order of one hour but the fibres spend only a few minutes over 1000°C.

A third processing step may include graphitization in a straight through process in an inert gaseous medium in the temperature range of 1900 to 2500 °C. The changes in this temperature range are in the physical structure of the carbon fibre; micro-crystallites extend in size and preferred orientation of the basal planes is improved. The fibre is changing to a more graphitic structure. Above 1900 °C the fibre can be stretched by the application of tension to improve the basal plane orientation and Young's modulus. The high temperature technology places a high cost on graphitized carbon fibre. As well, lower strain-to-failures result in progressing from carbonized and graphitized fibre with a loss in ultimate strength.

4.6 Surface Treatment and Sizing

Carbon fibres in their dry manufactured state do not bond well into resin matrices. Surface treatment enhances the bonding of the fibres with the resins without detriment to other fibre properties. This is achieved by incorporating oxygenated groups on the surface of the fibre. Methods of treatment vary from gaseous treatments, solution treatments, and electrolytic treatments. The importance of surface treatment in relation to matrix adhesion has been demonstrated for APC-2 [22].

Sizing of the carbon fibre is a protective process to improve the handleability but not the bonding characteristics of the carbon fibre. It involves the application of an epoxy or other resin to the carbon fibre through a solvent. The size content varies from 0.5 to 0.7% by weight.

4.7 Failure Strengths of Fibres

The strength of carbon fibres is largely dependent on the nature of surface flaws. The purity of the processing environment and quality of the processing parameters are critical. Fibre reinforcement consists of bundles of single fibre filaments. The testing of such bundles reveals random rupture of separate filaments with failure occurring in the filaments with a larger number of flaws. Bundle strength depends on the scattering of the strength properties of the fibres [26]. Flaws are in the form of impurities or voids created by particles, by mishandling, or by outgassing of volatiles during processing. The quality of the PAN precursor naturally affects the quality of the carbon fibre.

The matrix resin allows the use of the full strength and stiffness potential of carbon

fibres while reducing their susceptiblity to random brittle fracture. The behaviour of the composite material is radically different from the carbon fibres alone or the matrix alone. This is due to localization of the fibre rupture and subsequent stress transfer by the matrix. The failure of a single fibre does not necessarily weaken the composite as load transfer by a failed fibre can still take place and the matrix can transfer the remaining load to other fibres. It has been shown that when the degree of fibre fracture is 50% for a composite material the strength is equal to that of a fibre bundle where the degree of fracture is 20% [26].

5 Viscoelasticity

5.1 Introduction

In polymeric systems mechanical behaviour is dominated by viscoelastic behaviour. Creep is one facet of viscoelastic behaviour. In a polymer, each flexible threadlike molecule assumes an average volume much greater than atomic dimensions and is continually changing the shape of its contour due to thermal energy. Configuration or contour shapes are characterized by long-range contour relationships and correspondingly more localized relationships involving greater detail which eventually include the orientation of bonds in the chain backbone. These spatial relationships are referred to as *kinks*, *curls*, and *convolutions* (Figure 13) [27,28]. Rearrangements on the

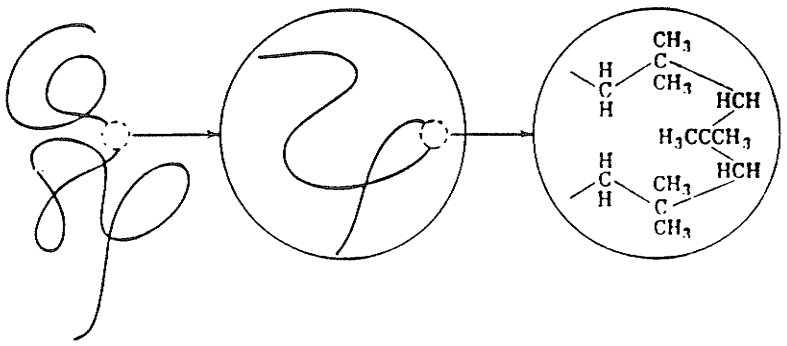

Figure 13: Symbolic representation of long-range contour relationshipes in a flexible polymer molecule (polyisobutylene) [28].

smallest scale are the most rapid. Under stress a new assortment of configurations are obtained and due to the different response times of the molecular arrangements there is a very wide and continuous range of time scale covering the response of such a system to external stress.

Every polymeric system has a glass transition temperature below which the writhing

thermal motions essentially cease. The glass transition temperature (T_g) is evident in a polymer by the reduction in properties of the polymer - typically in the modulus of elasticity. Long range convolutional adjustments are severely restricted below the glass transition temperature. The crystallinity of the polymer also has an infuence on the behaviour of the polymer. There is usually substantial disorder at the surface of the lamellae where the polymer chains are folded and reverse their directions. Two types of motion can then be expected [28]: short range configurational rearrangements and sliding of the lamellae with respect to each other with a frictional resistance related to the local viscosity of the disordered interface layers. When separate crystalline and amorphous phases can be identified, the macroscopic properties can be related to those of the individual phases.

For composite materials, the fibre reinforcement will complicate the nature of the viscoelastic behaviour of the composite material although the resin will play a dominant role in the performance of the composite material, particularly at higher temperatures near or above the glass transition temperature and especially in the transverse direction with respect to the fibre axis. For a unidirectionally reinforced composite material the behaviour of the material in the fibre direction will be fibre dominated and would not necessarily lend itself to the viscoelastic characterization used for an unreinforced thermoplastic polymer. Studies have also shown that the degree of crystallinity of the PEEK matrix in APC-2 influences the viscoelastic behaviour of APC-2 [29]. The processing conditions of APC-2 can affect the degree of crystallinity in the PEEK matrix, with faster cooling rates yielding lower crystallinities. A lower level of crystallinity results in greater mobility of the polymeric

backbone and a stronger ability to creep.

5.2 Viscoelastic Characterization

The viscoelastic behaviour of a material can be characterized by several methods which include constant load creep tests, stress relaxation tests, strain recovery tests, and dynamic mechanical analysis (DMA). Constant load creep testing and DMA are the most widely used tests and each provides insight into particular aspects of viscoelastic behaviour.

A constant load creep test is based on the fact that a viscoelastic material does not maintain a constant deformation with time under a constant load. In a polymeric system, viscoelastic behaviour is time and temperature dependent with temperature effects becoming more significant around the glass transition temperature. The disadvantage of a constant load creep test is the time involved in testing; these tests are time intensive.

A stress relaxation test involves monitoring the stress relaxation in a material under a constant displacement. The degree of stress relaxation will be a function of time and temperature. The material will not maintain a constant stress for a constant deformation but will relax with time. These tests are also time intensive.

A viscoelastic material will store some of its energy as elastic energy and dissipate some of the energy as heat while flowing under a given stress. This is the basis for a strain recovery test and DMA. Removing the load in a strain recovery test will cause the material to recover a portion of its deformation over a period of time. This information can then be used to characterize the viscoelastic behaviour of a material.

In dynamic mechanical analysis, a viscoelastic material is subjected to a sinusoidally oscillating stress or strain. If the material is subjected to a sinusoidally varying stress of constant amplitude then the strain will be neither exactly in phase (as for a perfectly elastic solid) nor 90 degrees out of phase (as for a perfectly viscous liquid) but somewhere in-between. Some of the energy is stored and recovered each cycle and some is dissipated as heat. If both the strain and the strain rate are infinitisimal then linear viscoelastic behaviour occurs and the ratio of stress to strain is a function of time (or frequency) alone and not of the stress magnitude.

For creep relaxation experiments, the stress as a function of time can be expressed as

$$\sigma(t) = \epsilon_o G(t) \tag{1}$$

where G(t) is called the relaxation modulus [27,28]. The relaxation modulus is analogous to Young's modulus in elasticity. For constant load creep tests a similar expression can be defined for strain as a function of time, i.e.,

$$\epsilon(t) = \sigma_o J(t) \tag{2}$$

where J(t) is the creep compliance[27,28]. G(t) and J(t) can be related to one another and have been modelled using spring-dashpot systems. The stress relaxation modulus G(t) and the stress compliance J(t) are usually plotted against log time. These plots of J(t) and G(t) are roughly the mirror image of each other reflected in the time axis. In certain regions G(t) is approximately 1/J(t) and the more slowly J(t) changes with time the more nearly is the reciprocal relation approached.

5.3 DMA

Dynamic mechanical analysis can be used to supplement transient (non-periodic) experiments and provide information corresponding to short transient times. A periodic experiment at a frequency ω is qualitatively equvalent to a transient experiment at a time $t = 1/\omega$. If the viscoelastic behaviour is linear and a sinusoidally varying stress is applied to a viscoelastic material the strain will also alternate sinusoidally but will be out of phase with the stress.

DMA can be performed by limiting the stress to a maximum amplitude ϵ° so that the strain varies as

$$\epsilon(t) = \epsilon^{\circ} sin\omega t \tag{3}$$

while the stress can be written as

$$\sigma(\omega) = \epsilon^{\circ}(G' sin\omega t + G'' cos\omega t) \tag{4}$$

which defines two frequency dependent relations; the storage modulus $G'(\omega)$ and the loss modulus $G''(\omega)$ [27,28]. The storage modulus $G'(\omega)$ is defined as the stress in phase with the strain divided by the strain and is a measure of the energy stored and recovered per cycle. G(t) and $G'(\omega)$ are measures of the stored elastic energy. Logarithmic plots of G(t) and $G'(\omega)$ are approximately mirror images of each other as a dynamic measurement at a frequency ω is qualitatively equivalent to one at $t = 1/\omega$. When G(t) is changing very slowly G(t) is approximately equal to $G'(1/t)$.

The loss modulus $G''(\omega)$ is defined as the stress 90 degrees out of phase with the strain divided by the strain and is a measure of the energy lost as heat per cycle. In frequency regions where $G'(\omega)$ changes slowly (corresponding to very little stress

relaxation in the equivalent plot of G(t)) the behaviour is more nearly perfectly elastic as very little energy is dissipated in periodic deformations. In these regions $G''(\omega)$ tends to be considerably less than $G'(\omega)$.

DMA can also be performed by applying a sinusoidal stress of a maximum amplitude σ^o and an expression similar to Equation 4 can be obtained:

$$\epsilon = \sigma^o(J' sin\omega t + J'' cos\omega t). \tag{5}$$

The storage compliance $J'(\omega)$ is defined as the strain in phase with the stress divided by the stress and is a measure of the the energy stored and released per cycle. $J'(\omega)$ resembles J(t) reflected in the compliance axis.

The loss compliance $J''(\omega)$ is the strain 90 degrees out of phase with the stress divided by the stress and is a measure of the energy dissipated or lost as heat as heat per cycle.

Based on these equations and this analysis, a complex relaxation modulus and complex creep compliance can be defined as follows [27,28];

$$G^* = \sigma^*/\epsilon^* = G' + iG'' \tag{6}$$

$$|G^*| = \sigma^o/\epsilon^o = \sqrt{G'^2 + G''^2} \tag{7}$$

$$J^* = \epsilon^*/\sigma^* = J' - iJ'' \tag{8}$$

$$|J^*| = \epsilon^o/\sigma^o = \sqrt{J'^2 + J''^2} \tag{9}$$

where ϵ^o and σ^o are the maximum stress and strain amplitudes reached per cycle. The complex relaxation modulus is exactly equal to the reciprocal of the creep compliance;

$$G^* = 1/J^*.$$

From these expressions the loss tangent is defined;

$$tan\delta = G''/G' = J''/J'. \tag{10}$$

The loss tangent is a dimensionless parameter and is a ratio of the energy lost and stored in a cyclic deformation. The loss tangent characterizes such physical properties as the damping capacity of a material, the attenuation of propagated waves and the frequency width of a resonance response. It can often be more conveniently measured than any other viscoelastic function but is less susceptible to direct theoretical interpetation than the other functions.

5.4 Effect of Temperature - WLF Equation

The preceding section does not incorporate the influence of temperature on viscoelastic behaviour, which for a polymeric system, is significant. To analyze the temperature dependence by seeking an analytical solution with time and temperature as independent variables would lead to complicated results. The method of reduced variables is used and allows simplification in separating the two principle parameters of time and temperature into a single function which can then be determined experimentally. This is the basis for the William-Landel-Ferry (WLF) equation.

The temperature-time (or frequency) dependence of the viscoelastic properties in the vicinity of the glass transition temperature (T_g) can be described using the WLF equation [27,28];

$$log(a_T) = \frac{-c_1(T - T_o)}{c_2 + T - T_o} \tag{11}$$

where a_T is the shift factor or the degree of horizontal shifting required to superimpose a given set of data points onto the reference data. T_o represents the reference

temperature and is typically taken as T_g. C_1 and C_2 are experimental constants. These constants were found to be 42.87 and 161.10 for a *standard processed* PEEK/ woven carbon fibre composite material [29]. The WLF equation allows data from several temperatures to be shifted to a reference temperature allowing the generation of a master curve for the polymeric system. The viscoelastic data is shifted with respect to time or frequency. The WLF equation generally applies at temperatures near and above T_g but its application may not be appropriate below T_g. The generation of a master curve will permit the prediction of the properties of the material on a frequency or time scale outside easily accessible testing ranges, particularly for DMA. Smooth master curves have been generated for the shear creep compliances of a cross-ply laminate of APC-2 at a reference temperature of 24 °C with testing temperatures ranging from 24 to 107 °C, well below the glass transition temperature [30]. In another investigation, a smooth master curve was not generated when high and low temperature data were shifted and superimposed to the same reference temperature for DMA in flexure in the transverse direction for a unidirectional laminate [31]. The WLF equation must be used with some discretion as its use with composite materials is not necessarily always appropriate.

The WLF equation was appplied to the transverse tests performed in this investigation. These results are shown and discussed in the Discussion. As well, plots of log compliance versus log time for longitudinal and transverse tests are shown and discussed with reference to viscoelasticity.

The processing conditions and the layup of APC-2 composite material influences its viscoelastic behaviour. The processing conditions affect the degree of crystallinity

in the PEEK matrix and this effect is reflected in the flexural storage modulus master curves in Figure 14 [29]. The quicker cooled material has a lower level of crystallinity and this results in a lower storage modulus. The lay-up and fibre orientation will determine the degree to which the properties of the matrix will play a role. In the transverse direction of a unidirectional composite material, the matrix plays a dominant role. In an off-axis lay-up, the matrix may still play a dominant role in determining the viscoelastic behaviour of the material. In these cases, the WLF equation may be used to characterize the viscoelatic behaviour of the material.

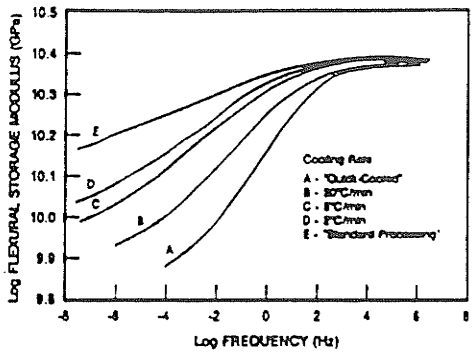

Figure 14: Effect of cooling rate on PEEK composite master curves [29].

6 Procedure

6.1 Background

Constant load creep testing in three point bending was chosen as the method of testing for this research. Tensile creep tests were attempted but fibre pull-out and premature failure (failure at the grips) were problems and were avoided with flexural testing. The material being investigated was unidirectional carbon fibre reinforced PEEK or APC-2 composite material. The material was supplied as fully prepared laminates by ICI (Imperial Chemical Industries). An investigation of the current literature showed that no similar work has been performed and that in general, little creep data is available. Some work has been performed to characterize viscoelastic behaviour in three point bending tests using DMA (Dynamic Mechanical Analysis) [29,31]. Constant load creep testing of cross-ply laminates of APC-2 in tension have been performed [30,32] but there has been no correlation with temperature dependence in the unidirectional direction. The procedures used follow ASTM Standard D790-86 [33] where applicable or follow those cited in similar research studies. ASTM Standard D790 encompasses the Standard Test Methods for Flexural Properties of Unreinforced and Reinforced Plastics and Insulating Materials and is the standard for three and four point bending tests for composite materials.

The three point bend test was chosen over the four point bend test as the test apparatus was simpler to construct for measurement of the maximum deflection at the midspan of the specimen. In a three point bend test the location of the point load coincides with the location of the maximum tensile or compressive stresses and

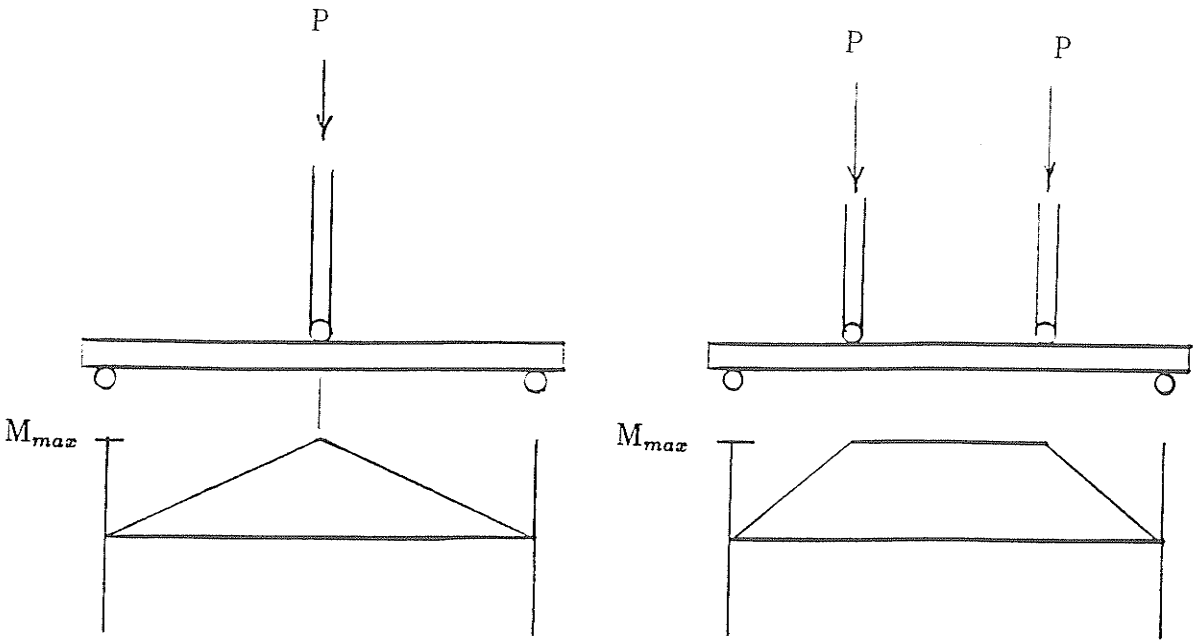

Figure 15: Three Point Bending Versus Four Point Bending.

coincides with the location of the maximum deflection or strain. For a three point bend test the displacement of the loading rod will give the displacement of the specimen (See Figure 15). The disadvantage of the three point bend test is that a severe stress gradient exists within the specimen, both along the length of the specimen and through the thickness of the specimen where the stress reverses from tensile to compressive. This means that only a small fraction of the fibres see the maximum stress and any imperfections or discontinuities in the location of the maximum stress will affect results.

The main advantage of the four point bend test (See Figure 15) is that a more uniform stress gradient exists within the specimen; a uniform stress field exists between the loading points, therefore, a much larger fraction of the fibres are subjected to the maximum stresses. One would therefore expect less scatter in data from four point

bend tests as compared to three point bend tests. The main disadvantage of the four point bend test is that the maximum deflection of the specimen and the location of the loading points do not coincide. A four point bend test requires a more elaborate test setup to measure the maximum deflection at the midpoint of the specimen.

6.2 Sample Preparation

Specimens were prepared from unidirectional laminate plates as supplied by ICI. These plates were approximately 9 by 13 inches and had nominal thicknesses of 0.06 inches. Specimens of 3-3$\frac{1}{4}$ inches by 0.5 inches were prepared from the laminates by shearing. The edges of the specimens were sanded down to 0.5 inches to remove the roughness and any damage which may have occurred due to sample preparation. The test span length was 2.5 inches giving a span-to-depth ratio of 40:1 or greater as recommended by ASTM D790 for highly anisotropic materials. At span-to-depth ratios of less than 40:1 shear deformation can significantly influence modulus measurements. The actual widths of the specimens were measured to within +/- 0.001 inches while the thickness of each sample was measured to within +/- 0.0001 inches. Three samples were tested at each condition, with testing occurring at eight temperatures with three different stress levels applied at each temperature in the unidirectional direction. Tests were run for a minimum of five hours or until failure occurred. A new sample was prepared for each test and conditioned at temperature for thirty minutes prior to testing. Testing concentrated on the behaviour of APC-2 in the fibre direction although some transverse tests were performed.

6.3 Apparatus

The testing apparatus consisted of a laboratory constructed stand and frame onto which a box furnace was attached (See Figure 16). The sample fixture was also made in-house according to ASTM D790. The fixtures were all made to within 0.001 inches. A lever arm using a 3:1 ratio was used to supply the load. A pull rod attached to the lever through the top of the furnace supplied the load to the sample. A DCDT (Direct Current Differential Transformer) attached to the top of the loading frame was used to measure the displacement in terms of voltage and recorded on a Honeywell chart recorder. The voltage was later converted to displacement in inches and used to calculate strain and other data. The recorder was calibrated with the DCDT using a micrometer to +/- 0.001 inches. The calibration did not change over the course of all the tests. An Omega temperature controller kept the temperature of the furnace at a constant level plus or minus one degree Celsius.

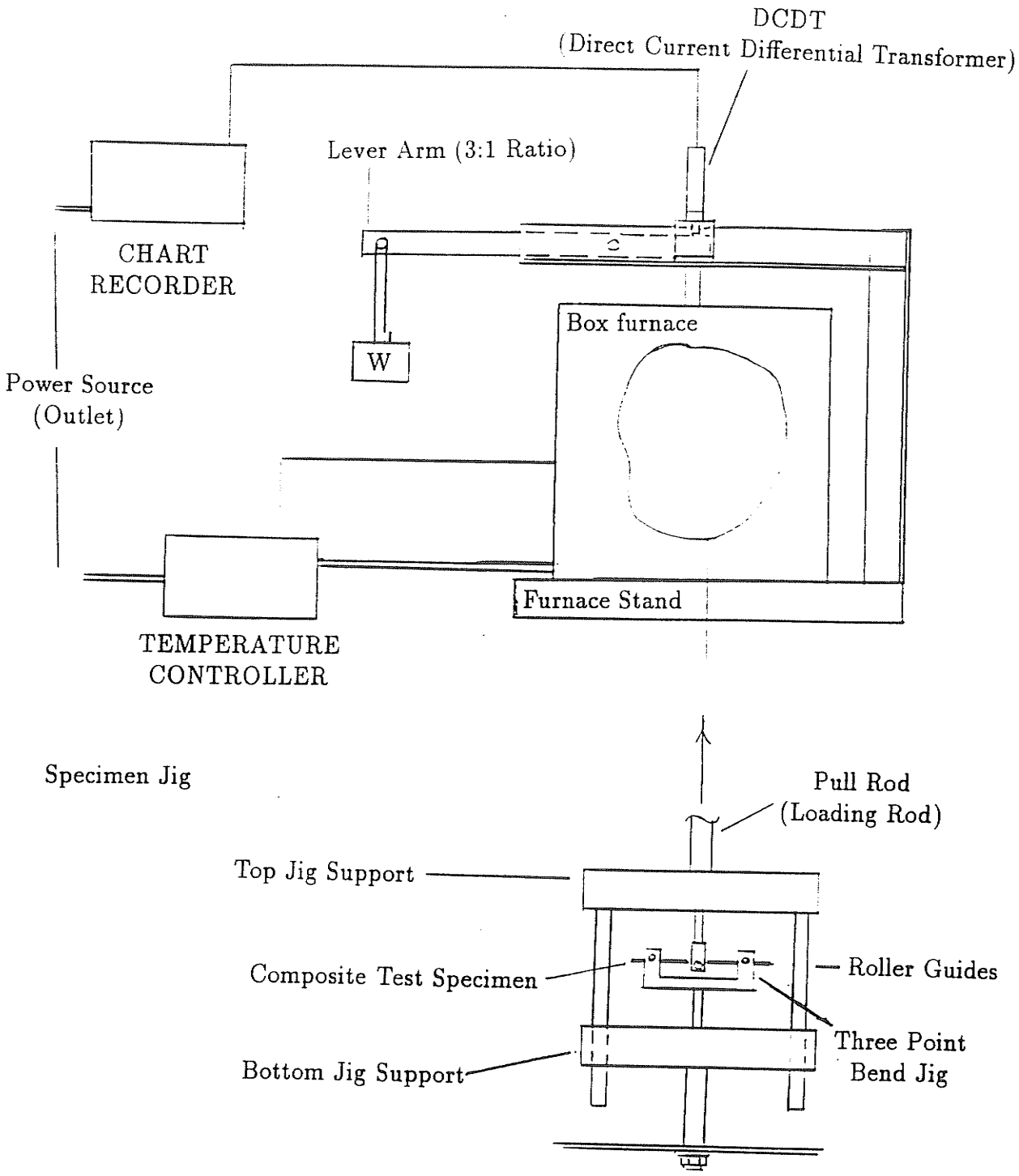

Figure 16: Constant Load Creep Testing Apparatus for Three Point Bending

7 Analysis

The applied stresses were calculated according to ASTM Standard D790. A stress level was chosen and the required load was calculated using the equation

$$P = \frac{2\sigma bd^2}{3L}$$

where b, d, and L are the width, depth and length of the sample. The stress (σ) in the above equation is the maximum tensile or compressive stress in the test specimen. The test was run at a chosen stress but due to the large deflections which occur as a result of the large span-to-depth ratios a stress correction may be applied as follows [33]:

$$\sigma = (3PL/2bd^2)[1 + 6(D/L)^2 - 4(d/L)(D/L)]$$

where D is the deflection of the sample when under load. This equation is usually applied for deflections in excess of 10% of the support span however it was applied to all the data for consistency.

The flexural modulus was calculated by dividing the corrected stress by the initial strain. Shear deformation will cause the flexural modulus to be underestimated so the following shear correction factor is applied if warranted [34]:

$$E_B = \frac{\sigma}{\epsilon}(1 + S)$$

where

$$S = \frac{3d^2 E_x}{2L^2 G_{xz}}$$

and from Table 5, taking a value of 20x10^6 psi for the longitudinal modulus and 0.8x10^6 psi for the in-plane shear modulus, the ratio E_x/G_{xz} gives a value of 25.

The thickness d averages around 0.06 inches giving a correction factor of 1.02 or a correction of 2%. For a thick beam shear deformation can be quite significant. The shear corection factor was not applied for the tests run in this investigation.

The strain was calculated from the equation [33]

$$\epsilon(in/in) = \frac{6Dd}{L^2}.$$

The deflection D is calculated from the calibration of the chart recorder where displacement is recorded in terms of voltage.

The WLF equation is used to generate a master curve by superpositioning the data at one temperature to some reference temperature, usually the glass transition temperature for the plots of log compliance versus log time. Three tests at three different temperatures are required to calculate the constants.

8 Results and Discussion

8.1 Axial Testing

The constant load creep tests performed display certain trends with temperature and stress (see Table 8). The results show that unidirectionally reinforced APC-2 does not creep significantly in the fibre or axial direction in flexure even at stresses at or near the ultimate stress (see Table 9 and Figure 20). The creep strain only makes up about 3% of the total strain observed at 200 °C and at 220 °C although for one test at 220 °C the creep strain was 4% of the total strain after a time of 20,000 seconds (@ 5 hours). Figure 17 and Figure 18 are typical curves (above and below the glass transition temperature) of strain versus time obtained in this investigation. The behaviour above and below T_g for APC-2 in the longitudinal direction is basically identical. Figure 17 and Figure 18 show only a portion of the creep curves; from the initial strain to the final strain. This region is where the creep strain occurs. Figure 19 shows the full curve from which Figure 17 was obtained. Figure 19 illustrates the small amount of creep which occurs in the longitudinal direction. This contrasts quite sharply with the tests performed in the transverse direction (see Figure 27 anf Figure 28). At room temperature the creep strain only makes up about 0.7 to 1.6% of the total strain observed after 20,000 seconds. The total failure strains observed ranged from 2% at room temperature to less than 1% at 200 and 220 °C (see Figure 21).

The applied stress also influenced the creep strain contribution of the total strain. Below 140 °C the higher stresses yield larger creep strain contributions while at 140 °C

Table 8: Unidirectional Testing: Strains

Test	σ ksi	$\epsilon_o(\%)$ in/in	$\epsilon_t(\%)$ $t = 20000s$	$\frac{\epsilon_t - \epsilon_o}{\epsilon_t}$x100	ϵ_{end} (%) in/in	Time of test (s)	$\frac{\epsilon_{end} - \epsilon_o}{\epsilon_{end}}$x100
$20A1$	236	1.67	1.68	0.95	1.69	72000	1.36
$20A2$		1.72	1.74	0.81	1.73	32400	0.23
$20A3$		1.75	1.76	0.23	1.76	61200	0.34
$20B1$	261	1.85	1.87	1.07	1.87	18000	1.07
$20B2$		1.88	1.90	1.00	1.90	52200	1.16
$20B3$		1.87	1.89	0.95	1.89	25200	0.95
$*20C1$	284	2.02			2.05	2580	1.56
$20C2$		1.93	1.96	1.54	1.96	32400	1.54
$20C3$		2.01	2.03	1.23	2.03	43200	1.23
$+100B1$	213	1.66			1.67	5520	0.23
$100B2$		1.66	1.66	0.30	1.66	50400	0.36
$100B3$		1.66	1.66	0.42	1.66	18000	0.42
$*100C1$	226	1.76			1.77	3720	0.23
$100C2$		1.72	1.74	1.09	1.74	81000	1.09
$100C3$		1.75	1.76	0.96	1.76	72000	0.96
$*100A1$	236	1.76	1.79	1.67	1.79	21600	1.67
$*100A2$		1.82			1.82	30	0.11
$*100A3$		1.84			1.86	2760	0.97
$130A1$	161	1.19	1.21	1.57	1.22	259200	2.06
$130A2$		1.30	1.31	0.76	1.31	252000	1.14
$130A3$		1.29	1.31	1.15	1.31	151200	1.45
$130B1$	169	1.37	1.38	0.72	1.39	162000	1.01
$130B2$		1.34	1.36	1.14	1.37	169200	1.51
$*130B3$		1.40			1.42	6240	1.42
$*130C1$	173	1.36			1.39	11040	1.73
$130C2$		1.42	1.44	1.52	1.45	97200	2.00
$130C3$		1.37	1.39	1.58	1.40	75600	1.93
$140A1$	152	1.21	1.22	1.15	1.24	252000	2.81
$140A2$		1.20	1.22	1.23	1.23	237600	2.04
$140A3$		1.33	1.35	2.07	1.36	158400	2.36
$*140B1$	164	1.32			1.33	174	1.13
$*140B2$		1.35			1.37	301	1.53
$140B3$		1.32	1.34	1.86	1.34	144000	1.86
$*140C1$	174	1.42			1.44	3600	1.59
$*140C2$		1.41			1.43	3960	1.534
$*140C3$		1.43			1.44	240	0.69

* - Sample failed.

+ - Test suspended after less than 20,000 seconds.

Table 8: Continued: Unidirectional Testing: Strains.

Test	σ ksi	$\epsilon_o(\%)$ in/in	$\epsilon_t(\%)$ $t = 20000s$	$\frac{\epsilon_t - \epsilon_o}{\epsilon_t}$x100	ϵ_{end} (%) in/in	Time of test (s)	$\frac{\epsilon_{end} - \epsilon_o}{\epsilon_{end}}$x100
$*150A1$	156	1.30			1.33	296	2.62
$*150A2$		1.27			1.29	4320	2.09
$150A3$		1.20	1.23	2.84	1.24	64800	3.16
$150B1$	144	1.12	1.15	2.36	1.15	18000	2.36
$150B2$		1.14	1.17	2.22	1.18	75600	2.64
$*150B3$		1.17			1.19	3840	2.26
$150C1$	133	1.05	1.08	2.56	1.09	64800	2.95
$150C2$		1.05	1.08	2.41	1.08	25200	2.41
$150C3$		1.03	1.05	2.38	1.05	52200	2.66
$175C1$	91	0.76	0.77	1.17	0.78	82800	2.06
$175C2$		0.78	0.79	1.65	0.793	68400	2.27
$175C3$		0.75	0.77	3.10	0.78	79200	3.72
$175B1$	112	0.88	0.92	3.70	0.92	32400	3.81
$175B2$		0.89	0.92	3.15	0.92	32400	3.36
$175B3$		0.92	0.96	3.96	0.96	32400	4.06
$175A1$	124	1.03	1.05	2.66	1.06	50400	2.75
$*175A2$		1.02			1.04	3420	2.12
$*175A3$		1.02			1.05	11580	2.23
$200B1$	89	0.78	0.80	2.26	0.80	55800	2.26
$200B2$		0.74	0.76	2.88	0.76	21600	2.88
$200B3$		0.77	0.79	2.53	0.79	50400	2.78
$*200A1$	102	0.83	0.84	1.79	0.84	4260	2.25
$200A2$		0.87	0.89	2.91	0.90	64800	3.23
$200A3$		0.86	0.89	2.82	0.89	23400	2.82
$*200C1$	112	0.94	0.96	2.30	0.97	230400	3.51
$*200C2$		0.96			0.98	3780	1.74
$*200C3$		0.96			1.00	10260	3.31
$220C1$	81	0.74	0.76	3.27	0.77	64800	3.40
$220C2$		0.70	0.72	2.64	0.72	25200	2.64
$220C3$		0.70	0.72	2.79	0.72	54000	2.79
$220B1$	91	0.81	0.84	4.16	0.84	27000	4.38
$220B2$		0.82	0.84	2.27	0.84	39600	2.39
$220B3$		0.80	0.82	2.93	0.82	79200	3.52
$220A1$	102	0.87	0.89	2.69	0.90	54000	3.01
$*220A2$		0.90			0.92	1140	1.75
$*220A3$		0.90			0.93	7560	2.70

* - sample failed.

Table 9: Failure Data: Longitudinal Tests

Test	Stress(psi)	$\epsilon_{t=0}(\%)$	ϵ_f (%)	TTF (s)	%Creep Contribution
$20C1$	284,000	2.02	2.05	2580	1.59
$100A1$	236,000	1.76	1.79	21600	1.70
$100A2$		1.82	1.82	30	0.11
$100A3$		1.84	1.86	2760	0.98
$100C1$	226,000	1.76	1.77	3720	0.23
$130C1$	173,000	1.36	1.39	11040	1.76
$130B3$	169,000	1.40	1.42	6240	1.55
$140C1$	174,000	1.42	1.44	3600	1.62
$140C2$		1.41	1.43	3960	1.56
$140C3$		1.43	1.44	240	0.70
$140B1$	164,000	1.32	1.33	17	1.14
$140B2$		1.35	1.37	301	1.55
$150A1$	156,000	1.30	1.33	296	2.69
$150A2$		1.27	1.29	4320	2.13
$150B3$	144,000	1.17	1.19	3840	2.32
$175A2$	124,000	1.02	1.04	3420	2.17
$175A3$		1.02	1.05	11580	2.35
$200C1$	112,000	0.94	0.97	230400	3.64
$200C2$		0.96	0.98	3780	1.77
$200C3$		0.96	1.00	10260	3.42
$200A1$	102,000	0.83	0.84	4260	2.30
$220A2$	102,000	0.90	0.92	1140	1.78
$220A3$		0.90	0.93	7560	2.78

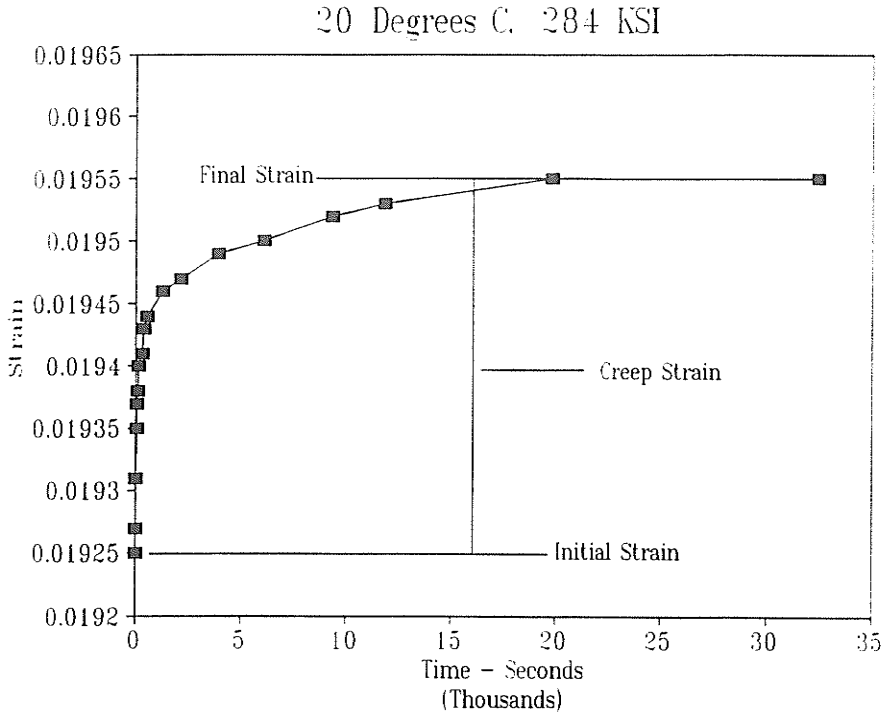

Figure 17: Strain versus Time(s), 20 °C, Longitudinal Testing.

and higher no clear conclusions could be made regarding the influence of stress. This means that APC-2 is not a linear viscoelastic material in the fibre direction below 140 °C. For a linear viscoelastic material creep is independent of stress for incremental strains and incremental strain rates. It is true that tests in the longitudinal direction were run at high stresses. However, typical stress-strain curves for unidirectional carbon fibre composite materials in the fibre direction are linear to failure due to the brittle nature of the carbon fibre reinforcement. Therefore, one would expect the relative percentage of creep to be independent of stress as well.

The plots of the creep strain (incremental strain) versus $\ln(t)$ yield a straight line relationship (see Figures 21 to 44, Appendix). Figure 22 and Figure 23 are typical plots of incremental creep strain versus $\ln(t)$. In general, the slopes (coefficients) of the curves increase with stress and temperature (see Table 12, Appendix A). Three

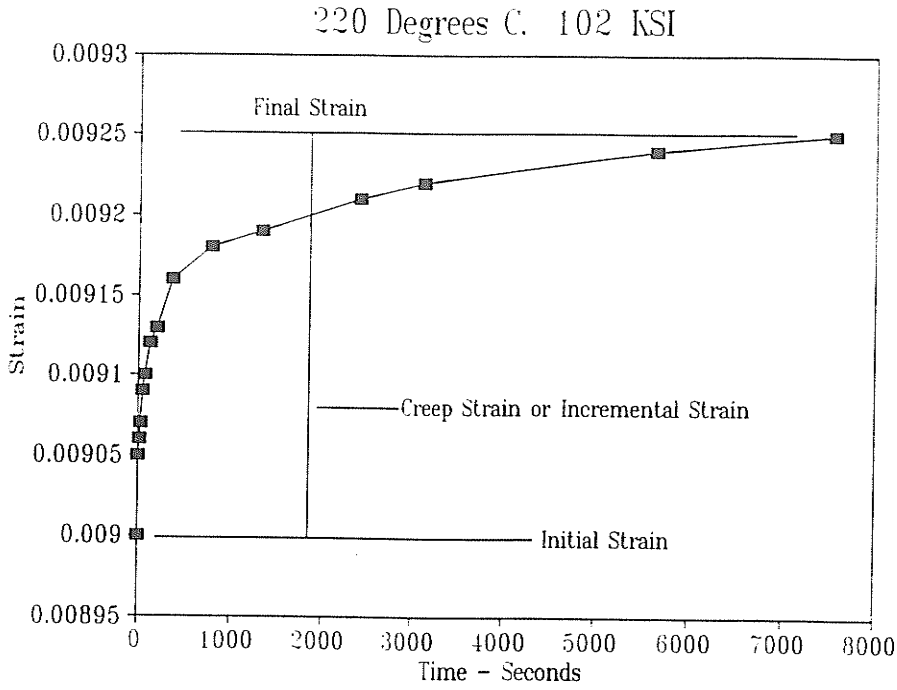

Figure 18: Strain versus Time(s), 220 °C, Longitudinal Testing.

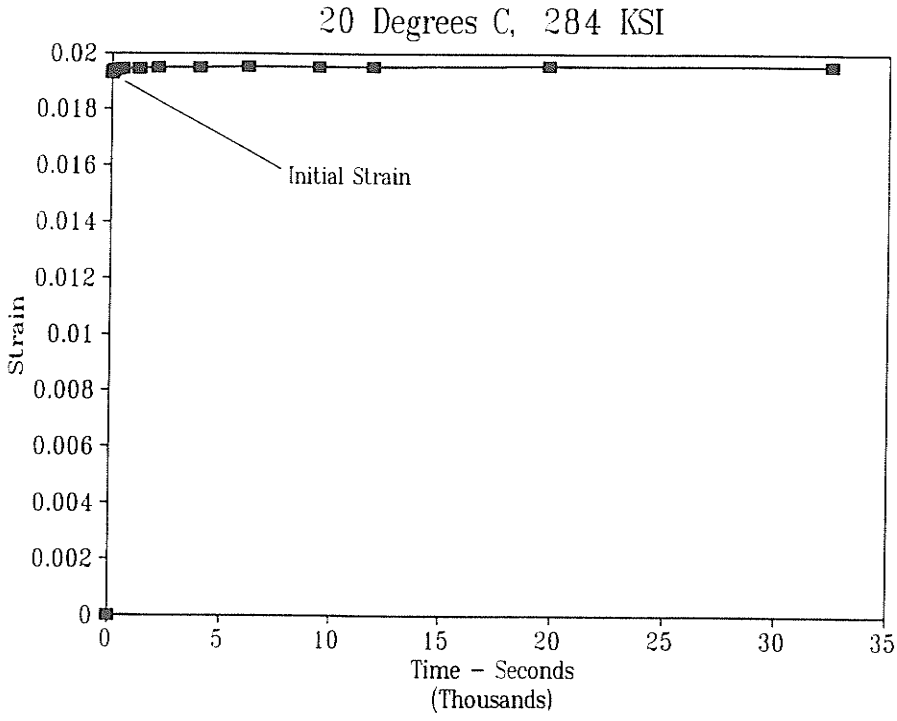

Figure 19: Strain versus Time: Creep Strain versus Total Strain, 20 °C, Longitudinal Testing.

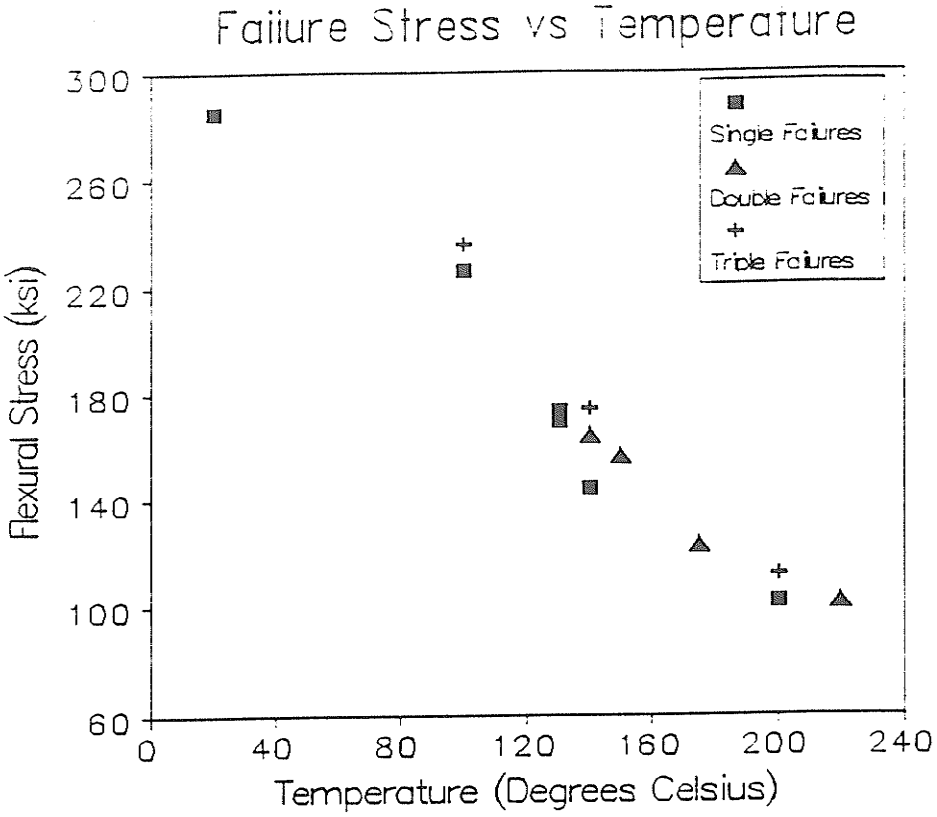

Figure 20: Failure Stress vs Temperature.

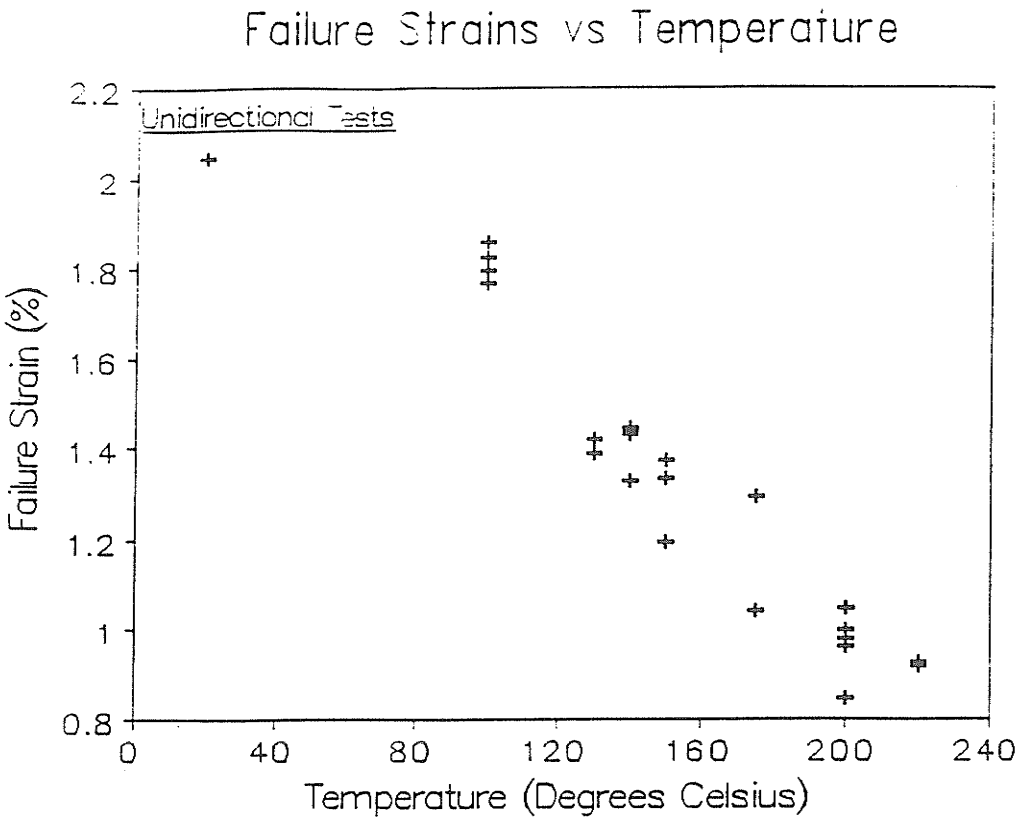

Figure 21: Failure Strains vs Temperature.

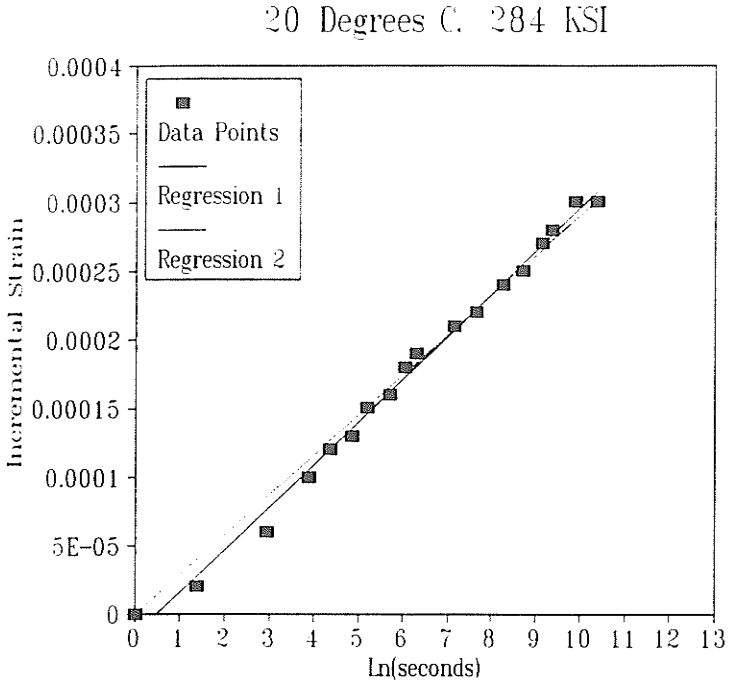

Figure 22: Creep Strain versus Ln(t), 20 °C, Longitudinal Testing.

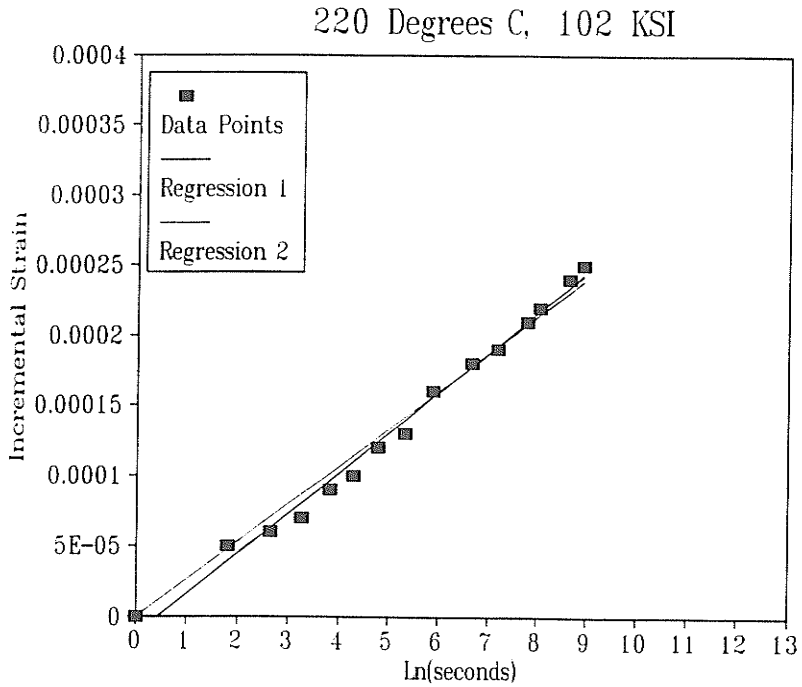

Figure 23: Creep Strain versus Ln(t), 220 °C, Longitudinal Testing.

tests were run at each condition and an average slope or coefficient was calculated for creep strain versus $\ln(t)$. The slopes or coefficients were determined by linear regression by two methods. For the first method the regression curve was calculated by forcing the y-intercept through the origin. The assumption here is that at one second ($\ln(1)=0$) creep strain is essentially zero and that this is known to be a real value. A regression curve was also calculated for which the slope and intercept were calculated. This curve more closely follows the actual data and may give a better indication of the creep rate. Some typical curves are shown for each case for 20 °C and 220 °C. For most of the curves the calculated intercepts are reasonably close to the origin although some variation does occur. A new sample was used for each test as outlined in the Procedure. A comparison of the average coefficient and the median coefficient gives an indication of the behaviour of the material and the range of behaviour with stress and temperature. Trends are visible with higher stresses and temperatures yielding larger coefficients (i.e. greater creep rates). Numerous deviations occur in the results but the trends are still apparent.

Some anomalies can be expected around the glass transition temperature between 140 and 150 °C. The nature of the 3-point bend test allows for the possibility of a larger degree of scatter due to the stress distribution in the specimen. Only a small fraction of the fibres see the maximum stress. The maximum tensile and compressive stresses occur in the extreme or outer fibres at the midspan of the specimen so the distribution of imperfections in a specimen will play a role in the range of behaviour observed. In a tensile specimen a constant stress exists through the cross section for most of the length of the specimen. The distribution of imperfections will therefore

not play as big a role in tensile testing as in flexural testing where the maximum stress and strain occur in a very small area, resulting in a smaller testing region which will not possess the same number of imperfections as in tensile testing. The presence of imperfections (or lack of them) will cloud results and result in flexural strength testing yielding greater values for ultimate strength than tensile testing. It is also for this reason that a test sample of three may not be totally sufficient to represent the true behaviour of the material especially given the subltety of the creep process in unidirectional APC-2. The creep process in APC-2 is not fully understood and the differences between tests are therefore even more difficult to explain.

Although APC-2 does not creep significantly in the fibre direction it is susceptible to creep rupture at stresses below the ultimate failure stress. Creep rupture is simply failure of a sample at a given load and stress after some amount of time has passed upon initial loading and after some creep has occurred. The most dramatic example of this is the failure of a sample after 64 hours at a stress of 112,000 psi and 200 °C (Table 9). The other samples at this stress and temperature failed after 1 and 3 hours respectively. The duration of most of the tests were 6 to 12 hours which means that had these tests run longer some may have eventually failed. For some tests failure will occur for two or three samples at one condition while failure may still occur for one or two samples at the same temperature but at a *lower* stress and usually after a longer period of time.

It is not known if the phenomenon of creep rupture is specific to flexural loading or whether or not unidirectional APC-2 under tension at stresses near the failure stress will behave similarly. This particular aspect of behaviour has not been reported in

the literature reviewed. However the stresses applied in other studies involved much lower stresses. No other investigations have been reported where flexural testing with large loads and with elevated temperatures were performed. The three point bend test is considered to be more of a structural and quality control test as shearing stresses, tensile stresses, and compressive stresses exist within the test specimen. This contrasts with a tension test which is a material test and involves only one constant stress through the length of the gauge section and a Poisson contraction. The 3-point bend test is more realistic of the stresses a structural component could be subjected to and is easier to perform but more difficult to analyze than a tensile test. Due to the nature of the stresses in flexural testing susceptibility to creep and creep rupture may be enhanced. Interlaminar shear stresses exist as the normal longitudinal stress changes from a maximum tensile stress at midspan to a maximum compressive stress at midspan going from top to bottom through the thickness of the beam. Because of this normal stress gradient shear stresses exist between the fibres and the matrix through the thickness of the beam. The effect of temperature on the weakening of the matrix, particularly above the glass transition temperature, is evident by the reduction in the modulus as temperature increases and with the reduction in the stress and strain-to-failure with temperature. The reduction in properties can be attributed to the weakening of the matrix and the inability of the matrix to keep the fibres from sliding with respect to one another. The adhesion of the fibres to the resin may still be very good but shearing of the PEEK resin or matrix occurs. One can assume this is occurring due to the reduction in properties, otherwise, the influence of temperature would not be observed. Once this shearing is allowed to take place complete load

transfer will not occur, resulting in failure and the full strength potential of the fibres will not be reached. The carbon fibres do limit the creep susceptibility of APC-2 but the matrix plays a dominant role in the creep rupture process and in the reduction of the physical properties of the composite material at elevated temperatures.

APC-2 is weaker in compression than in tension which causes the specimens to fail due to fibre buckling and delamination on the compression side of the specimens. All of the specimens which failed displayed features typical of compressive failure in bending. Observation of the fracture surfaces reveal the degree of compressive failure through the cross-section of the specimen. The division in the cross section between the areas where tensile and compressive failure occurs is very distinct. This division appears to occur at the mid-plane of the specimen which failed at room temperature, indicating that the compressive and tensile strengths are approximately equal. With an increase in temperature this division moves closer to the tension side of the specimen indicating a greater degree of compressive failure. At 200 and 220 °C it is apparent that only the very top layer of fibres are failing in tension indicating a substantial loss in compressive strength as compared to tensile strength as temperature increases. This is what is expected as the properties of the matrix are very important in determining the compressive properties of the composite material.

An initial modulus of bending was calculated for each test and an average initial modulus determined for each temperature (see Figure 24). This modulus was determined from the initial deflection just after the load was applied. The modulus was calculated by dividing the calculated stress by the initial strain. There is a wide range in the value of the modulus calculated from the results for the tests run. This

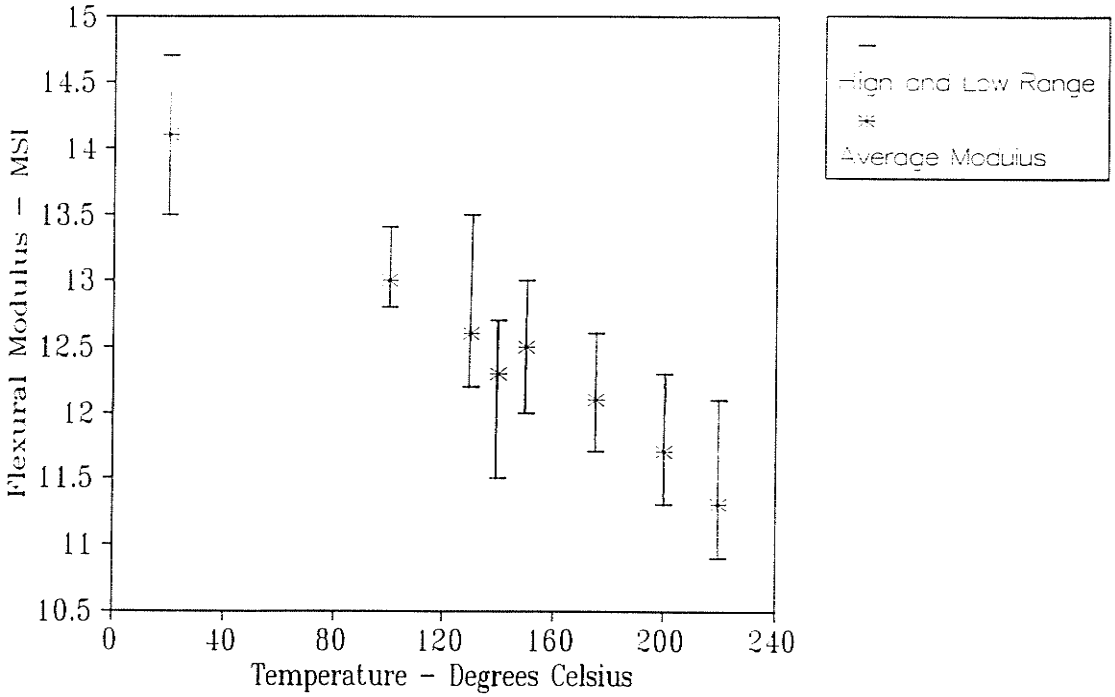

Figure 24: Flexural Modulus vs Temperature (Unidirectional Tests).

variation in the value of the flexural modulus (or Young's Modulus in bending) is due, in part, to the experimental procedure and setup. The purpose of this investigation was to study the creep behaviour of unidirectional APC-2. The tests were not setup to measure the modulus of elasticity with any great accuracy. Accurate determination of the modulus of elasticity would be determined from the stress - strain curve for a strength test for the material in question. The creep tests performed in this investigation were a constant load type test with the full load applied on the order of a few seconds. These types of tests will yield some variation and scatter for these reasons. However, calculation of a modulus and determination of its variation with temperature will help characterize the behaviour of the material. The modulus decreases with temperature although the behaviour near the glass transition temper-

ature (143 °C) transition temperature is slightly erratic. The flexural modulus of $14.1 \text{x} 10^6 lb/in^2$ (14.1 msi) recorded at room temperature is lower than the 19.4 msi cited in the literature [4]. The axial flexural strength (i.e. the strength of a unidirectionally reinforced fibre composite material in the fibre direction in bending) reported in the literature ranges from 301,000 psi [9] to 273,000 psi [4]. This compares with the failure of one sample at a stress of 285,000 psi and indicates reasonable agreement. The stress-strain relationships appear to be linear at the stress levels tested although slight differences exist. For most unidirectionally carbon fibre reinforced composite materials the stress-strain relationships are assumed to be linear until failure, usually given to be 2% strain at room temperature. One sample at 20 °C had a failure strain of just over 2%.

8.2 Compliance Results - Longitudinal Tests

An attempt was made to generate a master curve for the longitudinal creep tests using the William-Landel-Ferry equation. Due to the nature of the curves and the magnitude difference between the compliances at different temperatures generation of a master curve using the WLF equation was not possible. The WLF equation was developed for viscoelastic characterization of polymers and polymeric systems. The use of the WLF equation is not appropriate for viscoelastic characterization of unidirectionally reinforced APC-2 in the fibre direction. The PEEK matrix does have an influence on the behaviour of the material but the fibre reinforcement limits the creep strain even at elevated temperatures. This lack of creep results in little change in compliance, making the generation of a master curve impossible.

Plots of Log Compliance(S_{11}) vs. Log Time(s) for the unidirectional tests yield a straight line (see Figure 25). In general, compliance is independent of the stress although there is variance from test to test. There is a change in slope of the log compliance curves with temperature with higher slopes observed with higher temperatures (Table 10) with a dramatic change at the glass transition temperature. There

Table 10: Slopes of Log Compliance vs. Log t curves: Average Values

Temperature	Average Slope
20	0.00115
100	0.00079
130	0.00156
140	0.00197
150	0.00307
175	0.00286
200	0.00300
220	0.00310

is little change in the slope above T_g although the compliance still increases with temperature. Due to the nature of these curves and the small amount of creep in unidirectional APC-2, the application of the WLF equation is not appropriate and it is not possible to generate a master curve. The matrix does play a role in the lower strains-to-failure observed with an increase in temperature and in the creep rupture process however the carbon fibre reinforcement does not allow modelling in creep as for a cross-ply or transverse laminate. The change in compliance is too little for such modelling.

In the plots of Log(S_{11}) vs. Log(t) the curves shown are from regression analysis of the data. The linear regression plots are coincident with the actual data plots of Log Compliance vs Log(t) due to the very slight variation of compliance with time. For

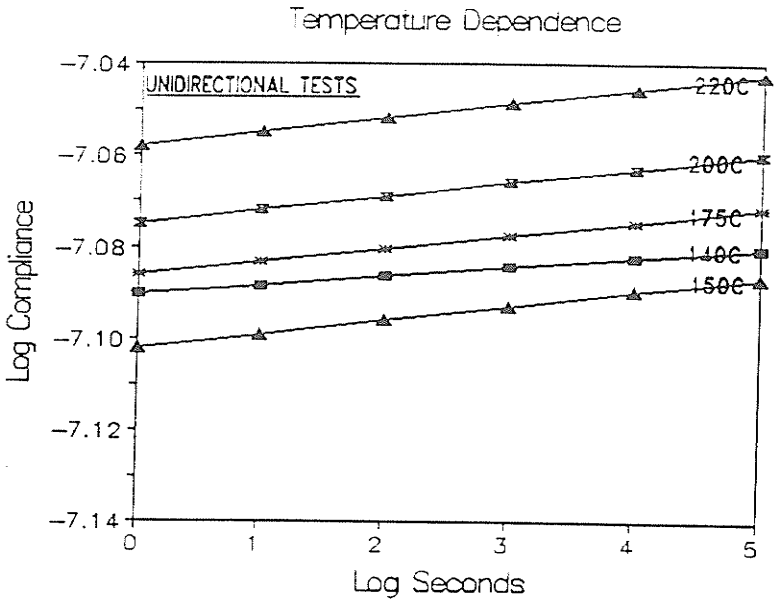

(a)

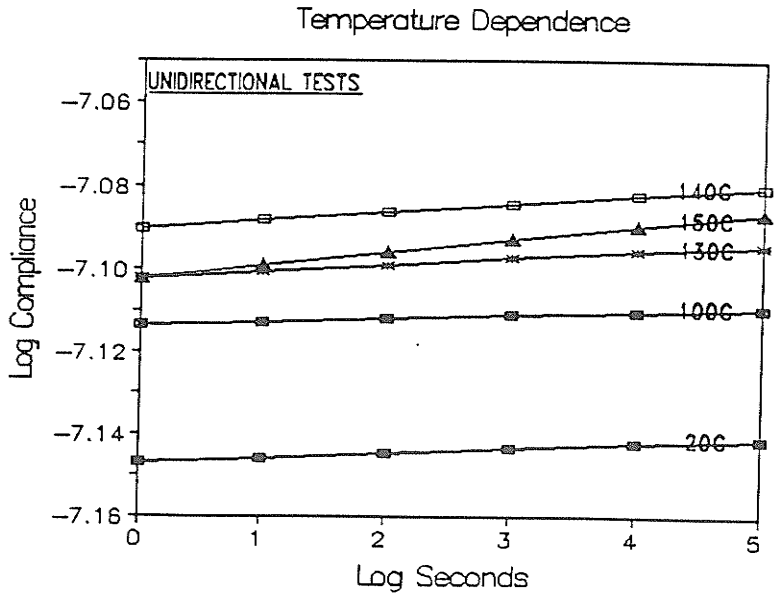

(b)

Figure 25: (a) and (b): Log Compliance(S_{11}) vs Log Time(s) for the unidirectional tests in three point bending

comparative and analytical purposes it is more convenient to present the regression curves.

8.3 Larson-Miller Parameter

Unidirectionally reinforced APC-2 does not follow the behaviour predicted by the William-Landel-Ferry equation in the fibre direction. APC-2 composite material is not dominated by viscoelastic behaviour when stressed in the fibre direction. The behaviour of APC-2 is fibre dominated parallel to the direction of the fibres. The creep behaviour may be better characterized by parameter test methods as used for metals and alloys. One such parameter is the Larson-Miller parameter [35], L-M, given by

$$L - M = R[log(tr) + C] \tag{1}$$

where R is the temperature in degrees Rankine, tr is the rupture time in hours and C is a constant which is about 20 for many metals. It is noted that the Larson-Miller parameter is highly unit dependent.

The Larson-Miller parameter for the present fracture results (Table 11) is plotted in Figure 26 where a value of 20 was assigned to the constant, C. The value of the constant can be determined experimentally but there was insufficient data available to do so in the present investigation. The determination of long term creep behaviour from short term creep tests performed is somewhat precarious. However the results do show promise for the Larson-Miller parameter as a method to predict the behaviour of APC-2 for creep and creep rupture. There is considerable scatter in the data but the greatest variation occurs under conditions of high stress at temperatures well below

Table 11: Fracture Data for APC-2 Unidirectional Composite Material Used for Larson-Miller Parameter.

Specimen	Stress (psi)	Temp (K)	Temp (R)	Failure Time(h)	Failure Strain(%)	L-M Parameter ($x10^{-4}$)
$20C1$	284,000	293	528	0.72	2.05	1.0
$100C1$	226,000	373	672	1.03	1.77	1.3
$100A1$	236,000	373	672	6.00	1.79	1.4
$100A2$	236,000	373	672	0.01	1.82	1.2
$100A3$	236,000	373	672	0.77	1.86	1.3
$130B3$	169,000	403	726	1.73	1.42	1.5
$130C1$	173,000	403	726	3.07	1.39	1.5
$140B1$	164,000	413	744	0.05	1.33	1.4
$140B2$	164,000	413	744	0.08	1.37	1.4
$140C1$	174,000	413	744	1.00	1.44	1.5
$140C2$	174,000	413	744	1.10	1.43	1.5
$150A1$	156,000	423	762	0.08	1.33	1.4
$150A2$	156,000	423	762	1.20	1.29	1.5
$150B3$	144,000	423	762	1.07	1.19	1.5
$175A2$	124,000	448	807	0.95	1.04	1.6
$175A3$	124,000	448	807	3.22	1.05	1.7
$200A1$	102,000	473	852	1.18	0.84	1.7
$200C1$	112,000	473	852	64.0	0.97	1.9
$200C2$	112,000	473	852	1.05	0.98	1.7
$200C3$	112,000	473	852	2.85	1.00	1.7
$220A2$	102,000	493	888	0.32	0.92	1.7
$220A3$	102,000	493	888	2.10	0.93	1.8

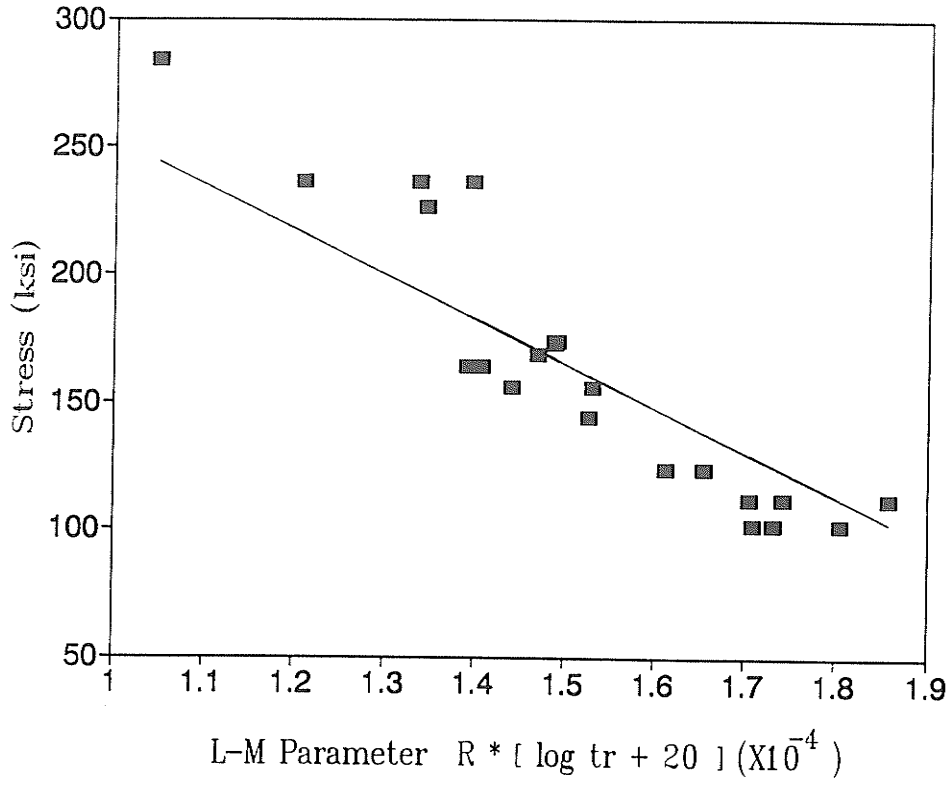

Figure 26: Larson-Miller Plot for PEEK-Carbon Fibre Composite Material(APC-2) Unidirectionally Reinforced in the Fibre Direction.

the glass transition temperature of 143 °C. One of the assumptions in the derivation of the Larson-Miller parameter is that failure strain is constant.

The results in Table 11 illustrate the problem in designing for high temperature-high stress applications of PEEK-Carbon fibre composite material. Creep failure occurs suddenly after very small creep deformations of only 0.01% to 0.04% and is, therefore, quite insidious in nature since imminent failure is difficult to detect.

8.4 Transverse Testing

Typical strain versus time curves are shown in Figure 27 and Figure 28. The tests in the transverse direction displayed much more creep as the strain versus time plots show as compared to the tests in the longitudinal direction. Figure 27 and Figure 28

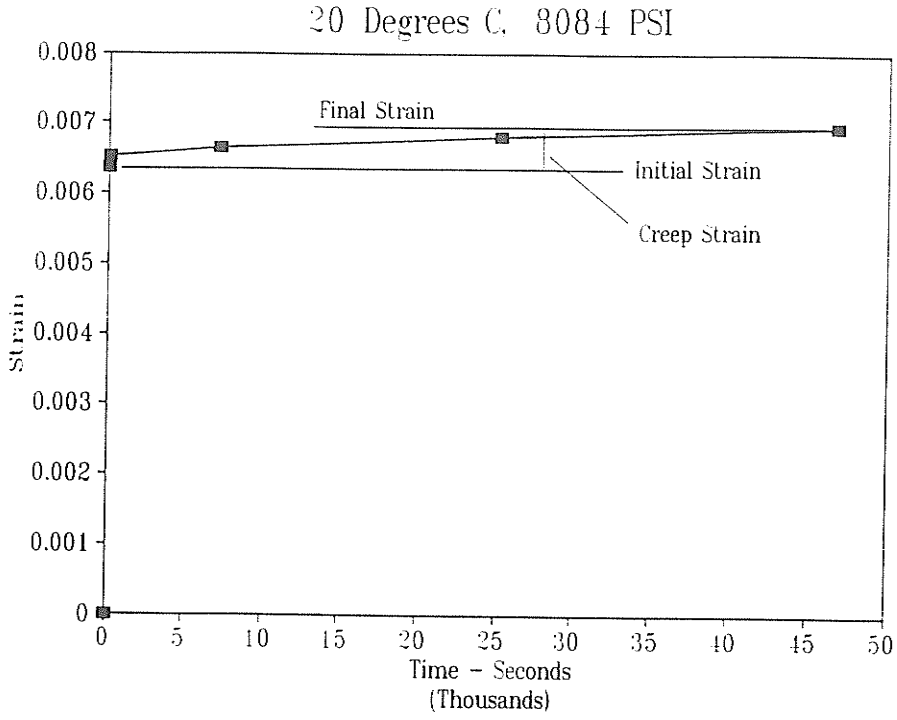

Figure 27: Strain versus Time(s), 20 °C, Transverse Testing.

show the influence of the PEEK resin on the behaviour of APC-2 in the transverse direction. Typical curves for creep strain versus $\ln(t)$ are shown in Figure 29 and Figure 30. The plots for all the temperatures tested are shown in the appendix. The slopes of the plots of incremental strain or creep strain versus $\ln(t)$ increase dramatically at 140 °C (near the glass transition temperature) and then remain static or increase very slightly. This phenomenon would suggest that creep rate in the transverse direction increases with temperature and experiences a 'quantum' leap at the glass transition temperature. The slopes of the incremental strain versus $\mathrm{Ln}(t)$ plots are shown in Table 12 and are plotted in Figure 31. These slopes were obtained using linear regression. Two methods were used; one where the intercept was made equal to zero and forced through the origin and one where the intercept was calculated. Both are shown for comparison and yield similar results. These

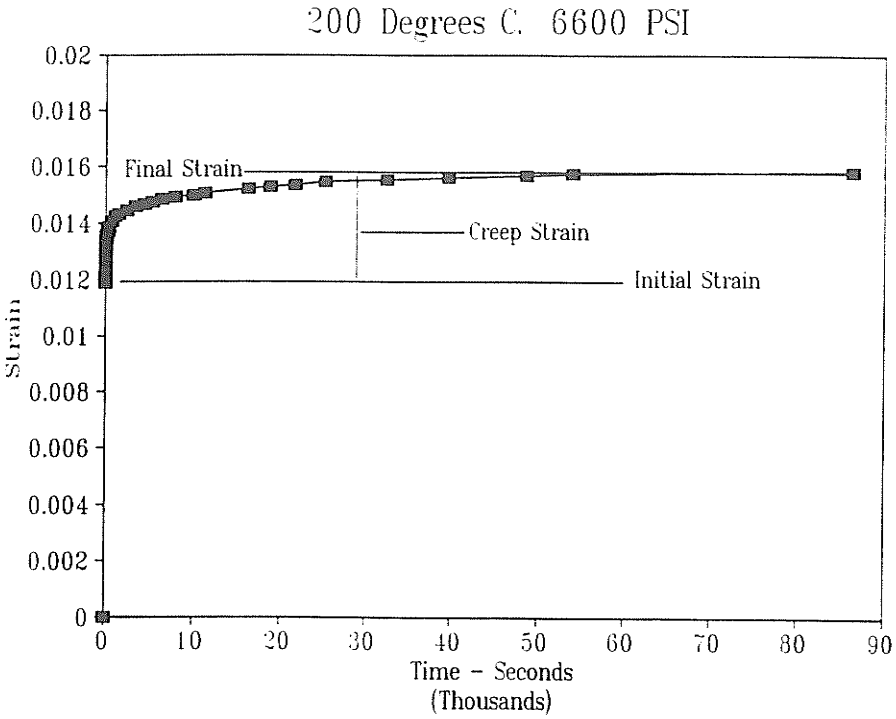

Figure 28: Strain versus Time(s), 200 °C, Transverse Testing.

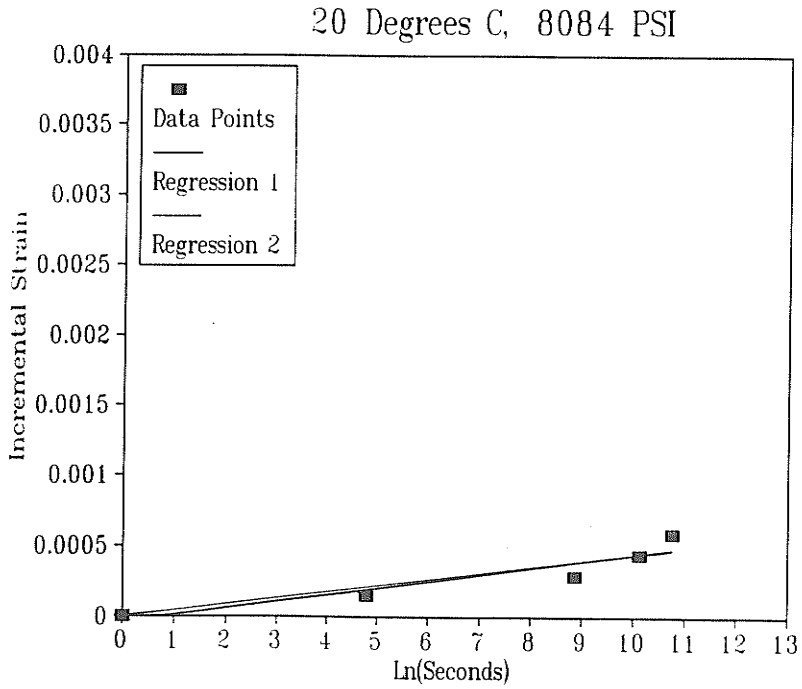

Figure 29: Creep Strain versus LN(t), 20 °C, Transverse Testing.

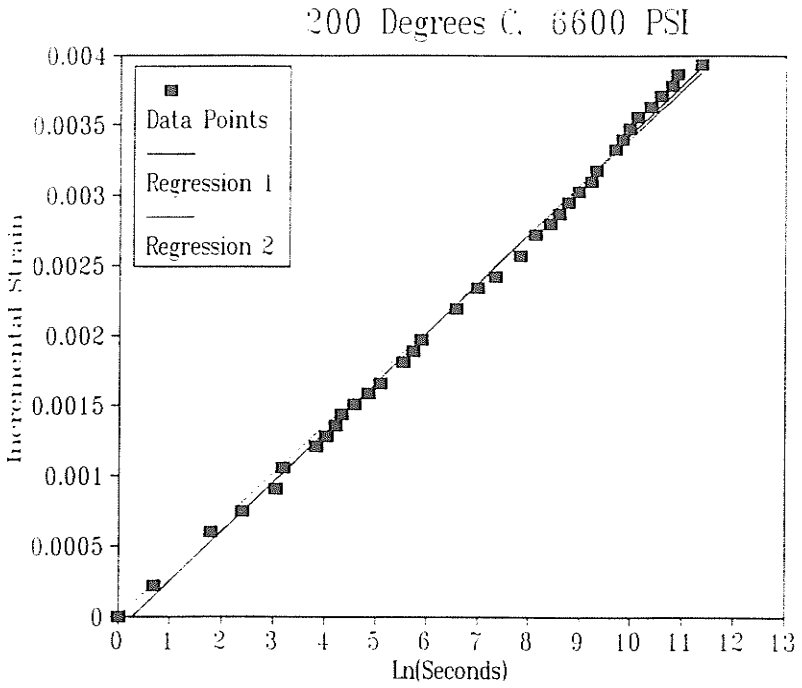

Figure 30: Creep Strain versus LN(t), 200 °C, Transverse Testing.

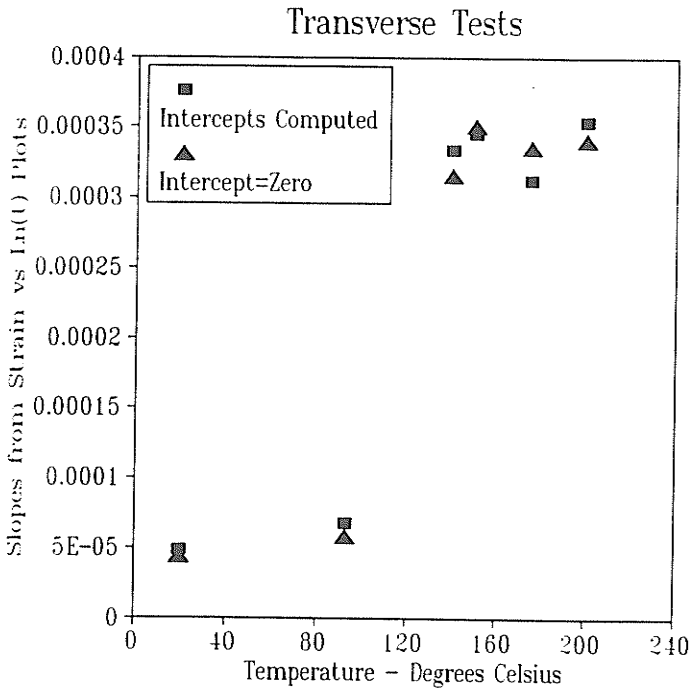

Figure 31: Strain/LN(t) versus Temperature (°C).

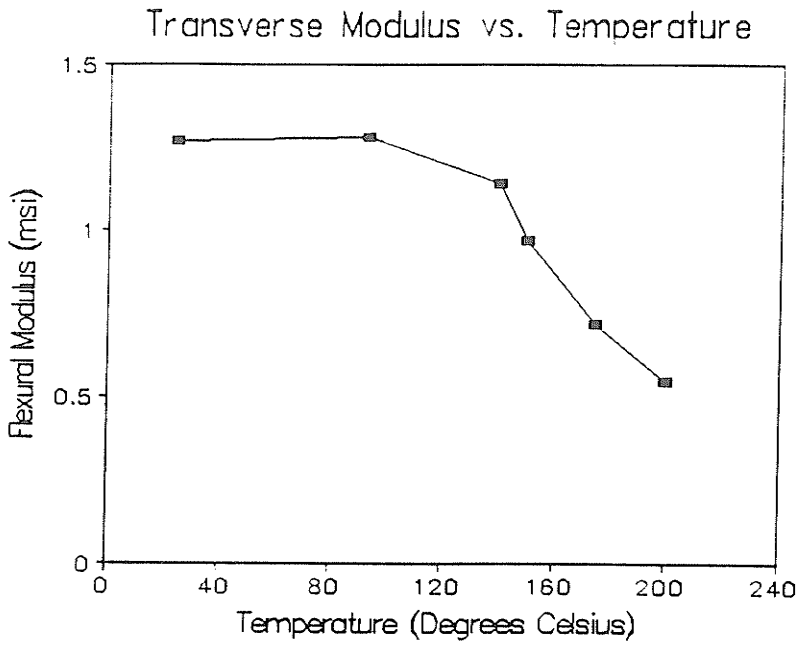

Figure 32: Transverse Modulus versus Temperature (°C).

tests were much more difficult to run due to the lower modulus in the transverse direction and the correspondingly larger deflections which resulted. Creep strain is much more significant in the transverse direction especially above the glass transition temperature. The creep strains in the transverse direction are about ten times higher than those measured at a similar initial strain for the longitudinal tests. At the higher temperatures it is difficult to measure an initial modulus as there is not a sudden change in slope upon application of the load, rather, a smooth and continuous displacement curve is generated.

The plot of transverse modulus versus temperature in Figure 32 behaves as expected with little change in modulus from room temperature to 93 °C. At 140 °C (i.e. at the glass transition temperature) and higher there is a marked decrease in

modulus as expected. This behaviour is typical and illustrates the behaviour of the PEEK matrix.

The contribution of the creep strain to the total strain is quite significant and greatly increases with temperature. At room temperature the creep strain makes up 6.0% of the total strain after 20,000 seconds (@ 5 hours) and 8.5% after 50,000 seconds (@ 14 hours). At and above 140 °C the contribution of the creep strain to the total strain ranges from 20 to 30% after a time of 20,000 seconds (see Table 13). This is much larger than before. In contrast to the specimens tested in the fibre direction, the specimens tested in the transverse direction were permanently distorted with very little strain recovery occurring.

8.5 Compliance - Transverse Tests

Plots of Log Transverse Compliance(S_{22}) versus Log(t) are non-linear and the curves appear as though they would conform to a master curve using the William-Landel-Ferry equation (See Figure 33). The range of values in compliances for the different tests have some overlap making generation of a master curve possible. An attempt was made to generate a master curve at a reference temperature of room temperature and at 93 °C and although a smooth curve could be generated the calculated constants greatly overestimated the shift factors at the higher temperatures. Using 140 °C as a reference temperature and using the data from the 150 °C and 175°C tests, the WLF constants were calculated to be -30 and 140 for C_1 and C_2. The shift factor for the 200 °C test was calculated to be 9.0 while the experimental value was found to be 9.5 indicating close correspondence. to the WLF equation. This

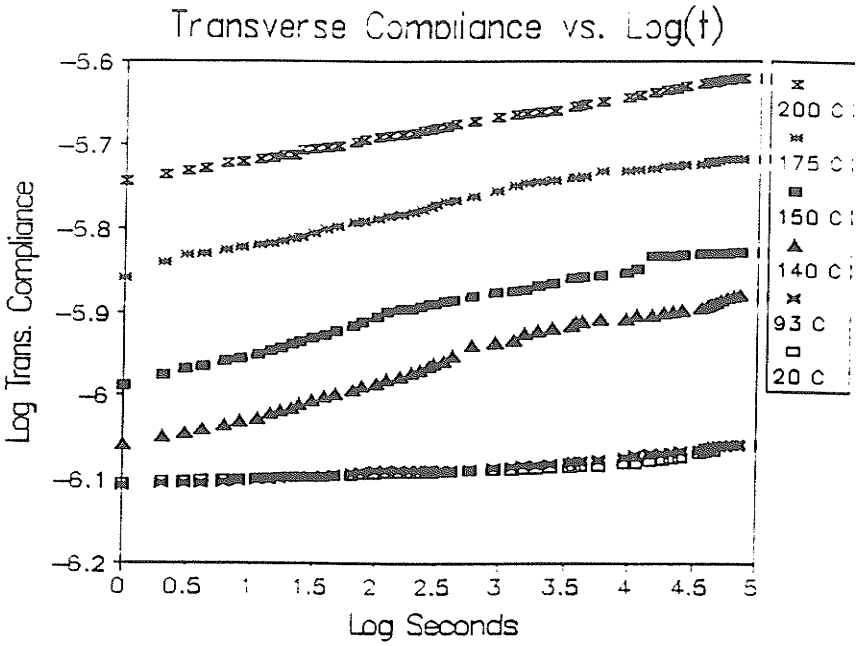

Figure 33: Log Transverse Compliance(S_{22}) versus Temperature(°C).

correspondence to the WLF equation is due to the dominance of the properties of the PEEK matrix in the transverse direction. This does not hold true for APC-2 tested in the longitudinal direction as discussed. Although more data could be obtained at higher temperatures for the transverse tests this aspect of the behaviour of APC-2 has been well characterized (see Figure 34).

Table 12: Regression Coefficients from Incremental Strain versus Ln(seconds) Plots, Transverse Testing.

Temperature (°C)	Stress (psi)	Regression (x10^5) Intercept Calculated	Regression (x10^5) Intercept=Zero
20	8100	4.84	4.40
93	8000	6.74	5.87
140	8100	33.4	31.6
150	8100	34.5	35.1
175	6500	31.2	33.6
200	6600	35.4	34.1

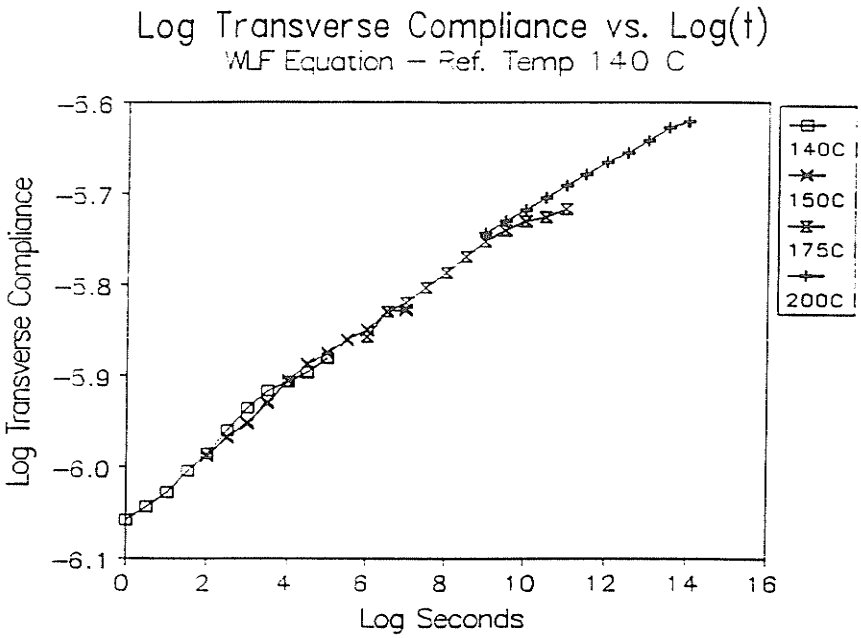

Figure 34: Master curve for transverse unidirectional APC-2, Log Transverse Compliance versus Temperature, WLF equation).

Table 13: Transverse Tests: Creep Strain Contribution

T (^oC)	Stress (psi)	$\epsilon_o(\%)$	$\epsilon_t(\%)$ $t = 20,000s$	$\frac{\epsilon_{creep}}{\epsilon_t}$x100 (%)	$\epsilon_t(\%)$ $t = 50,000s$	$\frac{\epsilon_{creep}}{\epsilon_t}$x100 (%)
20	8100	0.64	0.68	6.1	0.70	8.5
93	8000	0.62	0.68	8.8	0.70	10.5
140	8100	0.71	1.01	30.5	1.05	32.9
150	8100	0.84	1.20	30.2	1.21	30.7
175	6500	0.91	1.23	26.5	1.25	27.6
200	6600	1.19	1.53	22.4	1.57	24.2

9 Conclusions

9.1 Summary of Results

Constant load creep tests in three point bending of unidirectional APC-2 were performed at test temperatures ranging from room temperature to 220 ^{0}C. In the longitudinal direction the creep strain is almost negligible, even at 220 °C, and the integrity of APC-2 in the fibre direction is good in that little creep occurs. However, for large stresses (below the ultimate stress) failure can occur after creeping has occurred from anywhere from a few minutes to a few days at all the temperatures tested. The integrity of APC-2 in the fibre direction is questionable when considering the nature of the failures which occurred in this investigation. This form of failure (creep rupture) is insidious as it occurs without a large amount of creep first occurring.

The Larson-Miller Parameter shows some promise as a tool for use in the design of APC-2 in high stress-high temperature applications.

The tests performed in the transverse direction show a close correspondence to the WLF equation due to the dominance of the matrix properties in the transverse direction. The WLF constants C_1 and C_2 were found to be -30 and 140 respectively. Creep in the longitudinal direction is controlled by the properties of the carbon fibres although the matrix plays an important role in the failure process. The use of the WLF equation to predict the behaviour of APC-2 in the longitudinal direction is not appropriate.

9.2 Recommendations

Recommendations for further testing to answer some of the questions posed by the results of this investigation include the following:

1) Perform constant-load tensile creep tests in the longitudinal fibre direction at temperatures above and below the glass transition temperature to determine if the phenomenon of creep failure is specific to flexural loading. Transverse tests would aid in determining the role of the matrix.

2) Perform strength tests in three point bending and tension in conjunction with constant load creep tests. This would allow the susceptibility to creep failure to be determined by calculating the creep rupture stress as a percentage of ultimate strength (in tension and flexure). This data would be very valuable to design engineers.

3) Perform more constant load creep tests (flexural and tensile) over a wider stress range (at a given temperature) to determine whether or not there is a stress limit in constant load creep testing below which failure will not occur after a significant period of time, similar to the fatigue stress limit for some materials.

4) Investigate the use of the Larson-Miller parameter method as a method to predict long term creep behaviour. This would entail performing long term creep tests over a range of temperatures.

Further testing as outlined would allow a design envelope to be developed for APC-2 and would allow the material's behaviour to be determined in high stress and high temperature applications. The work in this thesis has been one of the steps in this process.

References

[1] A.C. Duthie. *Engineering Substantiation of Fibre Reinforced Thermoplastics for Aerospace Primary Structure.* 33rd International SAMPE Symposium. March 1988.

[2] G.R. Griffiths, W.D. Hillier, J.A.S. Whiting. *Thermoplastic Composite Manufacturing for a Flight Standard Tailplane.* Ibid.

[3] J.T. Hartness. *Polyetheretherketone Matrix Composites.* Sampe Quarterly, January 1983.

[4] W.I. Lee et al. *Effects of Cooling Rate on the Crystallinity and Mechanical Properties of Thermoplastic Composites.* Proceedings of The American Society for Composites, 1st Technical Conference, 1986, pp 119-128.

[5] N.J. Johnston and P.M. Hergenrother. *High Performance Thermoplastics: A Review of Neat Resin and Composite Properties.* 32nd International SAMPE Symposium, April 1987.

[6] Peggy Cebe et al. *Mechanical Properties and Morphology of Poly(etheretherketone).* ASTM STP 937, American Society for Testing and Materials, Philadelphia, 1987, pp 342-357.

[7] G.R. Belbin et al. *Carbon Fibre Reinforced Polyether Etherketone: A Thermoplastic for Aerospace Applications.* 2nd Intercontinental SAMPE Conference, Stresa, Italy, June 1982.

[8] ICI Literature.

[9] D.C. Leach, F.N. Cogswell. E. Nield. *High Temperature Performance of Thermoplastic Aromatic Polymer Composites.* 31st International Sampe Symposium, 1986.

[10] F.N. Cogswell and M. Hopprich. *Environmental resistance of Carbon Fiber - Reinforced Polyetheretherketone.* Composites, Symposium on Environmental Effects on Fibre - Reinforced Plastics, July 1983, pp251-253.

[11] Tsuneo Sasuga et al. *Electron Beam Irradiation Effects on Mechanical Properties of PEEK/CF Composite.* Journal of Material Science, 24(1989), pp1570-1574.

[12] G.F. Sykes et al. *Assessment of Space Environment Induced Microdamage in Toughened Composite Materials.* 18th International SAMPE Technical Conference, October 1986.

[13] G.T. Spamer and N.O. Brink. *Investigation of the Compression Strength After Impact Properties fo Carbon/PPS and Carbon/APC-2 Thermoplastic Materials.* 33rd International SAMPE Symposium, March 1988.

[14] D.J. Blundell and N.J. Osborn. *Crystalline Morphology of the Matrix of PEEK - Carbon Fiber Aromatic Polymer Composites: II. Crystallization Behaviour.* SAMPE Quarterly, Vol. 17. No. 1, October 1985.

[15] S.Mall, G.E. Law, M. Katouzian. *Loading Rate Effect on Interlaminar Fracture Toughness of a Thermoplastic Composite.* Journal of Composite Materials. Vol. 21. June 1987.

[16] R.M. Turner and F.N. Cogswell. *The Effect of Fibre Characteristics on the Morphology and Performance of Semi-Crystalline Thermoplastic Composites.* Sampe Journal, Jan/Feb 1987.

[17] D. Evans et al. *The Physical Properties of Carbon Fibre Reinforced PEEK Composites at Low Temperatures.* Proceedings of the 7th International Cryogenic Materials Conference, Advances in Cryogenic Engineering, V. 34, Plenum Publ. Corp., New York, NY, pp25-33.

[18] J.T. Hartness and R.Y. Kim. *A Comparative Study on Fatigue Behaviour of Polyetheretherketone and Epoxy with Reinforced Graphite Cloth.* 28th National SAMPE Symposium, April 1983.

[19] J Maxwell. *Novel Thermoplastic Composites in High Performance Components.* Int J of Vehicle Design, Technolgical Advances in Vehicle Design Series, SP6, Designing with Plastics and Advanced Plastic Composites, pp34-40.

[20] D.J. Blundell et al. *Spherulitic Morphology of the Matrix of Thermoplastic PEEK/Carbon Fibre Aromatic Polymer Composites.* Journal of Materials Science, 24(1989), pp. 2057-2064.

[21] P.J. Hine et al. *Failure Mechanisms in Continuous Fibre Reinforced PEEK.* Sixth International Conference on Composite Materials and ECCM2, Second European Conference on Composite Materials., Elsevier Applied Science, London, 1987, pp. 3.397-3.404.

[22] B. Fife, J.A. Peacock, C.Y. Barlow. *The Role of Fibre-Matrix Adhesion in Continuous Carbon Fibre Reinforced Thermoplastic Composites: A Microstructural Study.* Ibid, pp 5.439-5.447.

[23] D.J. Thorne. *Manufacture of Carbon Fibre from PAN.* Chapter XII, Handbook of Composites, Volume 1, Strong Fibres, Edited by W. Watt and B.V. Perov, 1985, Elsevier Science Publishers.

[24] W. Johnson. *The Structure of PAN Based Carbon Fibres and Relationship to Physical Properties.* Chapter X, Ibid.

[25] A.A. Konkin. *Properties of Carbon Fibres and Fields of Their Application.* Chapter VII, Ibid.

[26] A.M. Skudra. *Micromechanics of Failure of Reinforced Plastics*. Chapter I. Handbook of Composites. Volume 3. Failure Mechanics of Composites. Edited by G.C. Sih and A.M. Skudra. 1985. Elsevier Science Publishers.

[27] John D. Ferry. *Viscoelastic Properties of Polymers*. 2nd Edition. John Wiley and Sons.

[28] John D. Ferry. *Viscoelastic Properties of Polymers*. 3rd Edition. John Wiley and Sons. 1980.

[29] P.S. Gill and William Sichina. *Characterization of Composites Using Dynamic Mechanical Analysis*. 33rd International SAMPE Symposium, March 1988.

[30] R.Y. Kim and J.T. Hartness. *Time-Dependent Response of AS-4/PEEK Composite*. 19th International SAMPE Technical Conference. October 1987.

[31] Richard P. Lockwood. *Viscoelastic Behaviour of Polyetheretherketone (PEEK) Composite*. Masters Thesis. Air Force Institute of Technology, Wright-patterson Air Force Base, December, 1987.

[32] A. Horoschenkoff et al. *Creep Behaviour of Carbon Fibre Reinforced Polyetheretherketone and Epoxy resin*. New Generation Materials and Processes, edited by Franco Saporiti et al, Grafiche F.B.M., Milano 1988.

[33] ASTM D790-86. Annual Book of ASTM Standards, Vol. 08.01, pp.280-289, 1988.

[34] J.M. Whitney, I.M. Daniel, R.B. Pipes. *Experimental Mechanics of Fiber Reinforced Composite Materials*. Published by The Society for Experimental Stress Analysis, Monograph No. 4, Prentice-Hall, 1982.

[35] George E. Dieter. Mechanical Metallurgy, 2nd Edition, pp.485, 1976.

Appendix

Table 14, Regression Slopes or Coefficients of Plots of Incremental Strain vs. Ln(t)

Figures 35 to 52, Creep Strain vs. Ln Time

Table 14: Regression slopes or coefficents of plots of incremental strain vs ln(t).

Test	Slope ($x10^5$)		Slope ($x10^5$)		Slope ($x10^5$)	
20°C	Stress=236 ksi		Stress=261ksi		Stress=284ksi	
	S1	S2	S1	S2	S1	S2
	1.89	1.66	2.14	2.11	4.31	4.28
	1.42	1.17	2.13	1.71	3.11	2.90
	0.47	0.46	1.87	1.65	2.25	2.48
AVG	1.10	1.26	2.05	1.82	3.22	3.22
100°C	Stress=213ksi		Stress=226ksi		Stress=237ksi	
	S1	S2	S1	S2	S1	S2
	0.58	0.60	0.43	0.46	3.18	2.33
	0.56	0.48	2.39	1.62	NA	NA
	0.70	0.74	1.86	1.66	2.25	2.27
AVG	0.61	0.74	1.56	1.24	2.72	2.30
130°C	Stress=161 ksi		Stress=169ksi		Stress=173ksi	
	S1	S2	S1	S2	S1	S2
	2.66	1.51	1.30	0.93	2.27	1.51
	1.54	1.06	2.23	1.45	2.89	2.08
	1.79	1.35	1.91	1.53	2.53	2.07
AVG	2.00	1.31	1.81	1.39	2.56	1.89
140°C	Stress=152ksi		Stress=164ksi		Stress=174ksi	
	S1	S2	S1	S2	S1	S2
	3.38	1.91	NA	NA	3.24	2.33
	2.27	1.51	1.15	1.12	2.86	2.45
	3.22	2.33	2.51	1.86	1.90	1.73
AVG	2.96	1.92	1.83	1.49	2.67	2.17
150°C	Stress=133 ksi		Stress=144ksi		Stress=156ksi	
	S1	S2	S1	S2	S1	S2
	3.19	2.58	3.03	2.62	4.20	3.41
	2.95	2.22	3.20	2.47	3.53	3.39
	3.19	2.37	3.59	3.19	4.31	3.11
AVG	3.11	2.39	3.27	2.76	4.01	3.30
175°C	Stress=91 ksi		Stress=112ksi		Stress=124ksi	
	S1	S2	S1	S2	S1	S2
	1.34	1.05	3.80	3.11	2.95	2.75
	1.56	1.16	3.09	2.95	2.66	2.54
	2.65	2.51	3.99	3.50	2.63	2.10
AVG	1.85	1.57	3.63	3.19	2.75	2.46
200°C	Stress=89 ksi		Stress=102ksi		Stress=112ksi	
	S1	S2	S1	S2	S1	S2
	1.86	1.65	2.54	2.19	2.82	2.16
	2.48	2.13	2.81	2.39	2.21	1.85
	2.24	1.82	2.73	2.37	3.80	3.13
AVG	2.19	1.86	2.69	2.32	2.94	2.38
220°C	Stress=82 ksi		Stress=91ksi		Stress=102ksi	
	S1	S2	S1	S2	S1	S2
	2.56	2.13	3.88	3.14	2.73	2.36
	2.05	1.80	1.77	1.80	2.02	2.01
	2.12	1.92	2.66	2.28	2.86	2.67
AVG	2.24	1.96	2.77	2.41	2.54	2.35

S1=Regression Slope, Intercept Calculated
S2=Regression Slope, Intercept=0

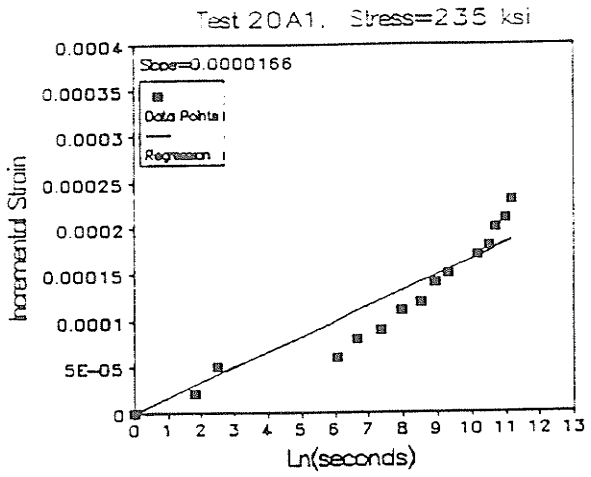

(a)

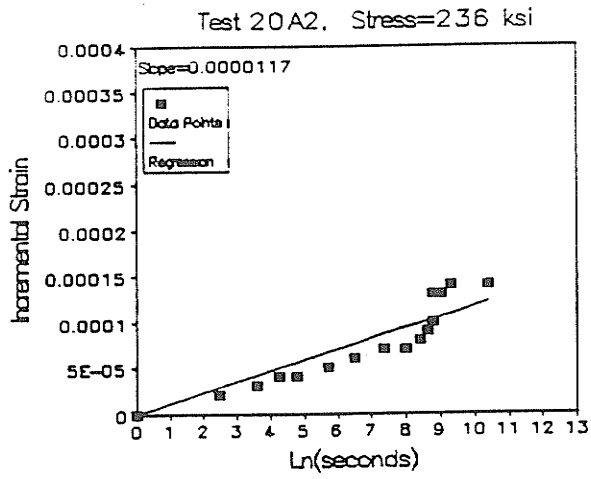

(b)

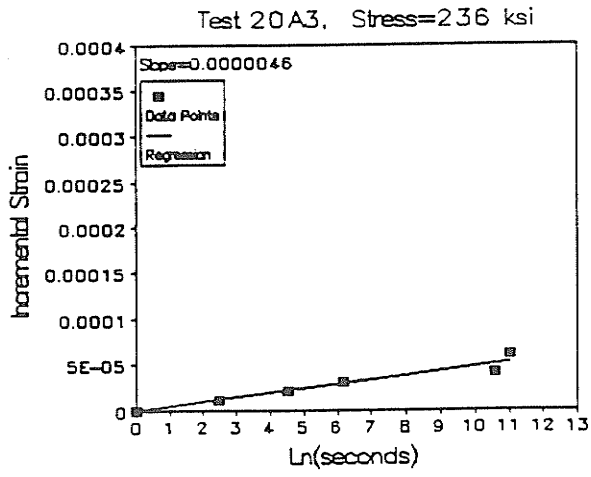

(c)

Figure 35: Incremental Strain vs Ln(time), Longitudinal Direction

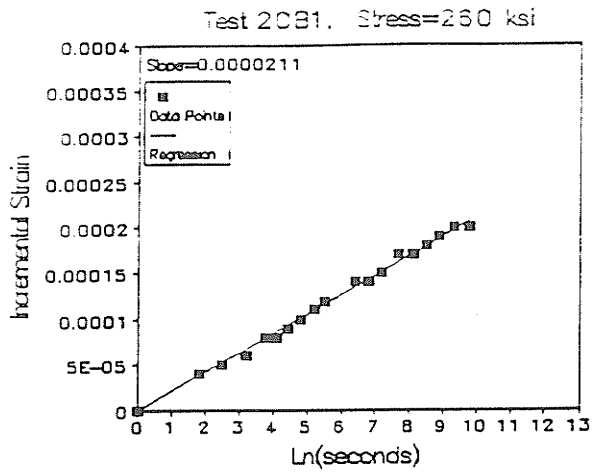

(a)

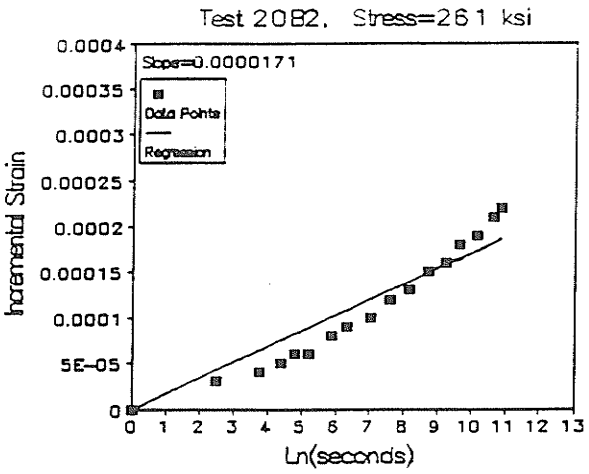

(b)

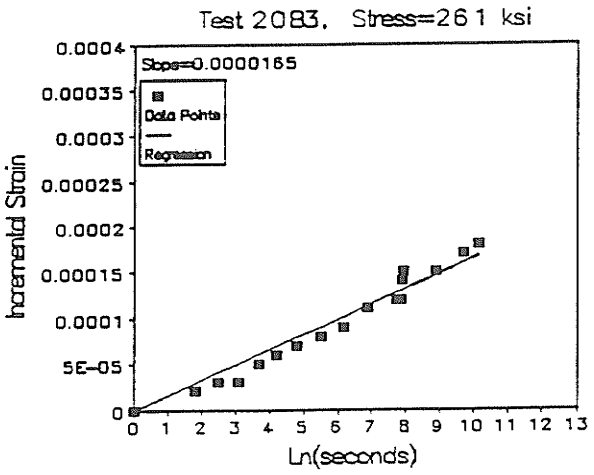

(c)

Figure 36: Incremental Strain vs Ln(time), Longitudinal Direction

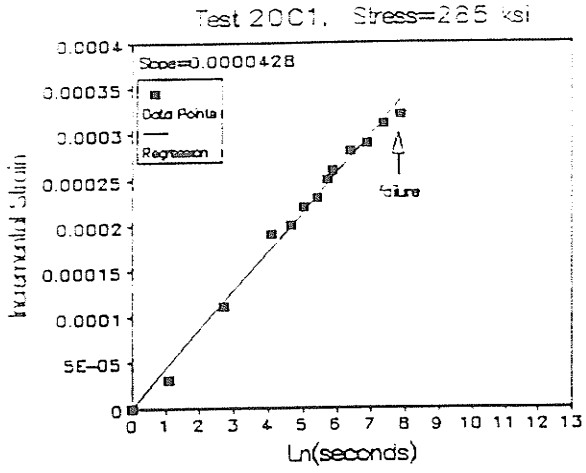

(a)

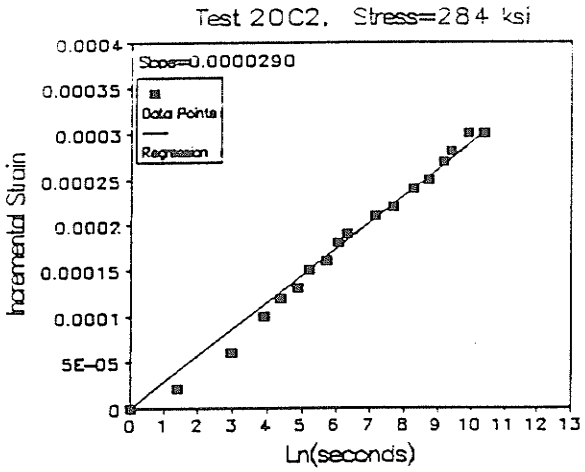

(b)

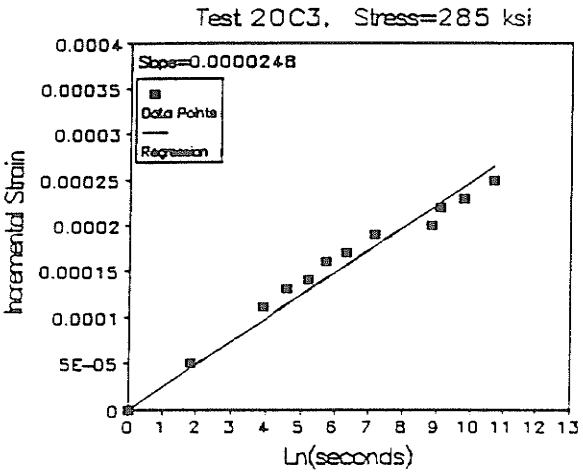

(c)

Figure 37: Incremental Strain vs Ln(time). Longitudinal Direction

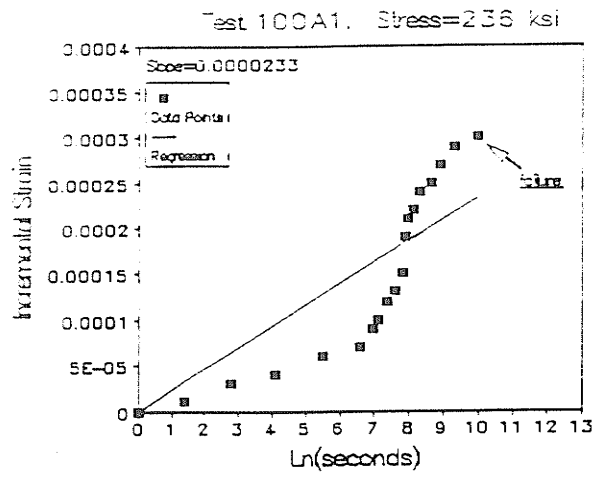

(a)

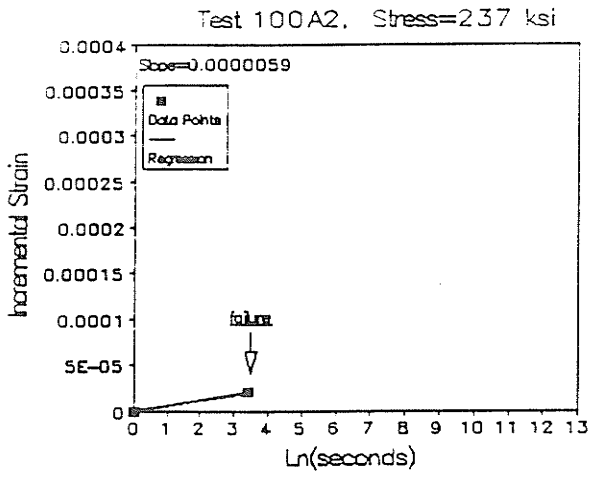

(b)

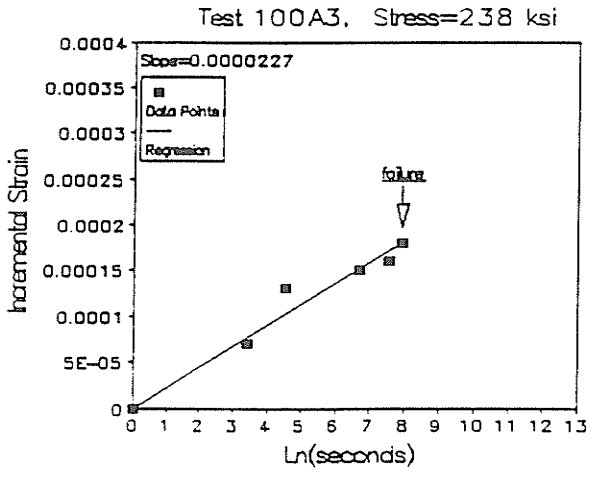

(c)

Figure 38: Incremental Strain vs Ln(time), Longitudinal Direction

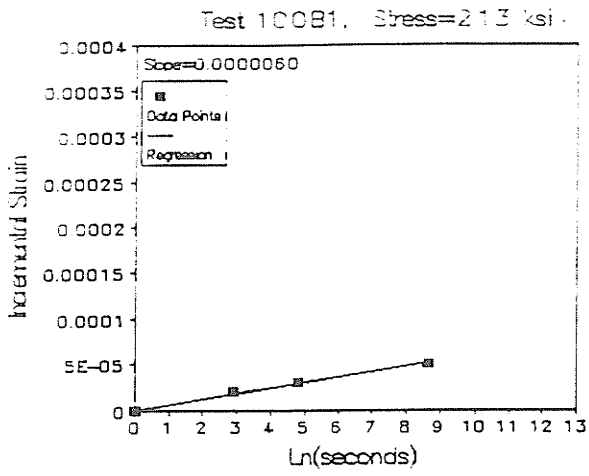

(a)

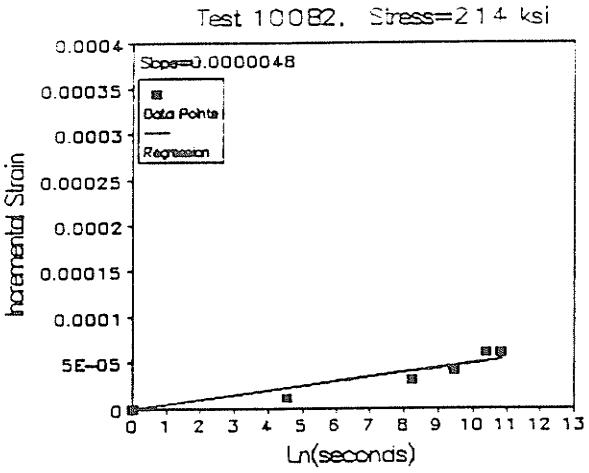

(b)

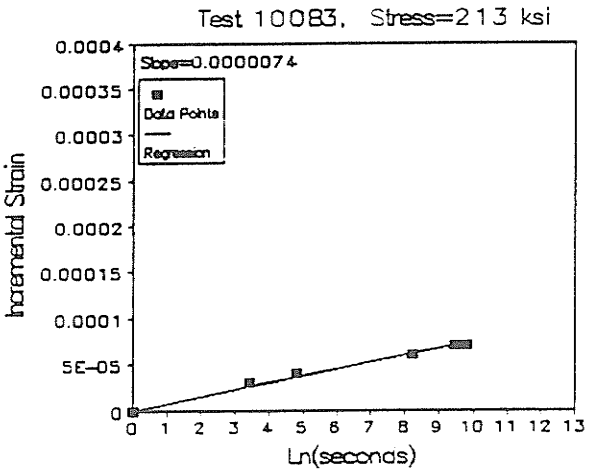

(c)

Figure 39: Incremental Strain vs Ln(time), Longitudinal Direction

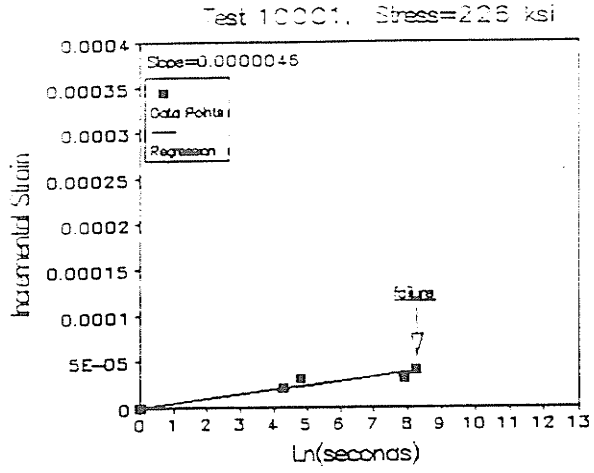

(a)

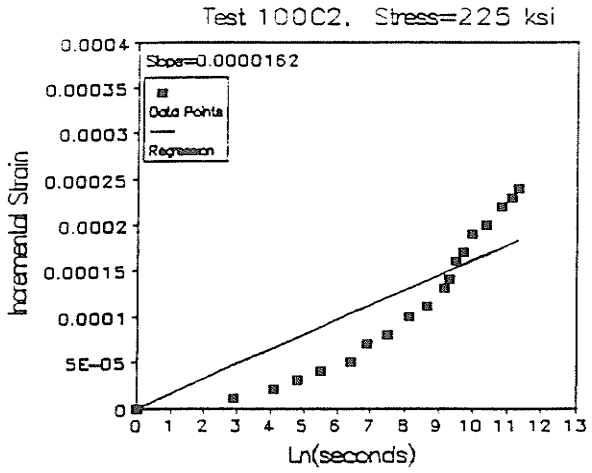

(b)

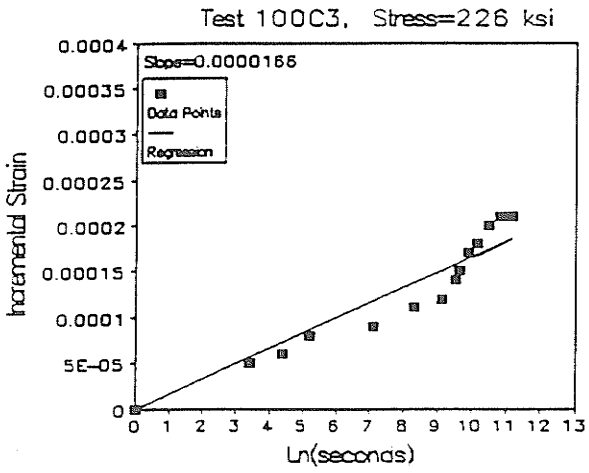

(c)

Figure 40: Incremental Strain vs Ln(time), Longitudinal Direction

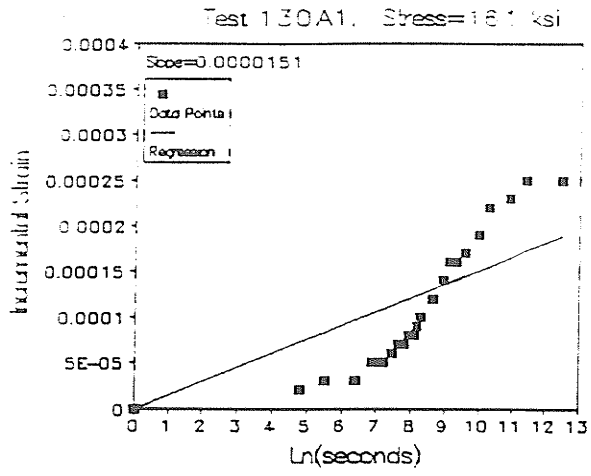

(a)

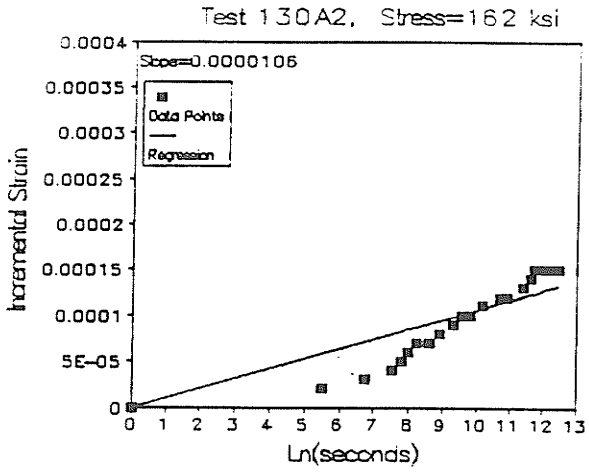

(b)

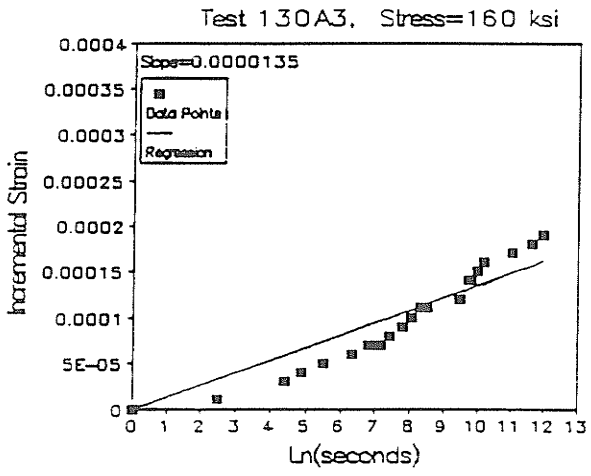

(c)

Figure 41: Incremental Strain vs Ln(time), Longitudinal Direction

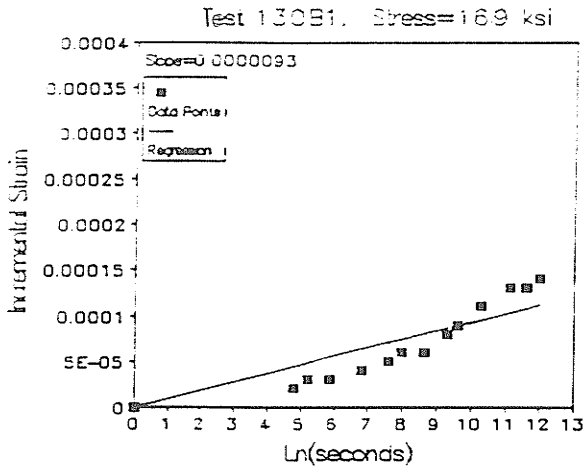

(a)

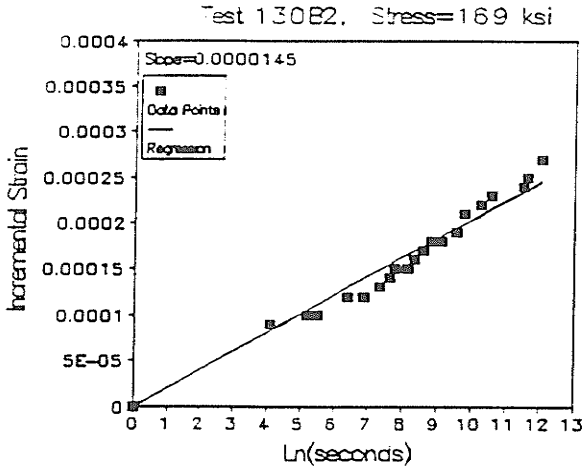

(b)

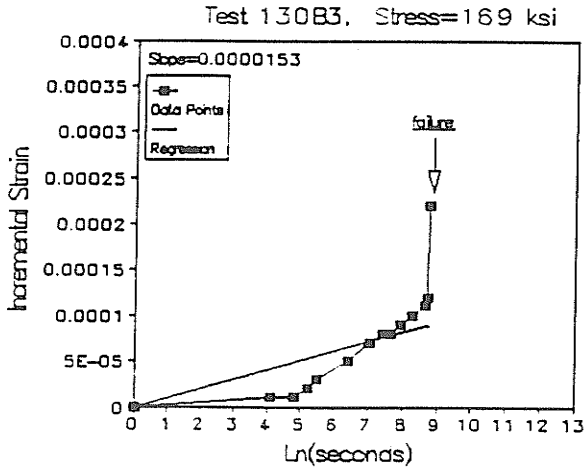

(c)

Figure 42: Incremental Strain vs Ln(time), Longitudinal Direction

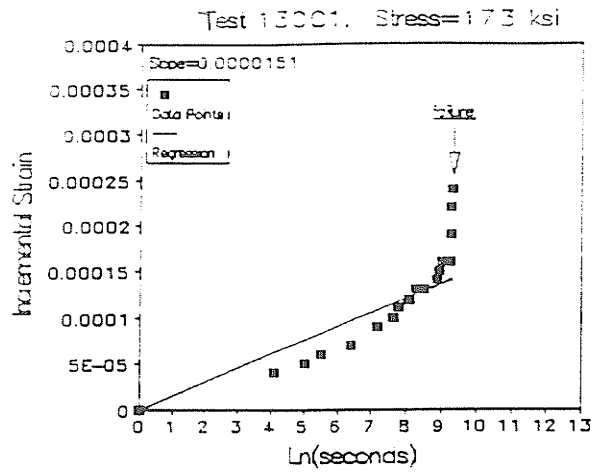

(a)

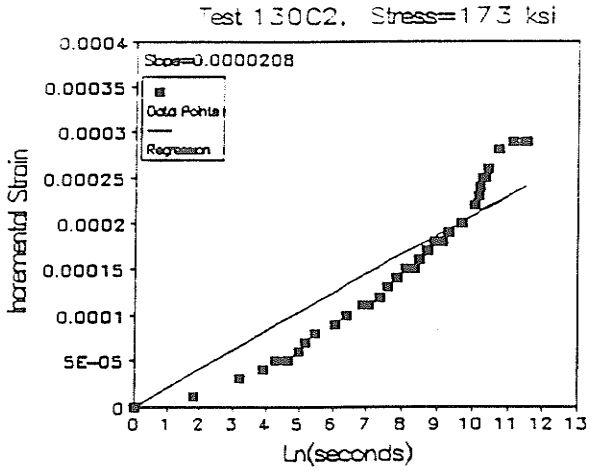

(b)

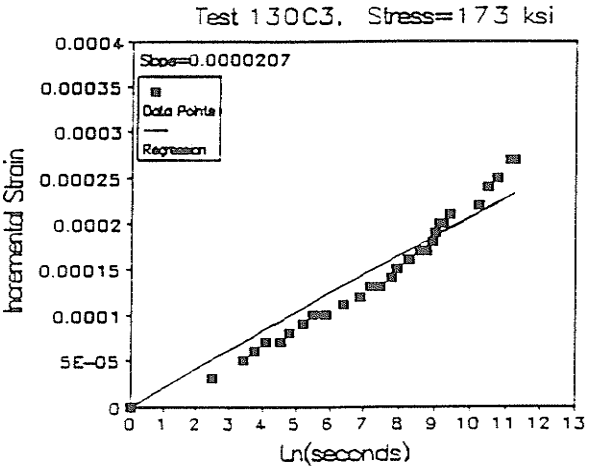

(c)

Figure 43: Incremental Strain vs Ln(time). Longitudinal Direction

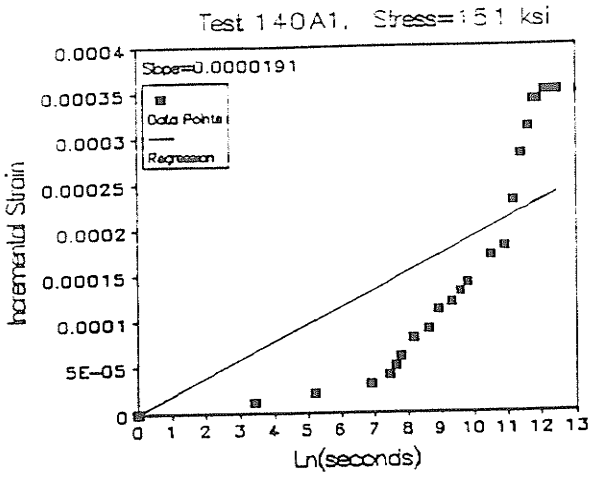

(a)

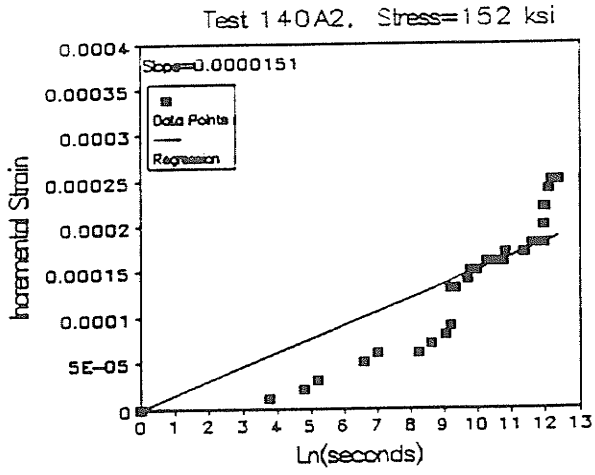

(b)

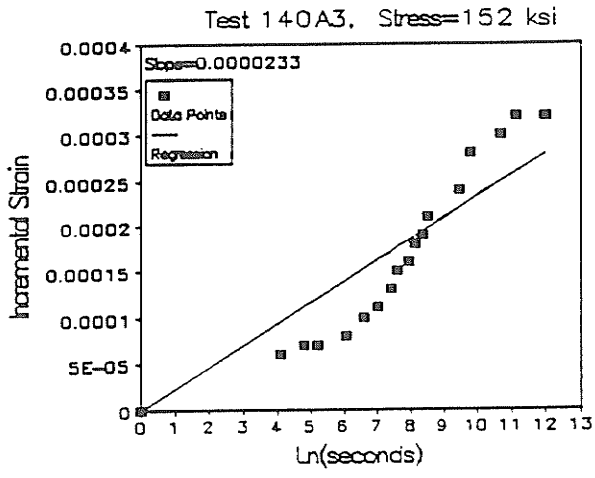

(c)

Figure 44: Incremental Strain vs Ln(time), Longitudinal Direction

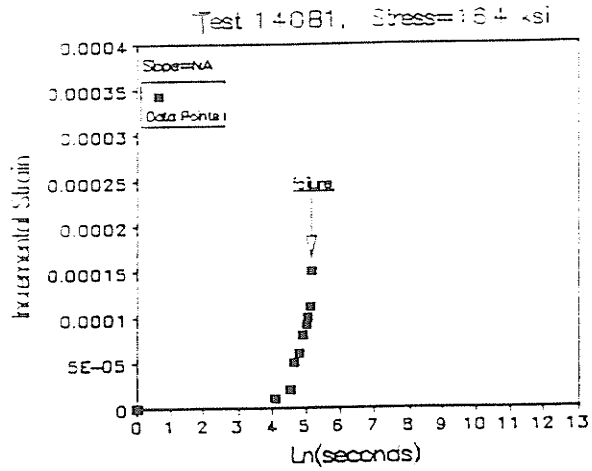

(a)

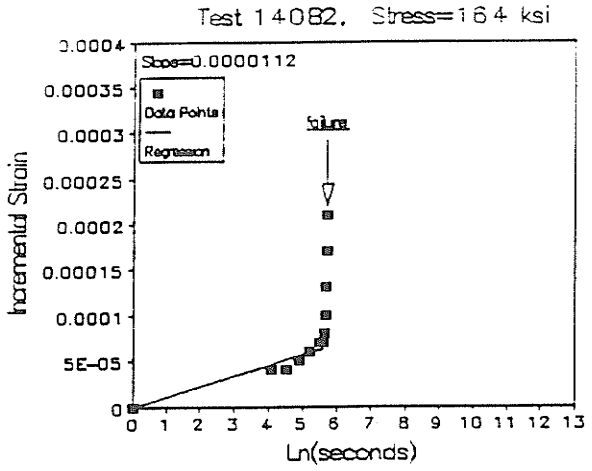

(b)

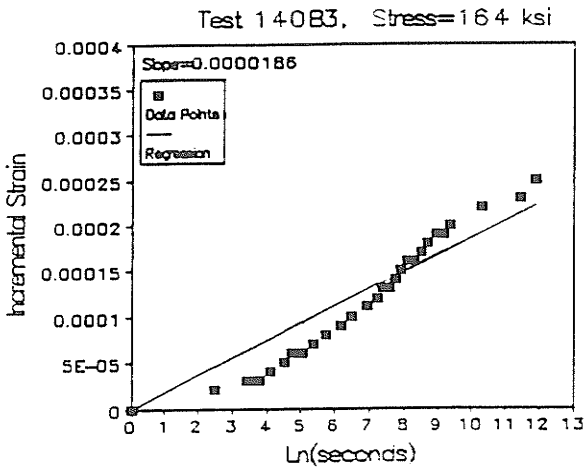

(c)

Figure 45: Incremental Strain vs Ln(time), Longitudinal Direction

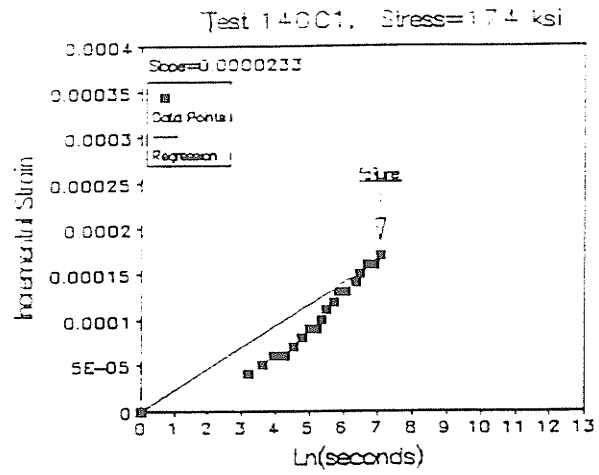

(a)

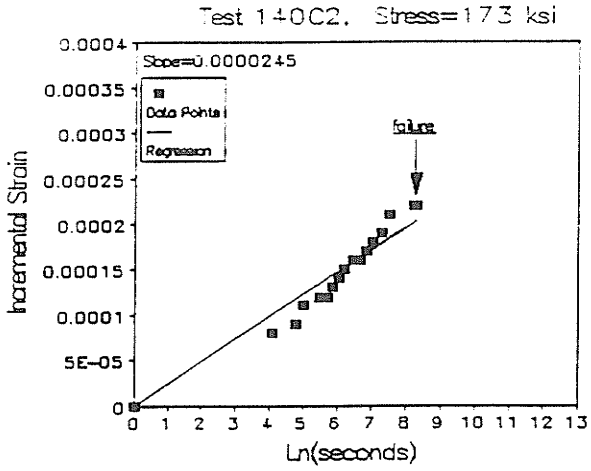

(b)

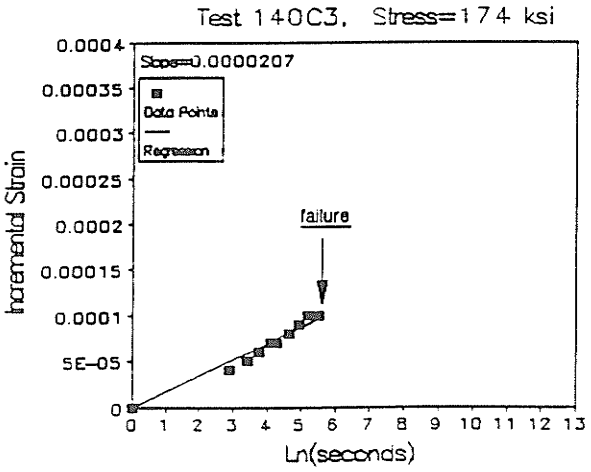

(c)

Figure 46: Incremental Strain vs Ln(time), Longitudinal Direction

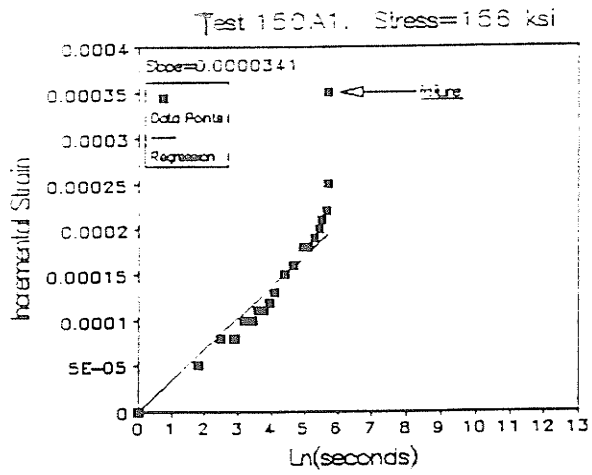

(a)

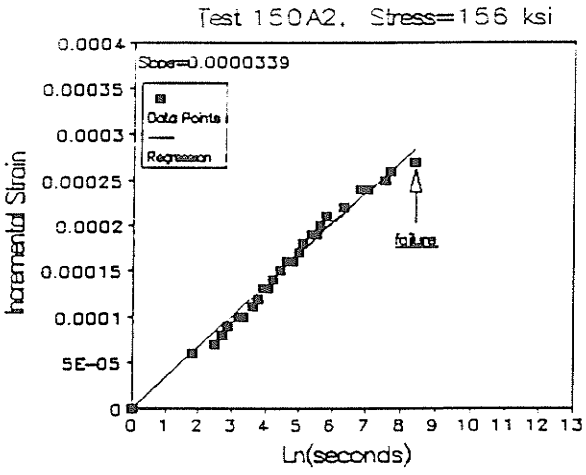

(b)

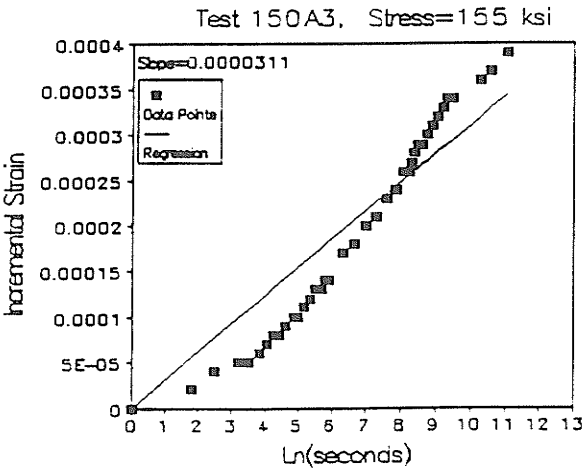

(c)

Figure 47: Incremental Strain vs Ln(time), Longitudinal Direction

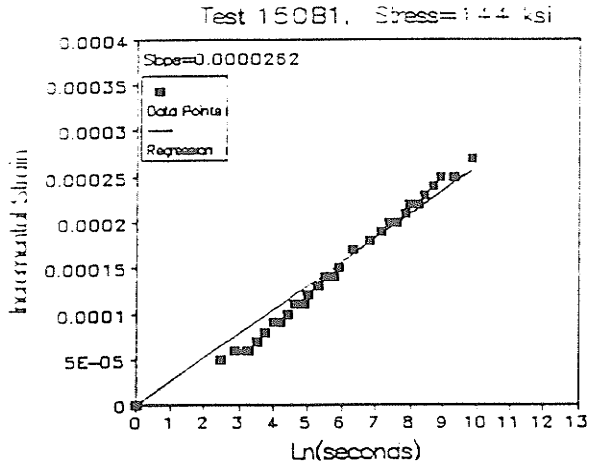

(a)

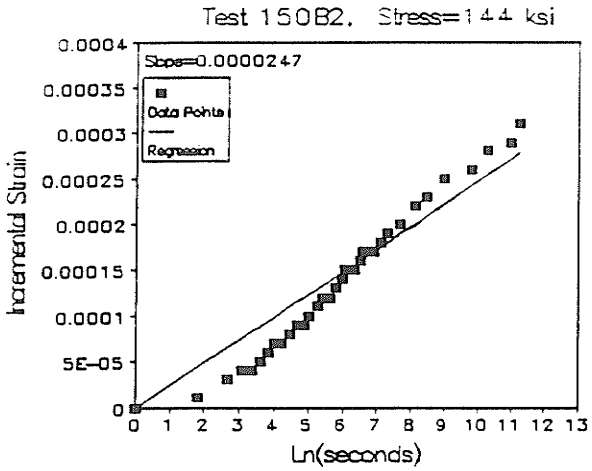

(b)

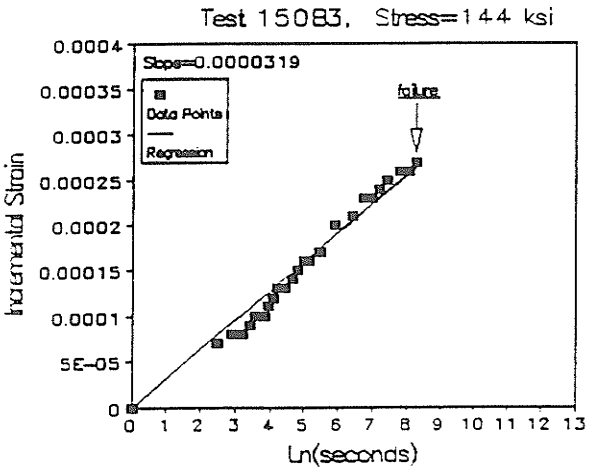

(c)

Figure 48: Incremental Strain vs Ln(time), Longitudinal Direction

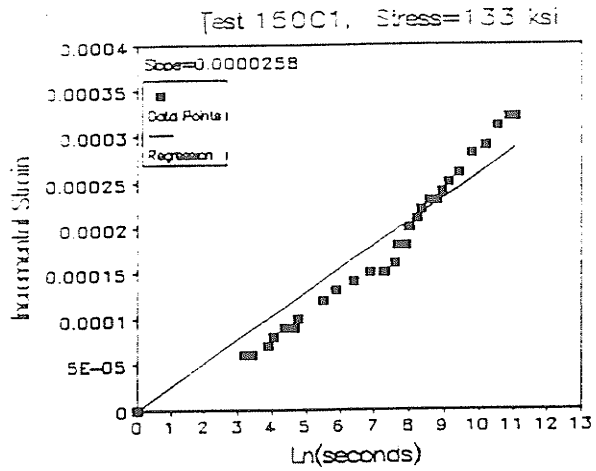

(a)

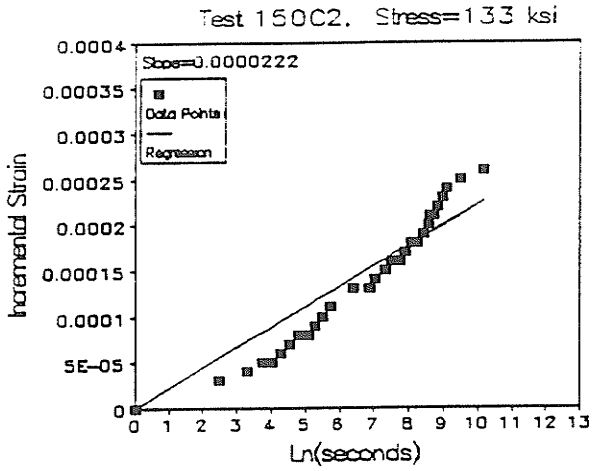

(b)

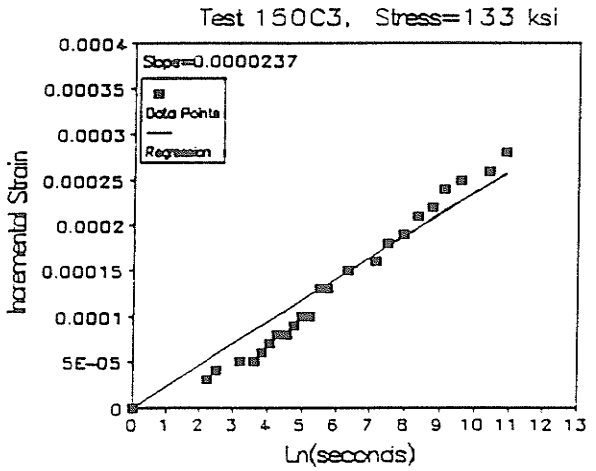

(c)

Figure 49: Incremental Strain vs Ln(time), Longitudinal Direction

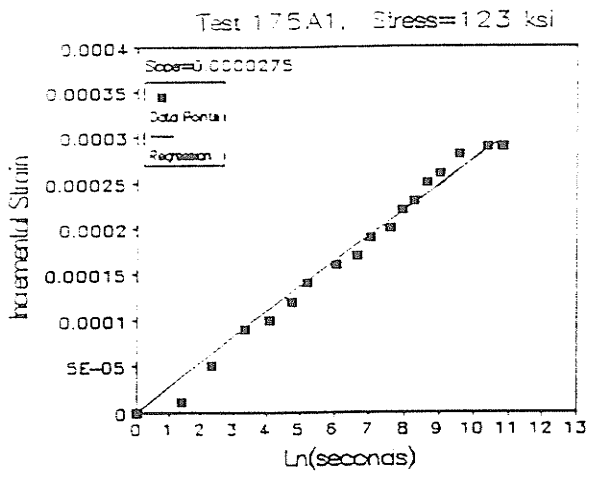

(a)

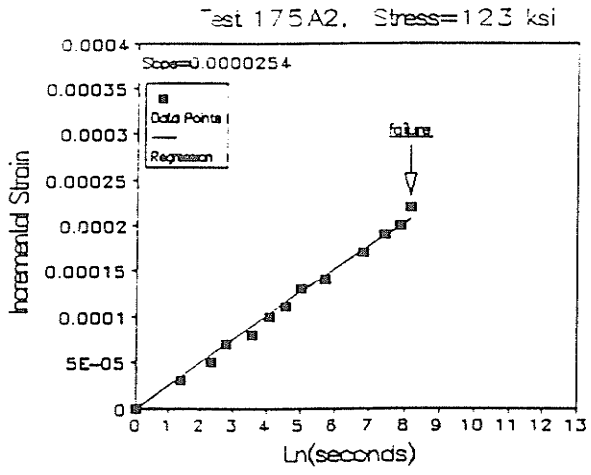

(b)

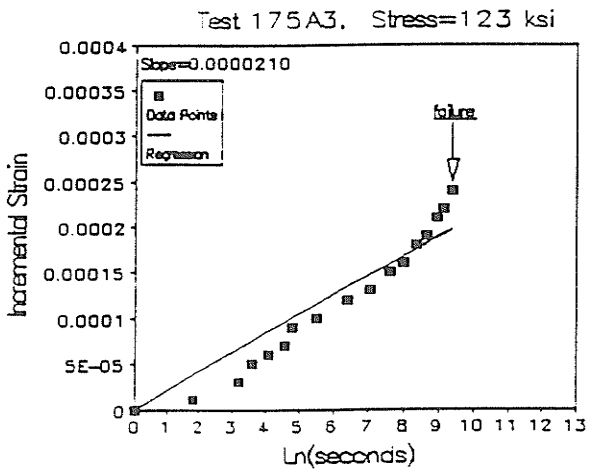

(c)

Figure 50: Incremental Strain vs Ln(time), Longitudinal Direction

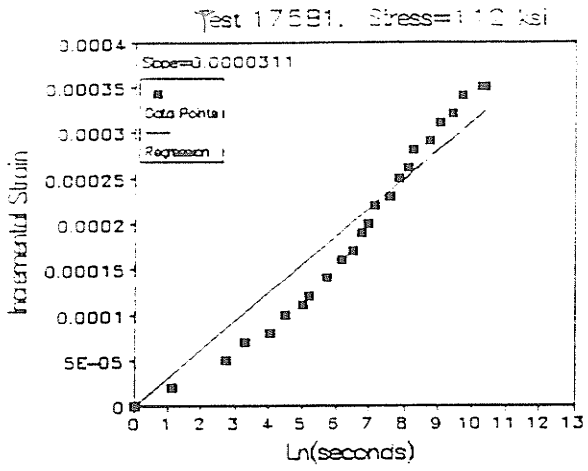

(a)

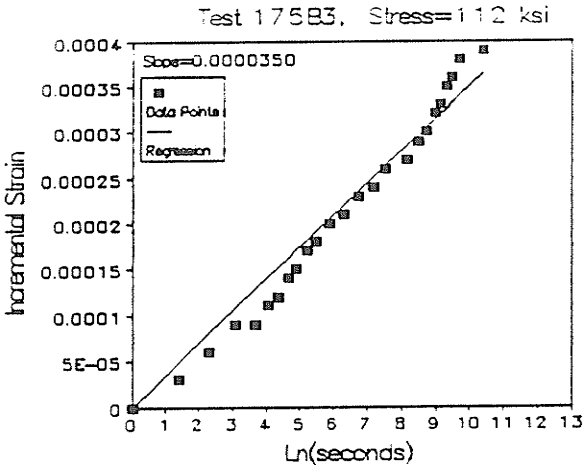

(b)

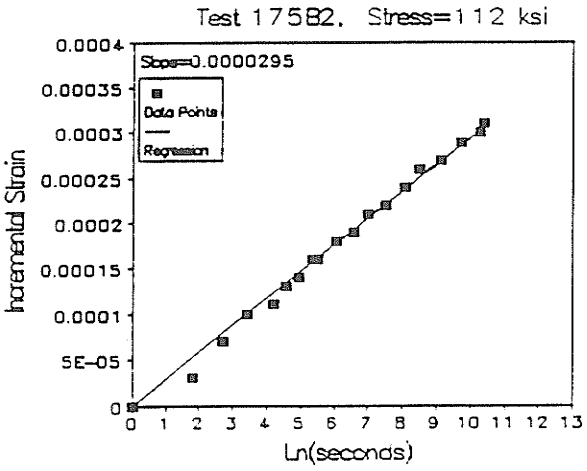

(c)

Figure 51: Incremental Strain vs Ln(time), Longitudinal Direction

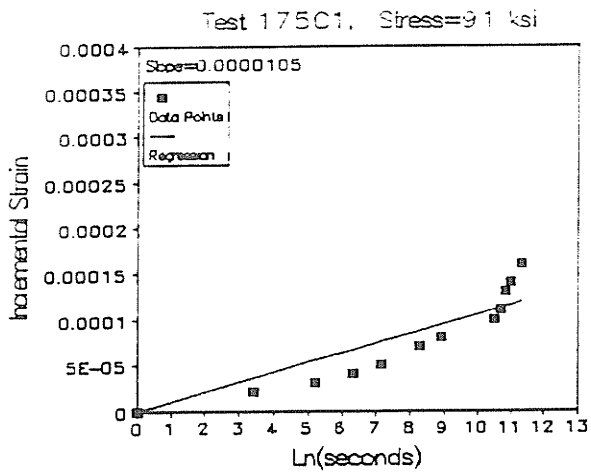

(a)

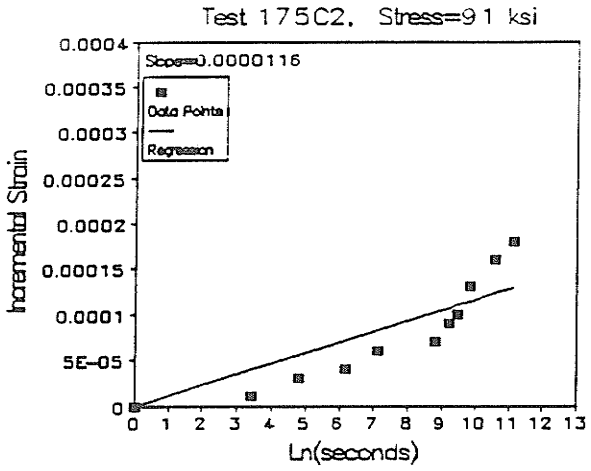

(b)

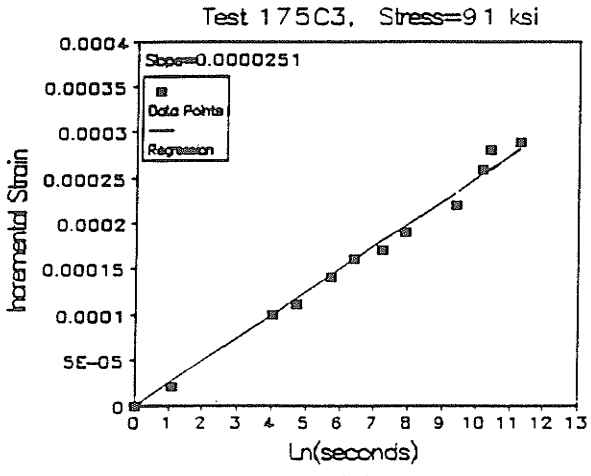

(c)

Figure 52: Incremental Strain vs Ln(time), Longitudinal Direction

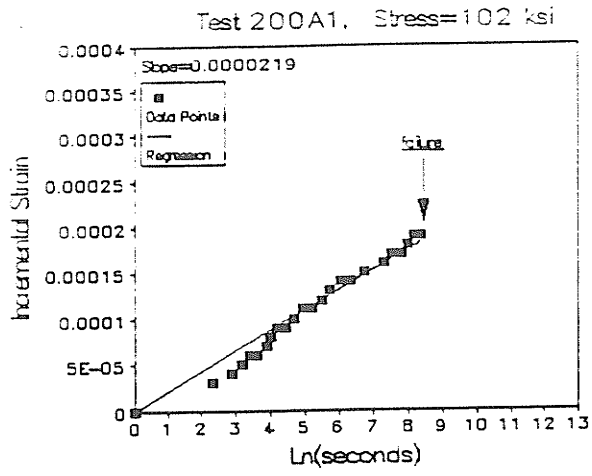

(a)

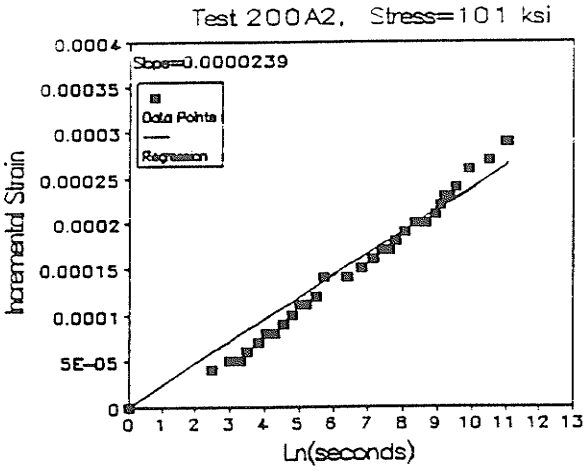

(b)

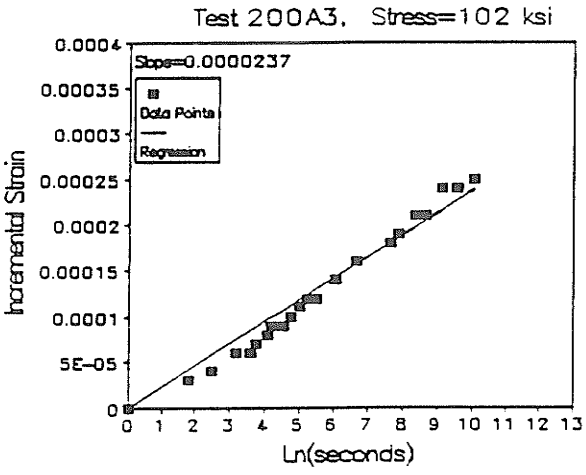

(c)

Figure 53: Incremental Strain vs Ln(time), Longitudinal Direction

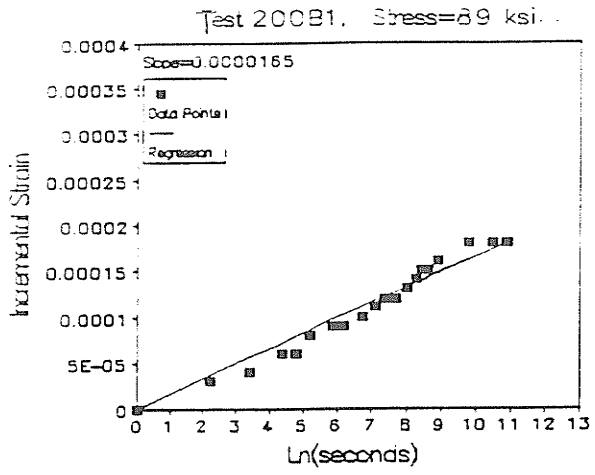

(a)

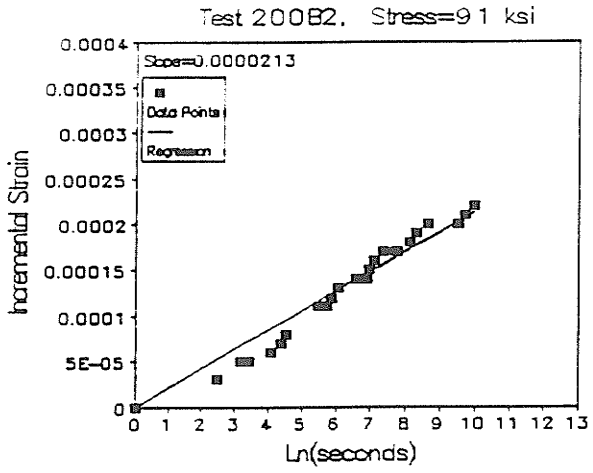

(b)

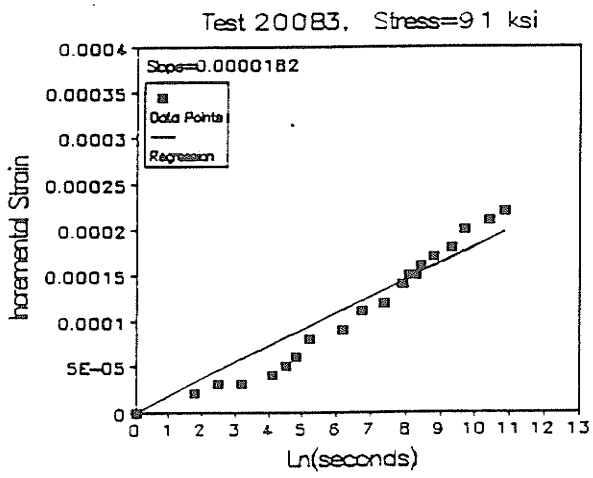

(c)

Figure 54: Incremental Strain vs Ln(time), Longitudinal Direction

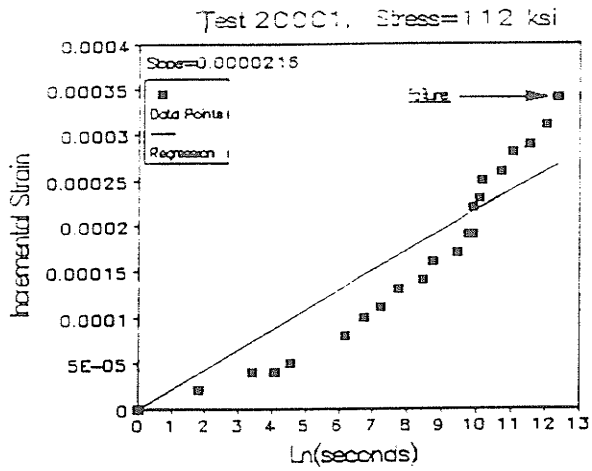

(a)

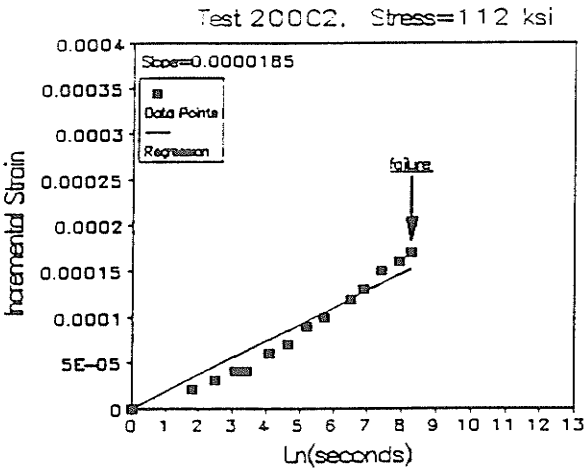

(b)

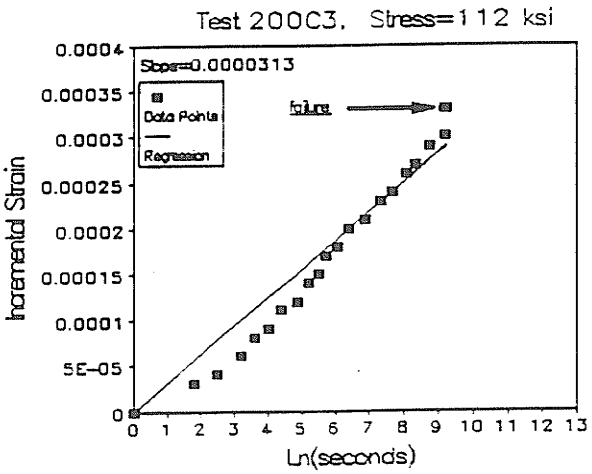

(c)

Figure 55: Incremental Strain vs Ln(time), Longitudinal Direction

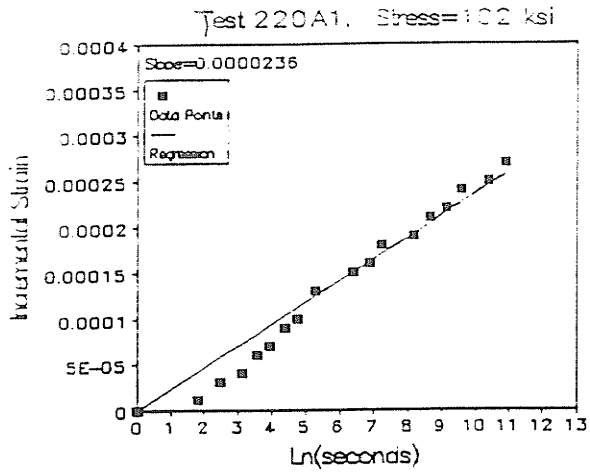

(a)

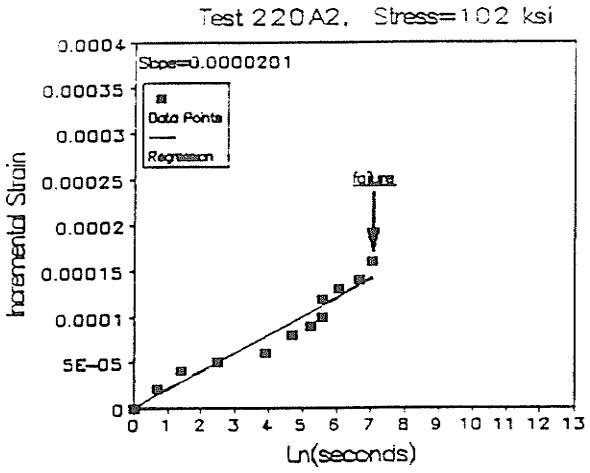

(b)

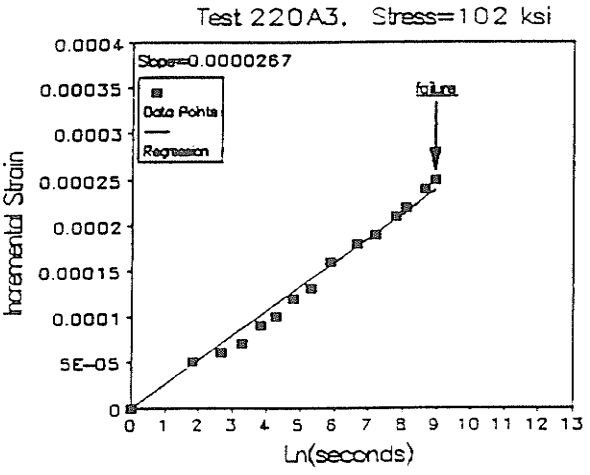

(c)

Figure 56: Incremental Strain vs Ln(time), Longitudinal Direction

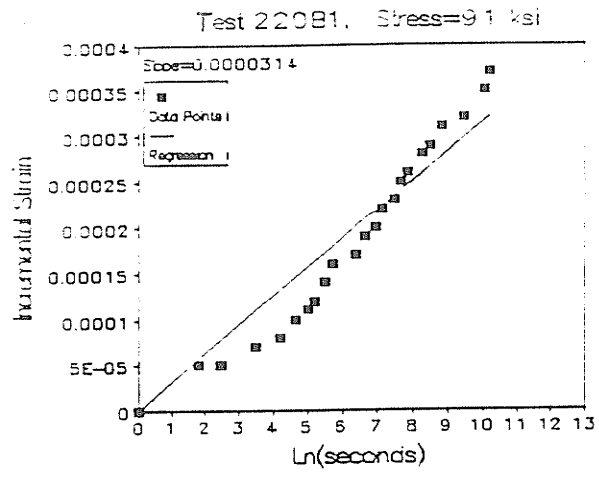

(a)

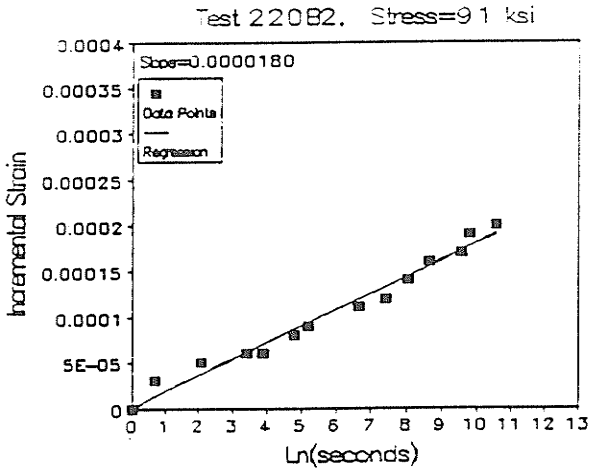

(b)

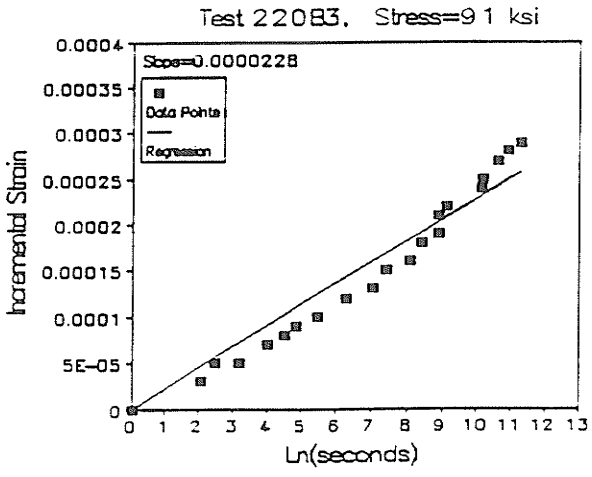

(c)

Figure 57: Incremental Strain. vs Ln(time), Longitudinal Direction

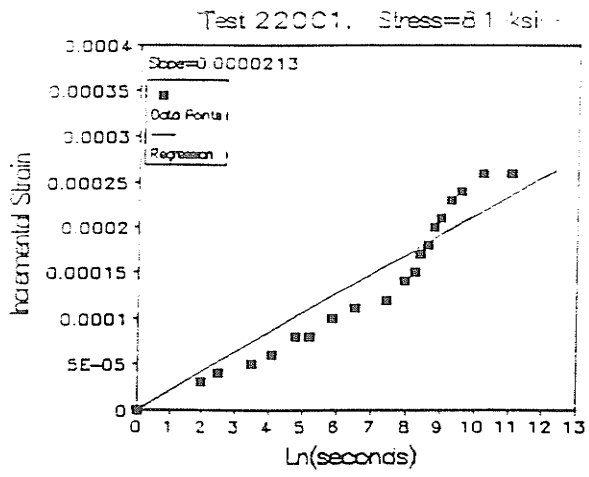

(a)

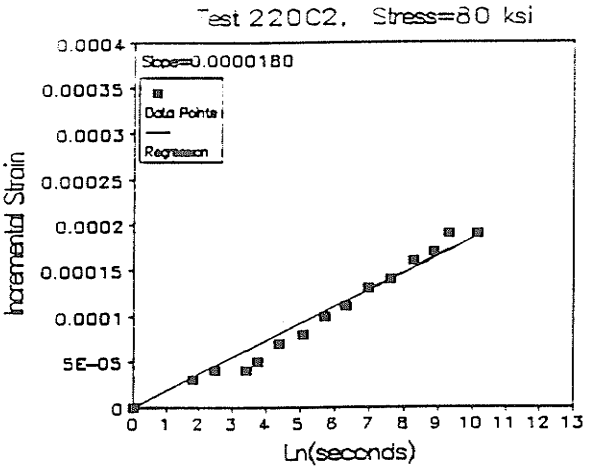

(b)

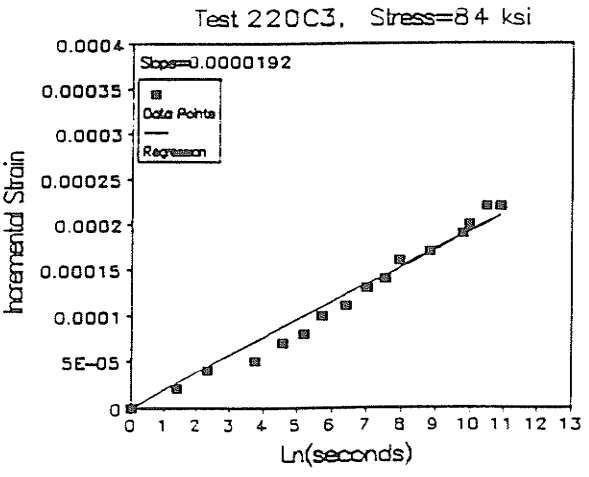

(c)

Figure 58: Incremental Strain vs Ln(time), Longitudinal Direction

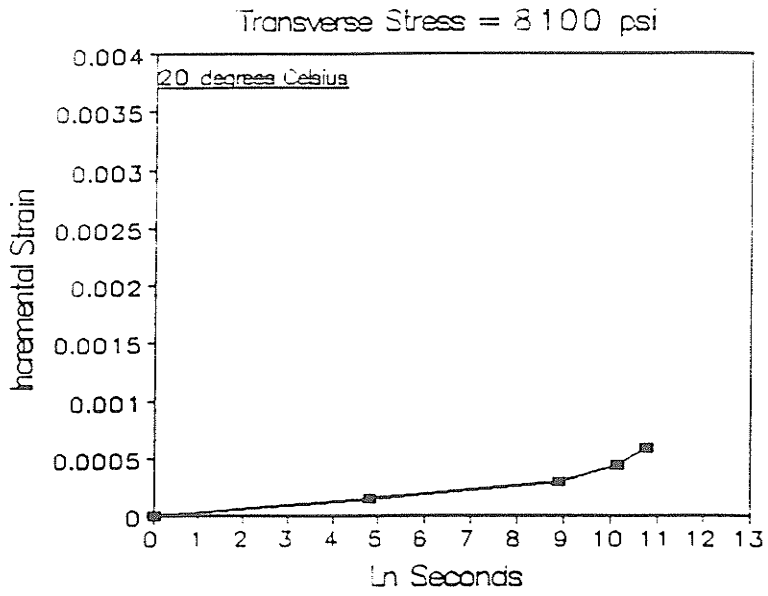

Figure 59: Incremental Strain vs Ln(time), Transverse Direction

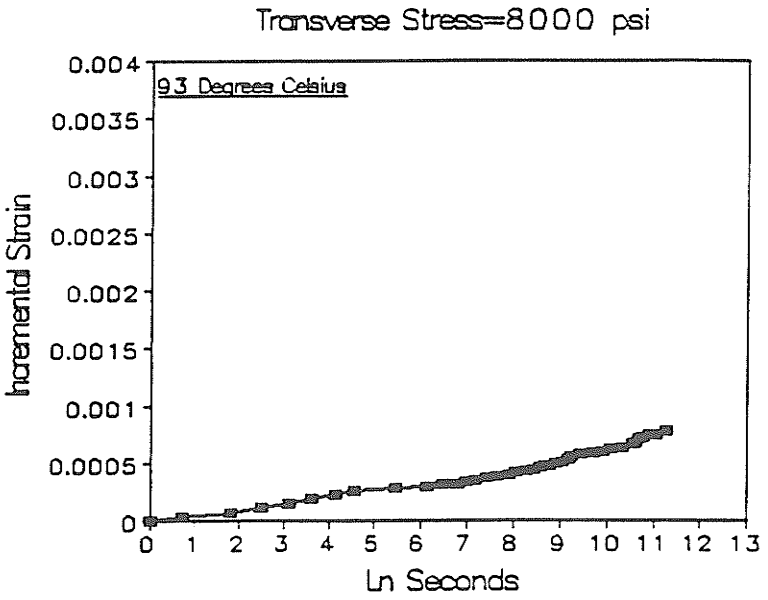

Figure 60: Incremental Strain vs Ln(time), Transverse Direction

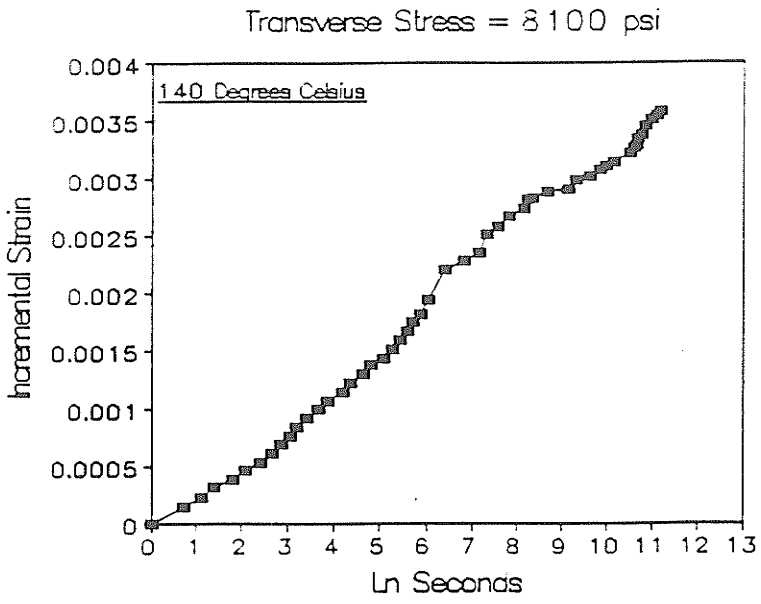

Figure 61: Incremental Strain vs Ln(time), Transverse Direction

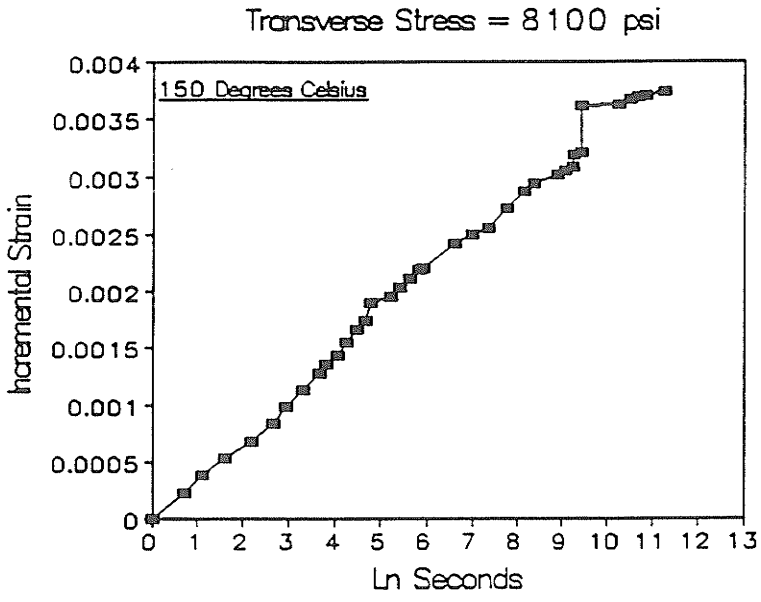

Figure 62: Incremental Strain vs Ln(time), Transverse Direction

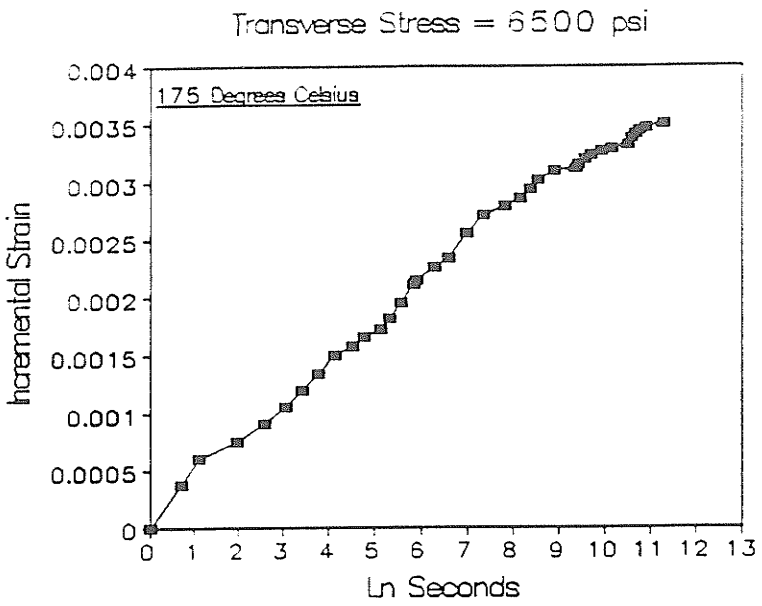

Figure 63: Incremental Strain vs Ln(time), Transverse Direction

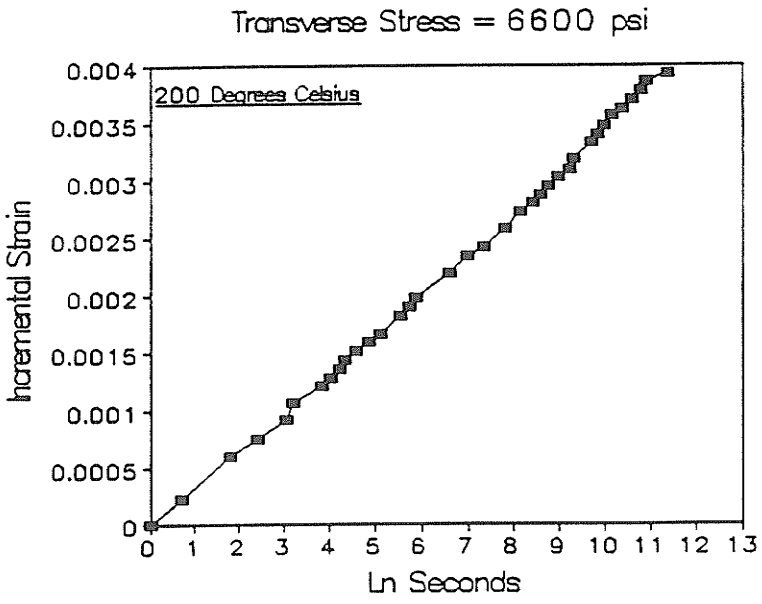

Figure 64: Incremental Strain vs Ln(time), Transverse Direction